AD-A267 984

UMENTATION PAGE

Form Approved
OMB No. 0704-0188

2. REPORT DATE	3. REPORT TYPE AND DATES COVERED
June 1993	THESIS/DISSERTATION

4. TITLE AND SUBTITLE

Modeling Teh Minimum Energy State Of The Earth's Magnetotail

5. FUNDING NUMBERS

6. AUTHOR(S)

Capt Markus Stephen Sorrells

7. PERFORMING ORGANIZATION NAME(S) AND ADDRESS(ES)

AFIT Student Attending: Utah State University

8. PERFORMING ORGANIZATION REPORT NUMBER

AFIT/CI/CIA- 93-123

9. SPONSORING/MONITORING AGENCY NAME(S) AND ADDRESS(ES)

DEPARTMENT OF THE AIR FORCE
AFIT/CI
2950 P STREET
WRIGHT-PATTERSON AFB OH 45433-7765

10. SPONSORING/MONITORING AGENCY REPORT NUMBER

11. SUPPLEMENTARY NOTES

12a. DISTRIBUTION/AVAILABILITY STATEMENT

Approved for Public Release IAW 190-1
Distribution Unlimited
MICHAEL M. BRICKER, SMSgt, USAF
Chief Administration

12b. DISTRIBUTION CODE

13. ABSTRACT *(Maximum 200 words)*

93-18994

93 8 16 063

14. SUBJECT TERMS	15. NUMBER OF PAGES 130
	16. PRICE CODE

17. SECURITY CLASSIFICATION OF REPORT	18. SECURITY CLASSIFICATION OF THIS PAGE	19. SECURITY CLASSIFICATION OF ABSTRACT	20. LIMITATION OF ABSTRACT

MODELING THE MINIMUM ENERGY STATE OF THE EARTH'S MAGNETOTAIL

by

Markus Stephen Sorrells

A thesis proposal submitted in partial fulfillment
of the requirements for the degree

of

MASTER OF SCIENCE

in

Physics

Approved:

W Farrell Edwards
Dr. W. Farrell Edwards
Major Professor

Jan J. Sojka
Dr. Jan J. Sojka
Committee Member

Kent L. Miller
Dr. Kent L. Miller
Committee Member

James P. Shaver
Dr. James P. Shaver
Dean of Graduate Studies

UTAH STATE UNIVERSITY
Logan, Utah

1993

ACKNOWLEDGMENTS

I would like to thank Dr. W. Farrell Edwards for all the guidance and support he gave me during my work on this thesis. I would also like to thank my other committee members, Dr. Jan J. Sojka and Dr. Kent L. Miller, for all their assistance throughout the entire process of picking a thesis topic to actually writing and defending it. Also, I would like to thank Dr. Anthony T. Y. Lui for providing me with data depicting typical magnetotail profiles during solar quiet times for the research in this thesis.

I also wish to thank Imad Barghouthi for providing assistance with the computer model programs in this thesis. Without the use of his considerable programming experience on the VAX computer system, I'm convinced I would still be programming the computer today.

I give a special thanks to my family, friends, and colleagues for their encouragement, moral support, and patience as I worked my way from the initial proposal writing to this final document. I could not have done it without all of you.

Markus S. Sorrells

CONTENTS

LIST OF TABLES

LIST OF FIGURES

ABSTRACT

Modeling the Minimum Energy State of the

Earth's Magnetotail

by

Markus S. Sorrells, Master of Science

Utah State University, 1993

Major Professor: Dr. W. Farrell Edwards
Department: Physics

For a system that remains in thermodynamic equilibrium, stable equilibria are determined by minimizing an appropriate potential energy function such as the Gibb's free energy. However, when a system does not remain in thermodynamic equilibrium (i.e. a radiating system), one cannot use a potential function to derive a state of stable equilibrium. If we assume this is the case for the earth's magnetotail, then we must come up with another method to determine stable equilibrium. We conjecture that this will be a minimum total energy.

By combining Poynting's theorem with the Lorentz force equation and Maxwell's equations, one can account for the energy advections into and out of a system containing a fully ionized plasma, as well as for the energy fluctuations caused by changing electric and magnetic fields. By minimizing the total energy equation representing an idealized model of the earth's magnetotail, one should be able to calculate its stable equilibrium state.

Although the idealized minimum energy model presented in this paper depicts many trends observed in the earth's magnetotail, this thesis concludes that more modifications are needed before it becomes a useful tool for analyzing the earth's magnetotail. (140 pages)

CHAPTER I

INTRODUCTION

Earth's Magnetotail

This thesis attempts to develop a model to determine if a minimum energy equilibrium state establishes itself within the earth's magnetotail. During quiet conditions, the earth's magnetotail receives and stores energy from the solar wind. At periodic intervals, the magnetotail releases all or a portion of this stored energy into the earth's ionosphere and interplanetary space in the form of geomagnetic storms, substorms, and plasmoid ejections. At this point in time, no one is quite certain how or why the magnetotail periodically releases its energy although there are a couple of theories available. One theory suggests that the solar wind may deposit energy into the magnetotail at a rate faster than the magnetotail can absorb it, causing the excess energy to be discarded during the energy storage cycle. Another theory states that the magnetotail has a finite energy storage capacity and when this critical level is reached, some unknown triggering mechanism causes the magnetotail to release its energy. Whatever the case, this energy release is probably the result of the magnetotail trying to establish an equilibrium state. It seems reasonable that the magnetotail would ultimately be trying to reach an equilibrium state having the lowest possible total energy. This thesis attempts to find out if the magnetotail releases enough of its energy at one time to ever reach this minimum total energy state.

The minimum energy model developed in this thesis calculates the minimum energy profiles of key parameters of the magnetotail such as magnetic field strength, ion and electron number densities, temperatures, and bulk flow velocities. By comparing the model's profiles with those observed in the magnetotail at the end of an energy release cycle, one should be able to ascertain whether the model works or not. Certain insights to the earth's magnetotail energy cycle may be gained if the model adequately describes the above situation. Before getting into the minimum energy model, a brief background into the magnetospheric/tail physics and

structure will be discussed in this chapter.

Magnetospheric/tail Models

Prior to the advent of space exploration, scientists had to rely solely on ground measurements to observe and come up with theories to explain the structure of the earth's magnetic field. As a result, early scientists pictured the earth's magnetic field as a perfect magnetic dipole (Fig. 1).

In 1931, Chapman and Ferraro brought the acceptance of a solar wind into the scientific community (Akasofu, 1981). Solar wind plasma originates from the sun's corona and flows radially outward at "supersonic" speeds that vary between 300 to 800 kilometers per second (Gosling, 1984). As the solar wind reaches the earth, it has a typical density of about 10 particles per cubic centimeter (Gosling, 1984) as compared to the 3×10^{19} particles per cubic centimeter found in the atmosphere at the earth's surface. During solar quiet times, the energy of the solar wind particles is normally a few eVs.

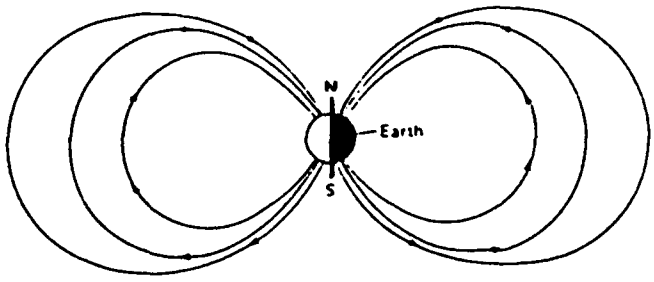

FIG. 1. The original undisturbed model with magnetic field lines extending into a vacuum [Gosling, 1984].

Scientists had to take into account the effects of the solar wind flow against the earth's magnetic field. They came up with what is now called the closed magnetospheric model in which magnetic field lines left one hemisphere of the earth and returned to the other hemisphere and were modified by the solar wind flow into the shape depicted in Fig. 2.

This model worked relatively well for describing some of the magnetospheric processes that were observed before the advent of space exploration. In 1955, a British geophysicist by the name of James W. Dungey attempted to apply hydromagnetic theory to calculate and determine the shape of the magnetotail (Carovillano et al., 1967). As it turned out, his calculations worked fairly well on the dayside portion of the magnetotail but it predicted that the magnetotail would close off relatively close behind the earth with something like a Mach angle. Of course current observations do not support this theory. As more magnetospheric processes were observed with the use of satellites, it became apparent that the closed magnetospheric model was not sufficient. For example, it could not explain how solar wind particles gained relatively easy access to the earth's polar regions nor could it explain the sharp outer boundary layer of the plasma sheet which separated the anti-parallel magnetic field lines of the magnetotail.

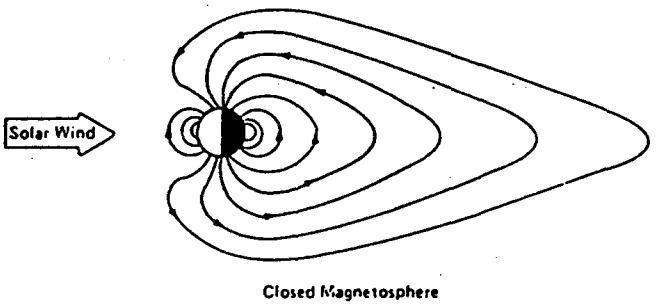

FIG. 2. A closed magnetospheric model in which the solar wind distorts the earth's magnetic field. All the earth's magnetic lines start and end on the earth. (For simplicity, the tilt of the earth's axis is not shown) [Gosling, 1984].

In the early 1960's scientists discovered that the solar wind contained a magnetic field. Since the sun has a dipolar magnetic structure, the solar wind carries "frozen" remnants of the sun's magnetic field within its flow. This "frozen in" magnetic field is known as the Interplanetary Magnetic Field or IMF. Due to the dipole nature of the sun, the IMF is either a sunward or anti-sunward orientation. A heliomagnetic current sheet separates these oppositely aligned magnetic fields, which prevents them from making contact and mutually annihilating one other. Due to the rotation of the sun and the current sheet's 7^{o} inclination (Tascione, 1988) to the solar rotational equator, the current sheet incurs a wavy structure depicted in Fig. 3. Because of the wavy nature of this current, the earth's orbit passes through it at least twice during each solar rotation. As the earth passes through this structure, the IMF will either have a northern or southern component to it depending on whether the earth is above or below the heliomagnetic current sheet. The acceptance of a magnetic field (or IMF) in the solar wind led scientists to develop an open magnetospheric model. In this model, some of the magnetic field lines flow from the earth out into interplanetary space instead of flowing back towards the earth at the

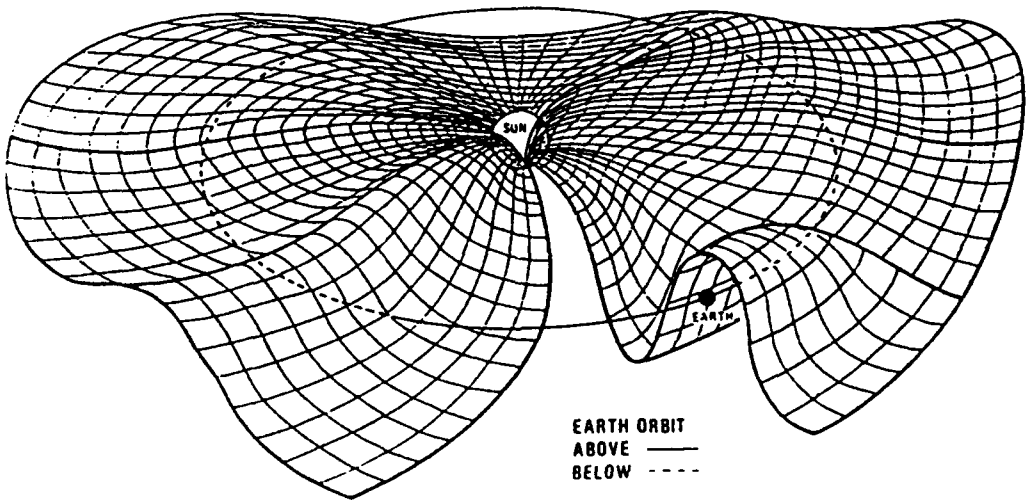

FIG. 3. Wavy structure of the heliomagnetic current sheet due to the current sheet's inclination to the sun's rotational equator [after National Research Council, 1981].

opposite hemisphere (Fig. 4). This model is able to explain many of the phenomena observed within the magnetosphere/tail that the closed model could not, such as how solar wind plasma and energy are able to move into and through the magnetosphere (Gosling, 1984). In fact, this model can also attempt to explain the dependence of the earth's magnetic activity on the IMF.

When the IMF points southward, as seen in Fig. 5(a), its magnetic field can easily merge with the earth's own field. According to the model, magnetic merging is one of the primary processes by which the solar wind transfers a portion of its mass/energy to the earth's magnetosphere/tail. As a result, the earth's magnetosphere/tail is relatively active during southward IMF.

However, magnetic merging occurs less often when the IMF points northward (Fig. 5(b)). This means the amount of solar wind mass/energy transferred into the earth's magnetosphere/tail is reduced. As a result, the earth's magnetosphere/tail experiences less geomagnetic activity when the IMF is pointing northward rather than southward.

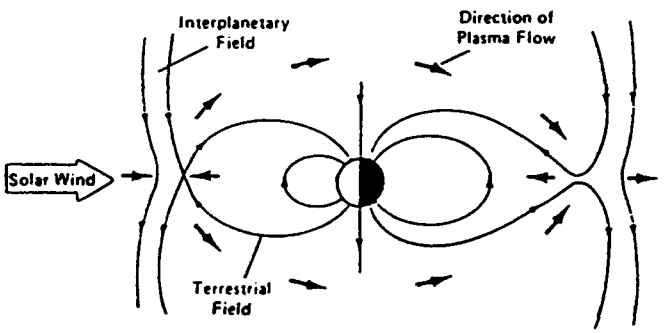

FIG. 4. An open magnetospheric model in which the terrestrial and interplanetary field lines connect. (Tilt of the earth's axis is not shown) [Gosling, 1984].

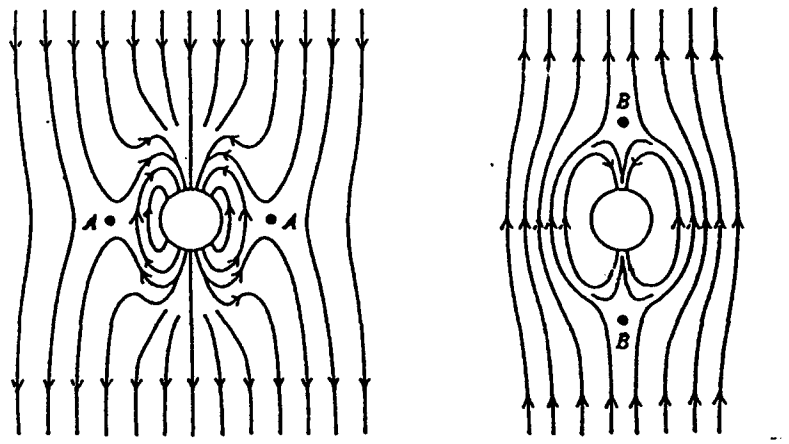

FIG. 5. The interaction of the earth's dipole magnetic field with (a) southern component of the IMF and (b) the northern component of the IMF.

Even with all its good points, the open magnetospheric model does not explain every situation within the magnetosphere/tail so most scientists today use a combination of the open and closed models to describe magnetospheric processes.

Magnetospheric/tail Physics

The "supersonic" plasma of the solar wind encounters the presence of the earth's magnetosphere at a boundary referred to as the "bow shock" (Fig. 6). This encounter is analogous to a shock wave created by an object moving at supersonic speeds through a fluid medium. The region directly behind the bow shock is called the "magnetosheath" and forms a physical boundary between the solar plasma at the bow shock and the magnetospheric plasma at the magnetopause. As the solar wind particles continue to flow past the earth's northward pointing magnetic field, they are acted upon by the Lorentz force $\vec{F} = q (\vec{v} \times \vec{B})$ which deflects the positive ions towards the dusk side of the earth and the negative electrons towards

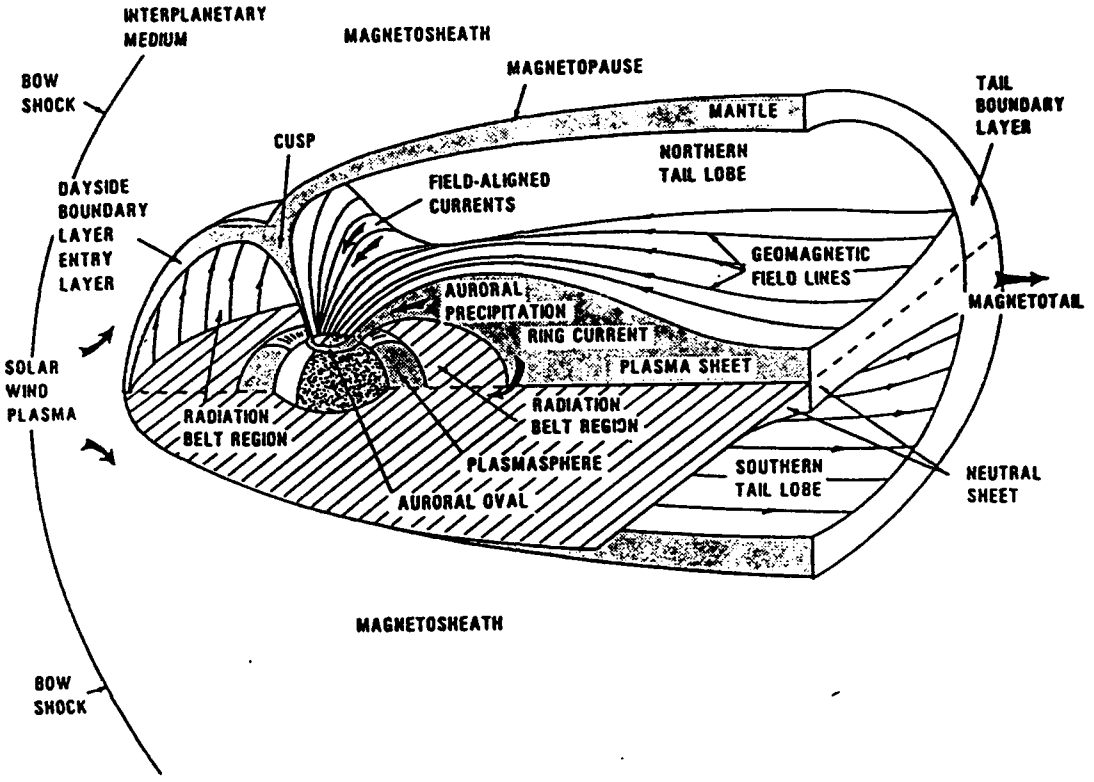

FIG. 6. Diagram showing the structure of the earth's magnetosphere system [National Research Council, 1981].

the dawn side (Fig. 7). This force sets up a magnetopause current that follows the path taken by the positive ions and flows around the outside of the magnetosphere and eventually merges with the magnetotail current, which flows around the exterior of the magnetotail from dusk to dawn as depicted in Fig. 8. The magnetotail current then merges with the current or plasma sheet current (Fig. 9), which flows from dawn to dusk in the interior of the magnetotail. The magnetotail and plasma sheet currents are enhanced by the earth's magnetic field, which points

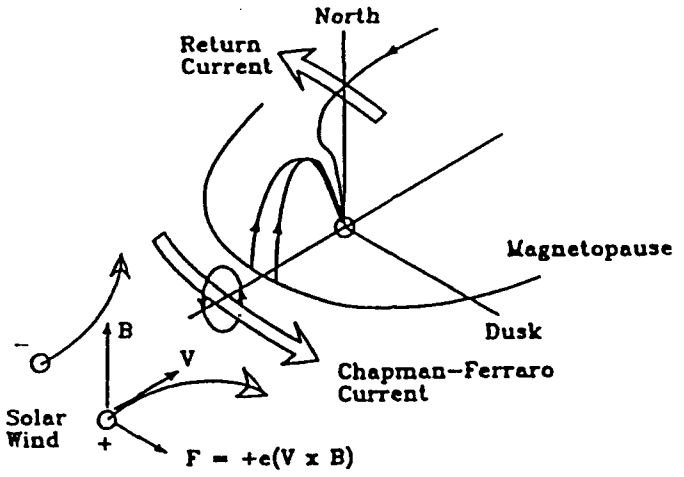

FIG. 7. Schematic showing how the Lorentz force creates the magnetopause current [from McPherron, 1991].

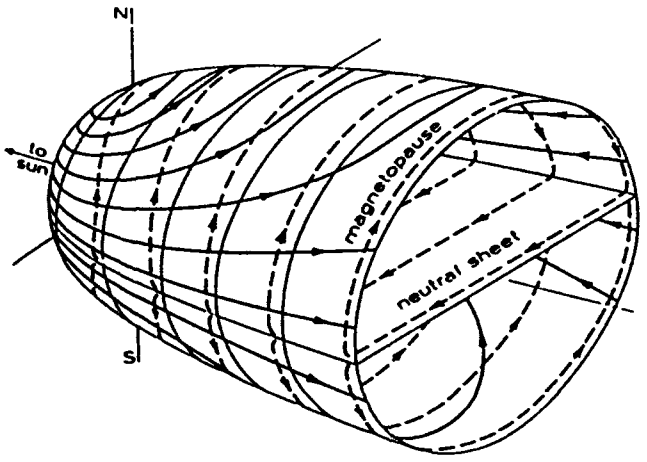

FIG. 8. Flow patterns of the two principal current systems which determine the configuration of the magnetosphere/tail [adapted after Axford, 1965].

sunward in the northern half of the magnetotail and anti-sunward in the southern half (Fig. 6). The ring current, which constitutes the earthward most regions of the plasma sheet, is due to drift of charged particles across the earth's magnetic field gradient. The drifts are charge dependent so that positive particles drift westward and negative particles drift eastward

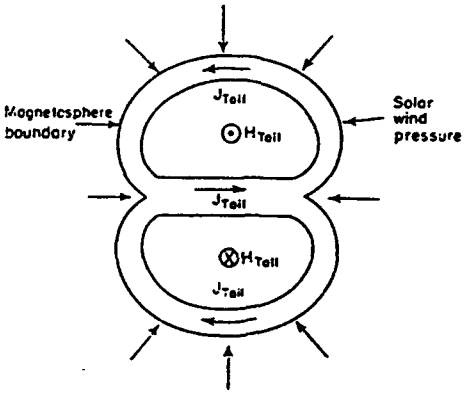

FIG. 9. Cross section of the earth's magnetotail showing the primary directions of the magnetopause and crosstail currents [following Axford et al., 1965].

(Fig. 10) producing a net westward current (Williams, 1987).

The field align currents (FACs), also known as Birkeland currents, connect the earth's ionosphere to the magnetosphere and interplanetary space. The net current usually flows into the ionosphere at the morning sector, across the polar cap (Auroral electrojet), and out of the ionosphere at the evening sector (Fig. 11). The magnetotail forms when the earth's magnetic field lines are stretched, as far as 1000 earth radii or R_e, downstream by the solar wind. The process starts when the IMF and the earth's magnetic field merge and connect on the sunward side of the earth near the magnetopause. The solar wind is then able to drag the interconnected magnetic field lines from the dayside portion of the magnetosphere down the magnetotail to the point where they reconnect (Fig. 12) (Sibeck, 1990).

As stated above, hydromagnetic theory was not able to explain the long nature of the magnetotail. The problem was that it assumed the solar wind slid smoothly along the boundary of the magnetotail without agitating it. Scientists soon concluded that there had to be some force exerted on the tail to allow it to be dragged out for such a distance. One explanation is that there must be a pressure p_1 within the tail region which tends to push out with just enough

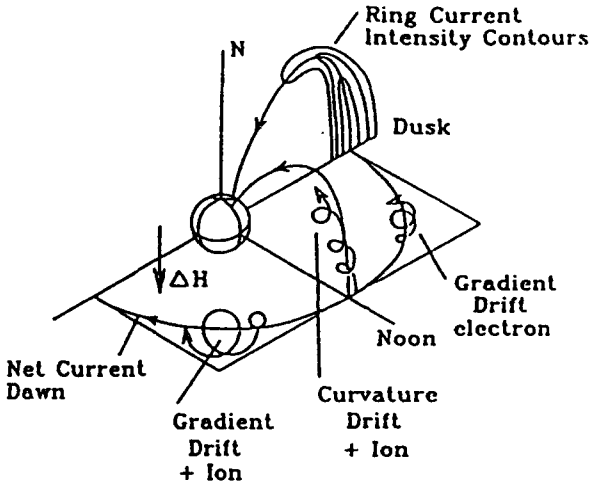

FIG. 10. A view of the dayside plasmasphere showing the creation of a westward ring current by particle drift [from McPherron, 1991].

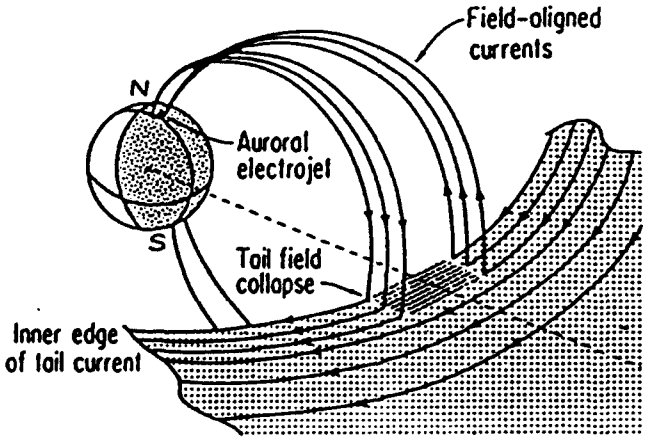

FIG. 11. Field aligned currents [from Clauer and McPherron, 1974].

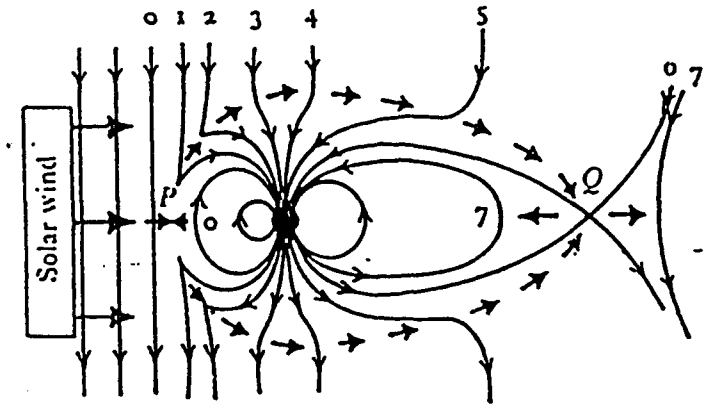

FIG. 12. Schematic showing magnetic merging process [Aeronomy Lecture, 1992].

pressure to equal the inward magnetic tension (or pressure) of the tail (Carovillano et al., 1967). This effect is expressed in Eq. (1).

$$P_1 = \frac{B^2}{8\pi} . \qquad (1)$$

However, there is also a pressure outside the tail p_2, which combines with the inward magnetic tension of the tail to push against the internal pressure. Therefore, in order for a transverse equilibrium condition to exist, the total pressure inside the tail p_1 must balance both the inward magnetic tension of the tail plus the pressure outside the tail p_2. This pressure balance is expressed in Eq. (2).

$$P_1 = \frac{B^2}{8\pi} + P_2 . \qquad (2)$$

Enhanced mixing of the solar wind plasma with the magnetopause boundary is also used to explain the magnetosphere's long tail. It is thought that this mixing could be due to surface instabilities on the magnetotail boundary or other unknown mechanisms. Whatever the cause, this mixing would allow particles from the solar wind to penetrate into the tail at large distances. The inertia of this penetration could then be the mechanism that stretches the magnetotail out to the long distances that we observe. The solar wind penetration can also be the source of the tension along the magnetic field lines. Calculations have shown that only $1/10^{th}$ of the total solar wind momentum is required to produce the necessary shape observed and tension required within the earth's magnetotail (Carovillano et al., 1967). It is these calculations which have caused the latter explanation to be widely accepted.

In order for solar wind plasma to interact within the earth's magnetic field, it must first get into the magnetospheric/tail system. One way this can happen is through the magnetic merging of the earth's magnetic field with an IMF as described above (Tascione, 1988). As the interconnected magnetic fields are pushed along by the solar wind, some of the solar wind particles are dragged along. When the magnetic field lines reconnect, a portion of the field line gets propelled earthward by the inward tension of the magnetic field, thereby injecting some of the trapped solar wind particles into the earth's magnetosphere (Fig. 12).

Solar wind particles can also get into the earth's magnetotail through diffusion across the magnetosheath boundary layer. A portion of the solar wind particles get through the bow shock and are able to diffuse through the magnetopause as they flow along it. Particles flowing across the top and bottom of the magnetosphere must travel through the magnetotail's lobes before they reach the plasma sheet (Fig. 13). Particles flowing along the equatorial region of the magnetosphere, also known as the Low-Latitude Boundary Layer (LLBL), are able to diffuse through the magnetopause and enter the plasma sheet from the sides (Fig. 14) (Lundin et al., 1991). Once the solar wind plasma is inside the magnetosphere/tail system, it initially flows

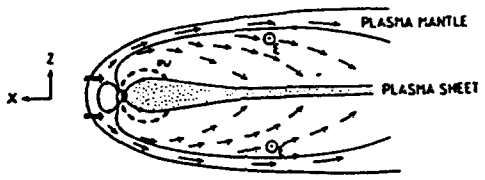

FIG. 13. Diagram showing access of solar wind particles through the northern and southern portions of the magnetosphere [Pilipp and Morfil, 1978, Cowley and Southwood, 1980].

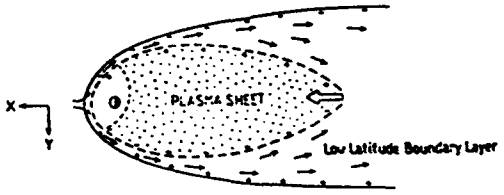

FIG. 14. Access through the LLBL [Heikkila, 1982, Eastman et al., 1985].

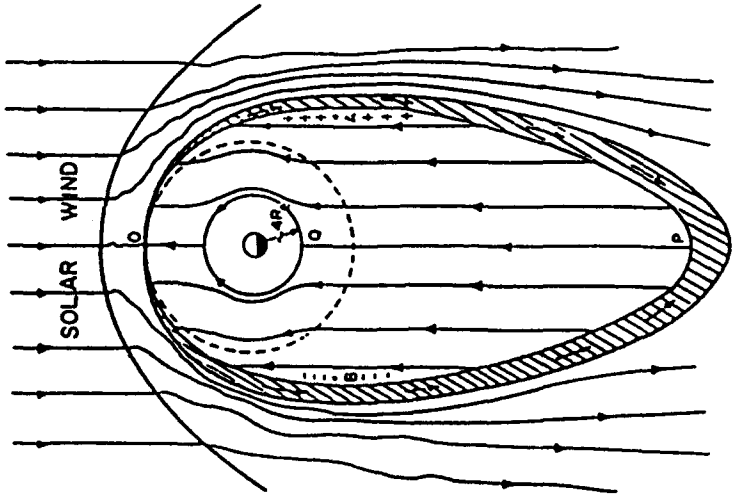

FIG. 15. Sketch of the equatorial section of the earth's magnetosphere looking from above the north pole showing idealized plasma flow [after Axford, 1964].

anti-sunward in the magnetosheath. Most of the plasma within the magnetosphere moves into the plasma sheet located in the equatorial region of the magnetotail. Once in the plasma sheet, the plasma flow is generally sunward (Fig. 15) from the earthward side of the magnetic field reconnection point (about 100 R_e). The plasma flow within the plasma sheet is due to either magnetic field line reconnections or the inward solar wind pressure on the earth's magnetic field.

As the plasma begins to flow earthward from the magnetic field reconnection site, several things happen to it. First, the plasma again experiences the Lorentz force $\vec{F} = q (\vec{v} \times \vec{B})$, which forces the positive ions to flow towards the dawnside of the magnetotail and the negative electrons to flow towards the duskside. The net effect of this action is to set up an electric field across the magnetotail which points from dawn to dusk (Fig. 16). Another way of looking at this is, since the plasma can be considered a collisionless medium, its motion sets up an electric field which satisfies the equation $\vec{E} = - \vec{v} \times \vec{B}$.

Since this plasma can be considered collisionless, it also experiences an $\vec{E} \times \vec{B}$ (electric field vector crossed with the magnetic field vector) drift (Hones, 1986). Near the earthward side of the reconnection site, the earth's magnetic field has a strong northerly component to it. As a result, the $\vec{E} \times \vec{B}$ drift directs the plasma towards the earth (Fig. 17). Midway between the reconnection site and the earth, the $\vec{E} \times \vec{B}$ drift forces the plasma towards the equatorial regions of the magnetotail due to the anti-parallel orientation of earth's magnetic fields at this point (Fig. 18). As a result of this action, the bulk of the magnetotail's plasma and energy is tied up within a relatively thin equatorial region called the central plasma sheet. This is where key processes such as energy storage and dissipation usually take place.

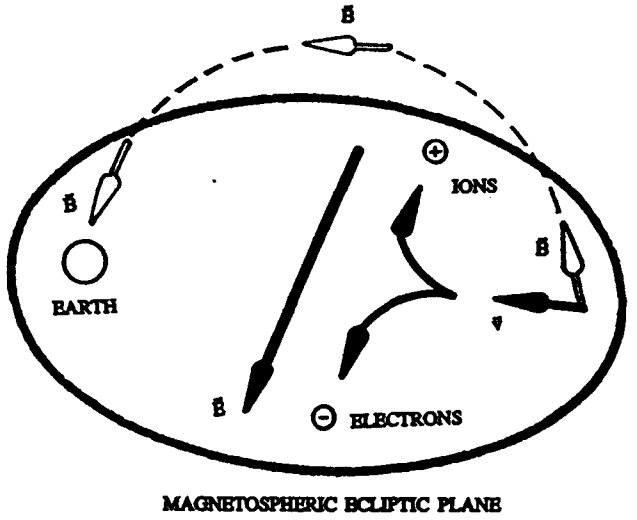

FIG. 16. Schematic showing the electric field set up as a result of the Lorentz force and $\vec{E} = -\vec{v} \times \vec{B}$.

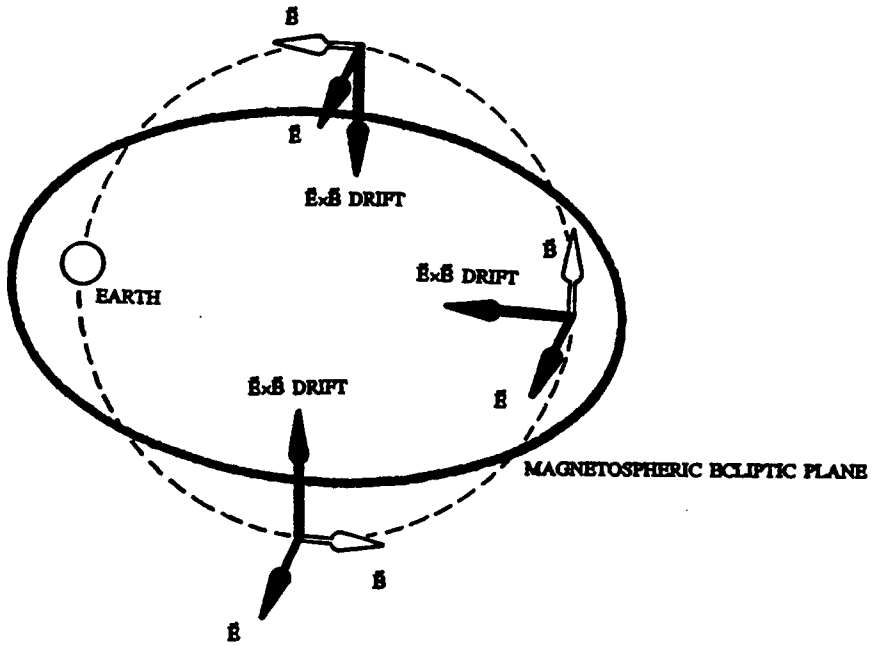

FIG. 17. Schematic showing the earthward $\vec{E} \times \vec{B}$ drift.

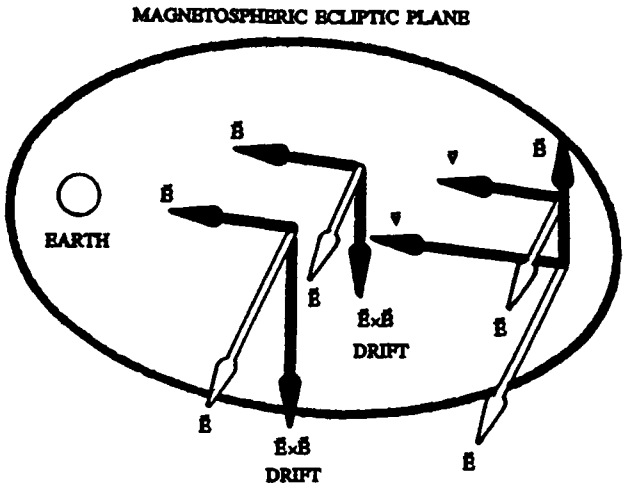

FIG. 18. Schematic showing the equatorial $\vec{E} \times \vec{B}$ drift.

Magnetotail Energy Storage and Dissipation Mechanisms

The solar wind/magnetospheric interaction basically converts the solar wind's kinetic energy into the electrical and magnetic energies observed within the magnetosphere/tail. The solar wind puts energy into the earth's magnetosphere/tail system at a approximate rate of 10^{19} ergs/sec (Lanzerotti and Krimigis, 1985). It appears that the earth's magnetospheric system has two models (Fig. 19) to describe the way it processes the energy it receives from the solar wind. One way is by direct dissipation of the solar wind energy into the earth's upper atmosphere where it manifests itself in the form of auroral storms (i.e. northern lights). This process is called the direct driven model and is depicted in Fig. 19(a) (Akasofu, 1987).

The other way the magnetospheric system handles the solar wind's energy is by storing it and releasing it periodically. This is called the driven reconnection model and is depicted in Fig. 19(b) (Akasofu, 1987). This model is analogous to a dripping faucet (Fig. 20) where "solar wind plasma seeps into the magnetosphere all along its boundary, accumulating in the tail until a

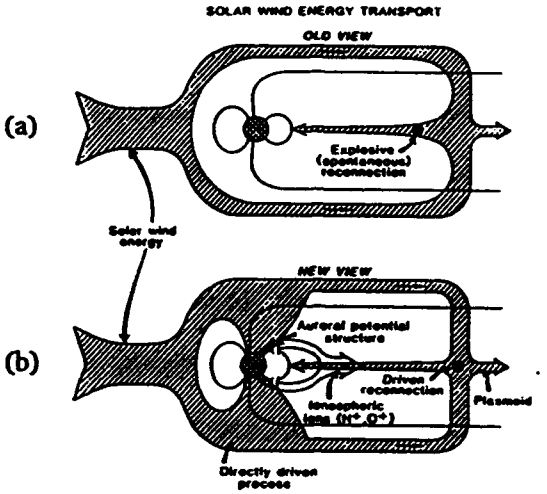

FIG. 19. (a) Schematic of how solar wind energy was thought to be transported to the earth. (b) Current view of how solar wind energy is thought to get to the earth [Akasofu, 1987].

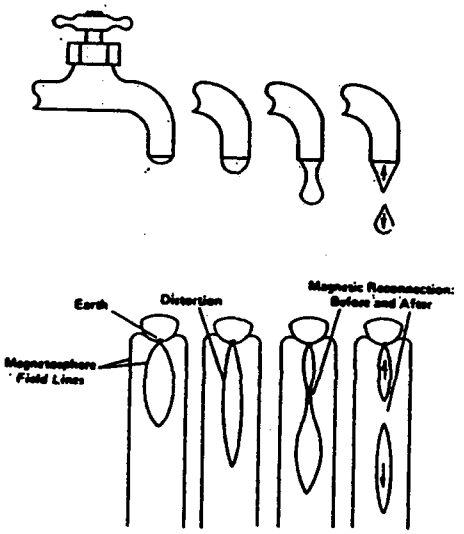

FIG. 20. Diagram showing how the magnetosphere's energy storing and release processes resemble a faucet drip [Gosling, 1984].

portion breaks off like a swollen drop of water from a faucet" (Gosling, 1984, p. 33). In this process, a portion of the stored energy is shed while another portion is directed towards the earth's poles. The shedding process has been directly observed in comets but not in the earth's magnetotail.

Most of the solar wind's energy, and particles, appears to be stored within the central plasma sheet of the magnetotail. Observations indicate, however, that plasma sheet energies are in the keV range while solar wind particles are only in the eV range. That means there must be some mechanism within the magnetotail which somehow accelerates the low energy solar wind particles to the higher plasma sheet energies observed. Magnetic field reconnection may be one possible mechanism. Scientists have predicted that when two anti-parallel field lines of the magnetotail lobes come into contact, they "explosively" cancel each other out with a resulting release of energy in the 5 kev range. This energy might be transformed into the high plasma kinetic energy observed within the central plasma sheet (Tascione, 1988).

Magnetotail Equilibrium/Steady State Condition

As it interacts with the solar wind, the magnetospheric/tail system appears to be trying to establish an equilibrium when it periodically releases some of its excess energy during magnetic storms. It seems possible that the magnetospheric/tail system may be trying to reach an equilibrium state having the lowest total energy. This is the assumption of this thesis and will be discussed in detail later.

In order to test this assumption, one needs to have measurements of the magnetotail while it is in a steady-state equilibrium condition. Unfortunately, due to the constant influx of energy from the solar wind, this condition rarely exists, but it may exist for some special cases. One case, as mentioned above, may exist for a brief period of time immediately after a magnetic storm when the magnetotail has released its excess energy. Another case may occur when the

earth's magnetic field is exposed to a large northerly component of the IMF for an extended period of time. When the IMF is pointing northward, the solar wind has minimal interactions with the earth's magnetic field. By looking at the specific parameters within the magnetotail system, one may be able to determine whether the system is in a minimum energy equilibrium state or not. This thesis explores this possibility.

Chapter II of this thesis explains a technique for finding the total minimum energy of a system not in thermodynamic equilibrium. This chapter discusses how the "Calculus of Variations" is used to determine which systems of equilibrium states are also minimum energy states.

Chapter III describes an idealized magnetotail model used in this research and discusses how the energy minimizing technique described in Chapter II is applied to it. Also, this chapter will explain what assumptions were used to create the idealized model and why.

Chapter IV addresses the computer program used to solve a series of differential equations which evolved from the calculus of variations technique. It also describes the model outputs and any associated graphs and plots.

Chapter V compares the model's results with real data from the actual earth's magnetotail. If the results approximate typical conditions observed in the magnetotail, then we will be able to say that we will have a working model for describing the earth's magnetotail energy state while it is in equilibrium. If, on the other hand, the model does not adequately simulate the magnetotail's energy state, then we will have eliminated one possible method for describing the earth's magnetotail energy structure.

Chapter VI draws conclusions based upon the results of this research and points out possible areas for further research.

Chapter II

MINIMUM TOTAL ENERGY

Systems in Thermodynamic Equilibrium

If a system is completely isolated from its surroundings, it is in thermodynamic equilibrium. Determining stable equilibria of systems in these states is done by minimizing the appropriate potential energy function for that thermodynamic equilibrium. Several potential energy functions and their specific uses are listed below (Adkins, 1968).

TABLE I. Potential Energy Functions.

Function	Description
Enthalpy	- can be used for determining the maximum amount of heat content available within a given system.
Helmholtz function	- can be used for determining the maximum amount of mechanical work which can be extracted from a given system.
Gibbs function	- can be used for determining the maximum amount of free energy available within a given system.

Therefore, in thermodynamic equilibria, minimizing a particular potential energy function yields a stable equilibrium state.

Systems Not in Thermodynamic Equilibrium

But what if the system does not remain in thermodynamic equilibrium. Such is the case where radiation is present (Pippard, 1957). We will assume that these equilibria have minimum total energy rather than minimum thermodynamic free energy (or potential energy). For such systems, we will attempt to find their stable equilibria by using calculus of variations to determine their minimum total energy states.

The first step prior to using this technique is to find an equation which adequately describes the energy of the system in question. The total energy, U, of our system, can be represented by adding up all of the applicable energy contributions, assuming that there are no dissipation and advection terms:

$$\begin{matrix}\text{Total}\\ \text{Energy}\\ \text{of a}\\ \text{System}\end{matrix}\ (U) = \begin{matrix}\text{Kinetic}\\ \text{Energy}\end{matrix} + \begin{matrix}\text{Magnetic}\\ \text{Field}\\ \text{Energy}\end{matrix} + \begin{matrix}\text{Electric}\\ \text{Field}\\ \text{Energy}\end{matrix} + \begin{matrix}\text{Kinetic}\\ \text{Pressure}\\ \text{Terms}\end{matrix}. \qquad (3)$$

The next step is to identify the constraining equations which apply to the problem. These include Maxwell's electrodynamic equations and equations of state for the plasmas in question.

The final step of this technique is to determine which functions appearing in the energy equations, Eq. (3), within the limits imposed by the constraint equations, yield a minimum total energy. These functions include variables such as magnetic fields, electric fields, particle densities, etc., which are dependent upon the independent space variables. One could randomly insert different functions for each of the dependent variables in Eq. (3), subject to the appropriate constraints, until the lowest possible value for U was reached. Unfortunately, this approach is very tedious and time consuming and would not guarantee, with any certainty, that

another combination of values may not generate an even lower value for U. It is due to this uncertainty that another technique must be used to find the lowest possible value for U, or minimum total energy. The technique uses the calculus of variations; it works as follows.

Calculus of Variations

Suppose, for example, we want to find the minimum total energy of a given system. Since the minimum total energy of a system is a special case of the system's total energy, we will look at the total energy first without restricting it to being a minimum. To illustrate this method, let us assume the total energy of the system can be represented as a function of two dependent variables, A and $B = \partial A/\partial z$, which are functions of one independent variable z. With this in mind, we can express the total energy of a given system as,

$$\underset{\text{ENERGY}}{\text{TOTAL}} (U) = \int_v f(A(z), B(z), z)\, dz . \tag{4}$$

In order to find the minimum total energy of the system, we must determine what functions A and B in Eq. (4) must be in order for U to achieve the lowest value possible. The trick is to discover, with some degree of certainty, what these functions are. Remember, the values of A and B may be constrained by one or more external equations as well as boundary conditions that may be imposed on the system. Therefore, in order to find A(z) and B(z), we must use the calculus of variations.

To use this technique we first assume that we know what the 'correct' values of A and B are, and express them as A_{min} and B_{min}. Substituting these new variables into Eq. (4) yields

$$\underset{\text{TOTAL ENERGY}}{\text{MINIMUM}}\ (U) = \int_V f(A_{min}(z), B_{min}(z), z)\, dz . \tag{5}$$

But how do we determine what the values of A_{min} and B_{min} are? To find out, we select some arbitrary functions, a(z) and b(z), multiply them by an infinitesimal dimensionless parameter α, and add them to A_{min} and B_{min} to generate two entirely new functions, A' and B'.

$$\begin{aligned} A'(z, \alpha) &= A_{min}(z, 0) + \alpha a(z); \\ B'(z, \alpha) &= B_{min}(z, 0) + \alpha b(z). \end{aligned} \tag{6}$$

One of the conditions of the calculus of variations is that all values of the 'correct' functions, A_{min} and B_{min}, must be the same as those of the new functions, A' and B', at the systems boundaries or endpoints. In this case, the endpoints are at the top, z_1, and bottom, z_2, of the system.

Rewriting Eq. (4) using the new functions A'(z,α) and B'(z,α) gives us the following expression,

$$\underset{\text{Energy}}{\text{Total}}\ U(\alpha) = \int_V f(A'(z, \alpha),\ B'(z, \alpha),\ z)\, dz . \tag{7}$$

By making αa and αb equal zero in Eq. (6), we see that A' and B' in Eq. (7) will have the same values as A_{min} and B_{min} in Eq. (5) and the system will be in a minimum total energy state.

We begin the process of minimizing by looking for cases where the derivative of U with

respect to α equals zero. Assuming $dU/d\alpha$ is a continuous function, the system will be in an equilibrium energy state when $dU/d\alpha$ equals zero.

$$\frac{\partial}{\partial \alpha} U(\alpha) = \int_V \left(\frac{\partial f}{\partial A'} \frac{\partial A'}{\partial \alpha} + \frac{\partial f}{\partial B'} \frac{\partial B'}{\partial \alpha} \right) dz = 0 . \tag{8}$$

Unfortunately, it is impossible to know for certain whether a particular equilibrium coincides with the system's minimum total energy state without doing any further tests. The reason for this is that a system may have many different equilibrium states (Fig. 21).

Another way to insure that an equilibrium state coincides with a system's minimum total energy is to take the limit of Eq. (7) as α goes to zero.

$$\begin{aligned} U_{min} &= \lim_{\alpha \to 0} U(\alpha) = \lim_{\alpha \to 0} \int_V f(A', B', z)\, dz ; \\ &= \lim_{\alpha \to 0} \int_V f(A_{min} + \alpha a, B_{min} + \alpha b, z)\, dz . \end{aligned} \tag{9}$$

We can see as α goes to zero, Eq. (9) begins to look like the minimum total energy equation (Eq. (5)). Therefore, in order to find the equilibrium state of a system which also coincides with its minimum total energy (U), we need to apply both the partial differentiation and limit to the energy equation at the same time as shown in Eq. (10) and Fig. 22.

$$\lim_{\alpha \to 0} \left[\frac{\partial}{\partial \alpha} U(\alpha) \right] = 0 . \tag{10}$$

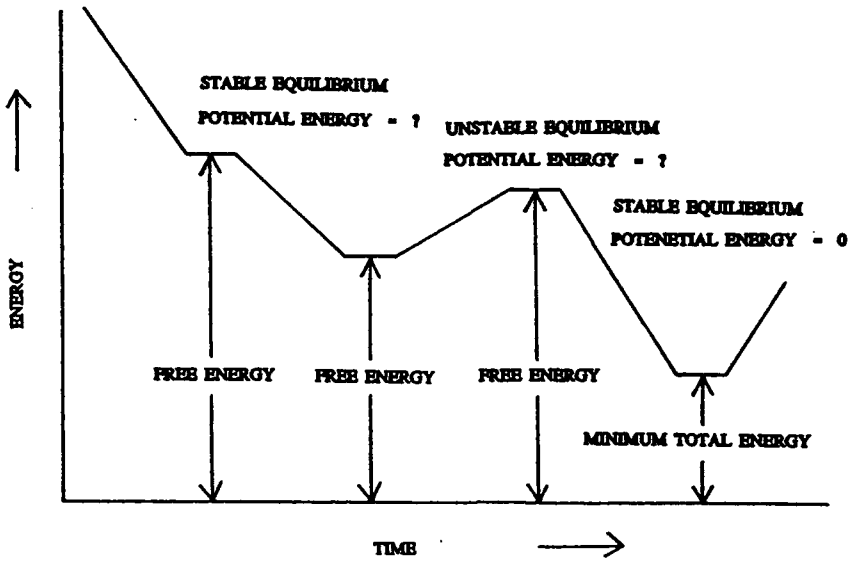

FIG. 21. Diagram showing that a system can have many equilibrium states (stable and unstable).

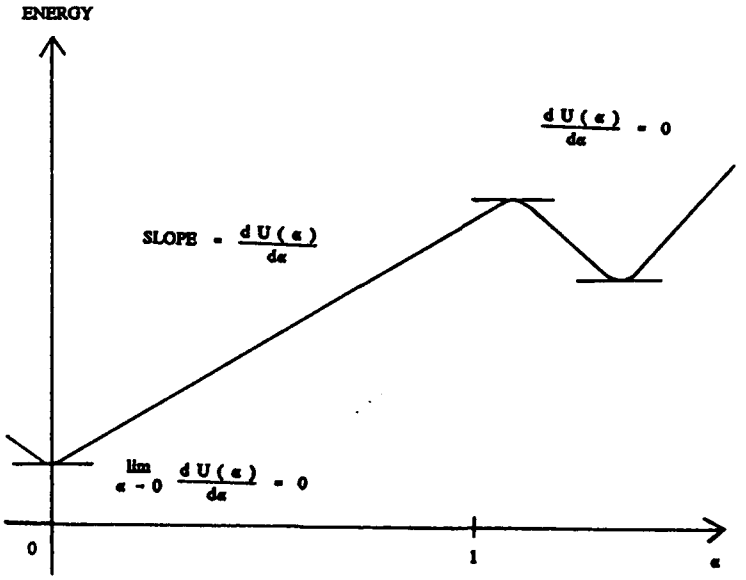

FIG. 22. Since the value for $U(\alpha > 0)$ will always be greater than $U(\alpha = 0)$, we can be assured that we will find the equilibrium condition with the least possible energy when α goes to zero.

Equation (10) must hold independent of the choice of functions a and b in Eq. (9) because as α goes to zero, A' and B' take on the values of A_{min} and B_{min}. By taking the limit as α goes to zero, however, we eliminate the values of the arbitrary functions, a and b, so how can we vary them so that we are left only with $A' = A_{min}$ and $B' = B_{min}$? The answer is to use integration by parts (Goldstein, 1980).

Integration by parts allows one to factor the arbitrary functions, a and b, out of Eq. (6) and leave only a differential equation within the integral based on the values A' and B'. Because $B' = \partial A'/\partial z$, the second integral of Eq. (8) is

$$\int_V \left(\frac{\partial f}{\partial B'} \frac{\partial B'}{\partial \alpha} \right) dz = \int_{z_1}^{z_2} \left(\frac{\partial f}{\partial B'} \frac{\partial^2 A'}{\partial z \partial \alpha} \right) dz ;$$

now we integrate by parts

$$\int_{z_1}^{z_2} \left(\frac{\partial f}{\partial B'} \frac{\partial^2 B'}{\partial z \partial \alpha} \right) dz = \frac{\partial f}{\partial B'} \frac{\partial A'}{\partial \alpha} \Big|_{z_1}^{z_2} - \int_{z_1}^{z_2} \frac{d}{dz} \left(\frac{\partial f}{\partial B'} \right) \frac{\partial A'}{\partial \alpha} dz . \qquad (11)$$

Since the correct and arbitrary functions must be equal at the system's endpoints/boundaries, z_1 and z_2, the partial derivative of A' with respect to α in the first part of Eq. (11) will disappear, leaving us with

$$\int_V \left(\frac{\partial f}{\partial B'} \frac{\partial B'}{\partial \alpha} \right) dz = - \int_{z_1}^{z_2} \frac{d}{dz} \left(\frac{\partial f}{\partial B'} \right) \frac{\partial A'}{\partial \alpha} dz . \qquad (12)$$

Therefore,

$$\frac{\partial}{\partial \alpha} U(\alpha) = \int_V \left(\frac{\partial f}{\partial A'} \frac{\partial A'}{\partial \alpha} - \frac{d}{dz} \frac{\partial f}{\partial B'} \frac{\partial A'}{\partial \alpha} \right) dz ,$$

$$= \int_V \left(\left(\frac{\partial f}{\partial A'} - \frac{d}{dz} \frac{\partial f}{\partial B'} \right) \left(\frac{\partial A'}{\partial \alpha} \right) \right) dz ,$$

or,

$$\frac{\partial}{\partial \alpha} U(\alpha) = \int_{z_1}^{z_2} \left(\left(F(z) \right) \left(\frac{\partial A'}{\partial \alpha} \right) \right) dz , \tag{13}$$

where,

$$F(z) = \frac{\partial f}{\partial A'} - \frac{d}{dz} \frac{\partial f}{\partial B'} . \tag{14}$$

We now have an expression F(z) that is written in terms of A' and B' only. Since the partial derivative of A with respect to α can be any arbitrary value, F(z) must be equal to zero in order to satisfy the condition we made in Eq. (8). Therefore, by solving the differential equation F(z) = 0 for A' and B', we are able to calculate the minimum total energy of the system. F(z) = 0 in Eq. (14) is called the Euler-Lagrange equation. This thesis will apply this method to an idealized model of the earth's magnetotail and compare the results with real data of the earth's actual magnetotail.

Chapter III

MAGNETOTAIL MODEL

Model Description

The model we use in this thesis to calculate the minimum total energy of the plasma sheet within the earth's magnetotail is depicted as a rectangular slab (Fig. 23) of infinite length and width and a finite height, h. The axes of this model magnetotail are defined by a right-handed Cartesian system where the positive x-axis, which represents the length of the slab, points towards the sun. The y-axis, which represents the width of the slab, is directed perpendicular to the x-axis in the duskward direction. Finally, the z-axis, which represents the height of the slab, points northward, perpendicular to both the x and y axis.

By using some key assumptions and applying an appropriate set of equilibrium equations to this magnetotail model, we should be able to calculate its minimum total energy. Comparing the results of the model's calculations to certain parameters observed in the plasma sheet of

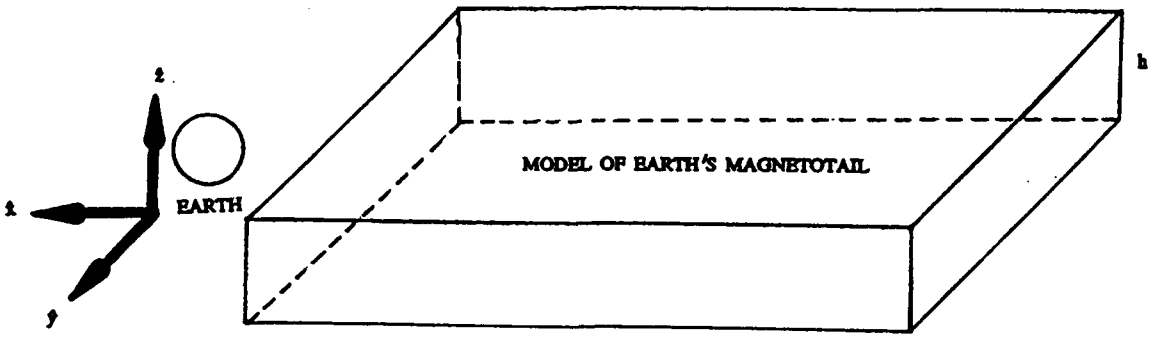

FIG. 23. Drawing showing the layout of the magnetotail model.

the earth's magnetotail during quiet (steady state) conditions will help determine the validity of this model.

As mentioned above, several assumptions are used in the model to keep it within the scope of this thesis. The assumptions used in the model are as follows:

a) System is in a steady-state condition ($d/dt = 0$).

b) System is in equilibrium.

c) Particle number densities, ions (n_1), and electrons (n_2) vary in the z direction only. In other words, the particle number densities remain constant within the x-y planes.

d) Ion velocities are restricted to the x-y plane to keep previous assumption true.

e) Only one species of particles (ions or electrons) moves, the other remains stationary, only ions possess velocity. This assumption is used to simplify calculations within this thesis.

f) The x and y components of the electric field equal zero ($E_x = E_y = 0$). Only the z component of the electric field has a value which varies only in the z direction ($E_z(z) = \text{value}$). Without this assumption, the ions, within the model, would experience a continuous acceleration within the infinite x-y planes due to a changing electric field. This condition would eventually cause the ions to reach an infinite velocity, an unrealistic situation.

g) The y and z components of the magnetic field equal zero ($B_y = B_z = 0$). Only the x component of the magnetic field has any value and this value varies only in the z direction ($B_x(z) = \text{value}$). The y and z components of the magnetic field are assumed to be zero because the model is approximating the center of the earth's magnetotail near the midnight sector. In this region of the earth's magnetotail, the magnetic field lines are very nearly parallel to the x axis with negligible y and z components.

h) Polarization and magnetization of the plasma are assumed to be negligible ($M = 0$, $P = 0$).

i) The plasma within the magnetotail model is fully ionized.

By using these simplifying assumptions, we are left with a very simple or zero order model which may not include all the necessary details to adequately describe the process observed within the central plasma sheet of the earth's magnetotail.

Magnetotail Model's Total Energy Equation

As stated in Chapter II, we must develop a total energy equation to describe the model system above which is not in thermodynamic equilibrium. To do this, we must determine what energy terms we want the total energy equation to have. Since we are attempting to model a region where electric and magnetic fields are prevalent, it seems logical that the total energy equation should contain terms describing the energy changes associated with these fields. We also need a kinetic energy term and an energy term that account for moving plasma particles (ions or electrons) and kinetic pressures found within the earth's magnetotail. Therefore, we want to develop a total energy equation for the model system that has the following form:

$$\text{Total Energy} = \int_V \left(\begin{array}{c}\text{E Field}\\ \text{Energy}\\ \text{Per}\\ \text{Unit}\\ \text{Vol}\end{array} + \begin{array}{c}\text{B Field}\\ \text{Energy}\\ \text{Per}\\ \text{Unit}\\ \text{Vol}\end{array} + \begin{array}{c}\text{Kinetic}\\ \text{Energy}\\ \text{Per}\\ \text{Unit}\\ \text{Vol}\end{array} + \begin{array}{c}\text{Energies}\\ \text{Associated}\\ \text{with}\\ \text{Kinetic}\\ \text{Pressure}\end{array} \right) \partial\tau \, .$$

Now we need an expression for each term in the total energy equation shown above. We can get expressions for the electric and magnetic field energies by combining Poynting's theorem with Maxwell's equations which results in the expression shown in Eq. (15).

$$\begin{array}{ccccccc} \text{Energy Change Per Unit Time} & = & \text{Electric/ Magnetic Field Strength Change Per Unit Time} & + & \text{Power Per Unit Vol} & + & \text{Energy Advection Per Unit Vol} \end{array}$$

$$\frac{d(U)}{dt} = \frac{\partial}{\partial t}\int_V \left(\frac{\epsilon_0 E^2}{2} + \frac{B^2}{2\mu_0}\right)\partial\tau + \int_V (\vec{J}\cdot\vec{E})\,\partial\tau + \oint_S \left(\frac{\vec{E}\times\vec{B}}{\mu_0}\right)\partial a\,, \tag{15}$$

where,

U = Total Energy of a System;
$\vec{E}$ = Electric Field;
$\vec{B}$ = Magnetic Field;
$\vec{J}$ = Electric Current;
ϵ_0 = Permittivity of Free Space;
μ_0 = Permeability of Free Space;
τ = Unit Volume;
a = Unit Area.

It is standard practice to define the $\epsilon_0 E^2/2$ and $B^2/2\mu_0$ terms in Eq. (15) as electric and magnetic field energy densities, respectively. These can be used in the total energy equation. We can also rewrite the energy advection term in Eq. (15) in terms of kinetic energy. Substituting these expressions into the total energy equation yields:

$$\begin{array}{ccccccccc} \text{Total Energy} & = & \int_V (& \text{E Field Energy Per Unit Vol} & + & \text{B Field Energy Per Unit Vol} & + & \text{Kinetic Energy Per Unit Vol} & + & \text{Energies Associated with Kinetic Pressure} &)\,\partial\tau\,, \end{array}$$

$$U = \int_V \left(\frac{\epsilon_0 E^2}{2} + \frac{B^2}{2\mu_0} + \frac{nmqv^2}{2} + Cn^{\gamma}\right)\partial\tau\,, \tag{16}$$

where,

n = Particle Number Density;
n_1 = Ions;
n_2 = Electrons;
m = Particle Mass;
q = Particle (Ion/Electron) Velocity;
C = Adiabatic Constant;
γ = Ratio of Specific Heats.

The last term of the total energy equation, Cn^{γ}, which accounts for the kinetic pressure found within the earth's magnetotail system, is derived from the Perfect Gas Law.

$$PV = \left(\frac{m}{N_A}\right)(R)(T) = (n)(k)(T);$$

or

$$P = \left(\frac{m}{V}\right)\left(\frac{R}{N_A}\right)(T);$$

$$P = (n)\ (k)\ (T);$$

where,

P = Pressure;
V = Volume;
R = Universal Gas Constant;
N_A = Avogadro's Number;
T = Temperature (in degrees Kelvin);
n = Number Density;
k = Boltzmann's Constant.

Assuming we have adiabatic conditions, we can say that the internal energy of a system is equal to the energy extracted from the system by the performance of work (First Law of

Thermodynamics).

$$\Delta u = -w .$$

However, the internal energy change for any process for an ideal gas can be rewritten as,

$$\Delta u = n C_v \Delta T ,$$

where C_v is the heat capacity of a system at a constant volume. In addition, the variable representing the performance of work can be rewritten as,

$$w = P \Delta V ,$$

where we assume that the pressure P remains approximately constant, for a very small change in volume δV. Substituting these new expressions into the thermodynamic equation yields:

$$n C_v \Delta T = -P \Delta V .$$

Now we want to write the above equation in terms of temperature and volume only. To do this we begin with the following form of the perfect gas law,

$$P = \frac{n R T}{V},$$

and substitute it into the rewritten thermodynamic equation yielding:

$$n C_V \Delta T = -\left(\frac{n R T}{V}\right) \Delta V;$$

$$\frac{\Delta T}{T} = -\left(\frac{R}{C_V}\right) \frac{\Delta V}{V} = -\left(\frac{C_P - C_V}{C_V}\right) \frac{\Delta V}{V} = -(\gamma - 1) \frac{\Delta V}{V}.$$

Integrating the above expression yields:

$$(T)(V)^{\gamma-1} = \text{Constant};$$

$$\left(\frac{P V}{n R}\right)(V)^{\gamma-1} = \text{Constant};$$

$$(P V)(V)^{\gamma-1} = \text{Constant}\,(n R);$$

$$(P)(V)^{\gamma} = \text{Constant};$$

but,

$$V = \left(\frac{R}{N_A}\right) \frac{(m)(T)}{(P)};$$

$$= (k) \frac{(1)\left(\frac{P}{n k}\right)}{(P)};$$

$$= (n)^{-1};$$

therefore,

$$
\begin{aligned}
P\,(V)^{\gamma} &= \text{Constant}: \\
P\,((n)^{-1})^{\gamma} &= \text{Constant}; \\
P\,(n)^{-\gamma} &= \text{Constant}; \\
P &= \text{Constant}\,(n)^{\gamma} = Cn^{\gamma}.
\end{aligned}
$$

For computing purposes, it is easier to deal with dimensionless equations than those with dimensions. In order to make Eq. (16) dimensionless, we redefine the dependent variables in such a way that each energy term becomes dimensionless. This has the same effect as setting

$$
\begin{aligned}
m &= 1; \\
q &= 1; \\
\epsilon_0 &= 1; \\
\mu_0 &= 1.
\end{aligned}
$$

which gives us the following equation,

$$
U = \int_V \left(\frac{E^2}{2} + \frac{B^2}{2} + \frac{nv^2}{2} + Cn^{\gamma} \right) d\tau . \tag{17}
$$

It is important to note here that the dependent variables in Eq. (17) are dimensionless and are not the same as the dimensioned variables shown in Eq. (16). It will be shown later in this thesis that by multiplying the dimensionless variables in Eq. (17) by an appropriate scaling quantity, we can end up with the dimensioned variables shown in Eq. (16). Therefore, unless specified, the dependent variables presented in this paper are dimensionless.

In order to account for the two different particle species, ions (n_1), and electrons (n_2), we must apply some of the assumptions discussed earlier in this chapter to Eq. (17). They are as follows:

$$\begin{aligned} E_x &= E_y = 0, && \text{(E Fld only has a z component);} \\ B_y &= B_z = 0, && \text{(B Fld only has an x component);} \\ v_z &= 0, && \text{(No vertical velocities);} \\ n_2 v_x &= 0, && \text{(Electron velocities are zero).} \end{aligned}$$

Applying these assumptions to Eq. (17) yields:

$$U = \int_V \left(\frac{E_z^2}{2} + \frac{B_x^2}{2} + \frac{n_1 v_x^2}{2} + \frac{n_1 v_y^2}{2} + C_1 n_1^{\gamma} + C_2 n_2^{\gamma} \right) \partial\tau \, . \qquad (18)$$

Rewriting Eq. (18) in an expanded form gives us Eq. (19). This new equation represents the total energy, U, of the model magnetotail system described earlier in this chapter. For the remainder of this thesis, Eq. (19) will be referred to as the total energy equation.

$$U = \int_0^h \int_{-\infty}^{+\infty} \int_{-\infty}^{+\infty} \left(\frac{E_z^2}{2} + \frac{B_x^2}{2} + \frac{n_1 v_x^2}{2} + \frac{n_1 v_y^2}{2} + C_1 n_1^{\gamma} + C_2 n_2^{\gamma} \right) \partial x \partial y \partial z \, . \qquad (19)$$

In order to come up with the lowest possible value for the total energy, U, of the model system, we must first find the minimum values of each of the terms in Eq. (19). Of course one way to do this would be to arbitrarily set each term in Eq. (19) to zero and make the total energy, U, of the system equal to zero, but this would depict a very unrealistic situation in the

real world.

Since we are looking for a minimum total energy of a system in equilibrium, the variables within Eq. (19) must be governed by one or more equilibrium equations. These equilibrium equations, in turn, will be constrained to some degree by conditions outside the system. Therefore, a proper set of boundary conditions must be defined along with the appropriate set of equilibrium equations. By having the appropriate set of equilibrium equations and boundary conditions, we will be able to define a range of values (Appendix C) for each term in Eq. (19).

Equilibrium Solutions

Maxwell's Equilibrium Equations

The equilibrium equations derived from Maxwell's equations are used to govern/restrict the electric and magnetic fields defined within the model system. The first of these equilibrium equations is Gauss' Law of Electric Charge and is expressed as

$$\nabla \cdot \vec{E} = \frac{\partial E_x}{\partial x} + \frac{\partial E_y}{\partial y} + \frac{\partial E_z}{\partial z} = \frac{\rho_{total}}{\epsilon_0} . \qquad (20)$$

We know the total charge density in Eq. (20) can be written as

$$\rho_{total} = \frac{m}{vol} = \frac{(+q)(n_1) + (-q)(n_2)}{vol} = q\,\frac{n_1 - n_2}{vol} . \qquad (21)$$

Therefore, by substituting Eq. (21) into Eq. (20) and applying the following assumptions,

$$E_x = E_y = 0 ;$$

we end up with the following expression:

$$\frac{\partial E_z}{\partial z} = n_1 + n_2 . \tag{22}$$

Eq. (22) provides us with the first equilibrium equation derived from Maxwell's equations which governs the model magnetotail's electric field and particle number densities.

The second equilibrium equation derived from Maxwell's equations is Faraday's Law of Induction and is expressed as

$$\begin{aligned} \nabla \times \vec{E} &= -\frac{\partial \vec{B}}{\partial t} ; \\ &= \left(\frac{\partial E_z}{\partial y} - \frac{\partial E_y}{\partial z} \right) \hat{x} \\ &\quad + \left(\frac{\partial E_x}{\partial z} - \frac{\partial E_z}{\partial x} \right) \hat{y} \\ &\quad + \left(\frac{\partial E_y}{\partial x} - \frac{\partial E_x}{\partial y} \right) \hat{z} . \end{aligned} \tag{23}$$

Using the assumption that the z component of the electric field only varies in the z direction ($E_z(z)$) and that the model system is in a steady state, we can see that Eq. (23) reduces to

$$\nabla \times \vec{E} = 0 . \tag{24}$$

The third equilibrium equation derived from Maxwell's equations is Gauss' Law of Magnetism and is expressed as

$$\nabla \cdot \vec{B} = \frac{\partial B_x}{\partial x} + \frac{\partial B_y}{\partial y} + \frac{\partial B_z}{\partial z} = 0 , \tag{25}$$

which is covered by the assumptions previously mentioned. This equilibrium equation states that magnetic field lines do not start or stop in space.

The final equilibrium equation derived from Maxwell's equations is Ampere's Law and is expressed as

$$\begin{aligned} \nabla \times \vec{B} &= \left(\frac{\partial B_z}{\partial y} - \frac{\partial B_y}{\partial z} \right) \hat{x} + \left(\frac{\partial B_x}{\partial z} - \frac{\partial B_z}{\partial x} \right) \hat{y} + \left(\frac{\partial B_y}{\partial x} - \frac{\partial B_x}{\partial y} \right) \hat{z} ; \\ &= \mu_0 \left(\vec{J} + \nabla \times \vec{M} + \epsilon_0 \frac{\partial \vec{E}}{\partial t} + \frac{\partial \vec{P}}{\partial t} \right) . \end{aligned} \tag{26}$$

Using the assumptions that the y and z components of the magnetic field equal zero ($B_y = B_z = 0$), the x component of the magnetic field varies in the z direction only ($B_x(z)$), the polarization and magnetization aspects of the electric and magnetic currents equal zero ($\vec{M} = \vec{P} = 0$), the permittivity of free space is dimensionless ($\mu_0 = 1$), and the system is in steady state ($d/dt = 0$), we can rewrite Eq. (26) as

$$\hat{y}\left(\frac{\partial B_x}{\partial z}\right) = J_t = (\rho)(\vec{v}) = (n_1 - n_2)(v_x\hat{x} + v_y\hat{y} + v_z\hat{z}). \qquad (27)$$

At this point, we use one of the model's assumptions that electrons (n_2) have no velocity. Normally when considering velocities due to $\vec{E} \times \vec{B}$ drifts, both the ions and electrons within a plasma drift. However, results from other works attempting to model the Venus flux ropes indicate that models, such as the one presented in this paper, may work better by keeping one of the species of particles stationary (private conversation with Dr. Edwards). With this in mind, combining like unit vector terms in Eq. (27) yields

$$\frac{\partial B_x}{\partial z} = n_1 v_y . \qquad (28)$$

This expression provides us with the second useful equilibrium equation derived from Maxwell's equations. This equation governs the model's magnetic field and ion velocities (or kinetic energies).

In summary, the equilibrium equations derived from Maxwell's equations are shown below.

$$\begin{aligned} \nabla \cdot \vec{E} &= \frac{\partial E_z}{\partial z} = n_1 - n_2 ; \\ \nabla \times \vec{E} &= 0 ; \\ \nabla \cdot \vec{B} &= 0 ; \\ \nabla \times \vec{B} &= \frac{\partial B_x}{\partial z} = n_1 v_y . \end{aligned} \qquad (29)$$

Kinetic/Force Equilibrium Equations

The equilibrium equations derived from the force equation are used to govern/restrict the kinetic energies and number densities of the particles contained within the model magnetotail. The force equation is expressed as follows:

$$\vec{F} = m\,\vec{a}\,. \tag{30}$$

However, since we are dealing with a specific volume, we need to express the force in Eq. (30) as a force per volume (Eq. (31)).

$$\frac{\vec{F}}{vol} = \frac{m}{vol}\,\vec{a}\,. \tag{31}$$

Rewriting Eq. (31) so that $\vec{f}$ represents the force per volume and ρ_m represents the mass per volume, we get

$$\vec{f} = \rho_m\,\vec{a}\,. \tag{32}$$

However, we also know

$$\vec{f} = \text{Lorentz Force} + \text{Pressure Gradient Force}$$

$$\vec{f} = \rho_m\,(\vec{E} + \vec{v} \times \vec{B}) - \nabla\vec{P}\,; \tag{33}$$

and,

$$\rho_m = \frac{m}{vol} = \frac{(+q)(n_1) + (-q)(n_2)}{vol} = N = \begin{matrix}\text{Total number}\\ \text{of particles}\\ \text{per unit vol}\end{matrix}, \tag{34}$$

and the acceleration is given by the convective derivative,

$$\vec{a} = \left(\frac{\partial \vec{v}}{\partial t} + (\vec{v} \cdot \nabla)\vec{v}\right). \tag{35}$$

Applying Eqs. (33, 34, and 35) to Eq. (32) yields the following equation(s).

$$\vec{f} = (\rho_m)(\vec{a});$$

$$(\rho_m)(\vec{E} + \vec{v} \times \vec{B}) - (\nabla \vec{P}) = (N)\left(\frac{\partial \vec{v}}{\partial t} + (\vec{v} \cdot \nabla)\vec{v}\right). \tag{36}$$

But according to Eq. (34), ρ_m=N, therefore Eq. (36) can be written as

$$(N)(\vec{E} + \vec{v} \times \vec{B}) - (\nabla \vec{P}) = (N)\left(\frac{\partial \vec{v}}{\partial t} + (\vec{v} \cdot \nabla)\vec{v}\right). \tag{37}$$

Applying the Perfect Gas Law ($P = nkT = Cn^{\gamma}$) to the pressure gradient force in Eq. (37) yields

$$(N)(\vec{E} + \vec{v} \times \vec{B}) - (C\gamma (N)^{\gamma-1} \nabla (N)) = (N)(\frac{\partial \vec{v}}{\partial t} + (\vec{v} \cdot \nabla)\vec{v}) . \quad (38)$$

Dividing both sides by the total number density (N) yields

$$(\vec{E} + \vec{v} \times \vec{B}) - (C\gamma (N)^{\gamma-2} \nabla (N)) = (\frac{\partial \vec{v}}{\partial t} + (\vec{v} \cdot \nabla)\vec{v}) . \quad (39)$$

Using the assumption that the electric field has only one component z, which varies only in the z direction, we can say

$$\vec{E} = (E_z)\hat{z} . \quad (40)$$

Since we have also assumed the y and z components of the magnetic field equal zero ($B_y = B_z = 0$) and the x component varies only in the z direction ($B_x(z)$), we get the following equation(s):

$$\begin{aligned} \vec{v} \times \vec{B} &= (v_y B_z - v_z B_y)\hat{x} \\ &\quad + (v_z B_x - v_x B_z)\hat{y} \\ &\quad + (v_x B_y - v_y B_x)\hat{z} ; \\ &= (-v_y B_x)\hat{z} . \end{aligned} \quad (41)$$

Since the pressure gradient force only varies in the z direction in this model, we get

$$(C\gamma (N)^{\gamma-2} \nabla (N)) = (C\gamma (N)^{\gamma-2} \frac{\partial (N)}{\partial z}) \hat{z} . \quad (42)$$

Looking at the right-hand side of Eq. (42) only, we can derive the following expression

$$(\frac{\partial \vec{v}}{\partial t} + (\vec{v} \cdot \nabla) \vec{v}) = (0 + (\vec{v} \cdot \nabla) \vec{v}) = 0 . \quad (43)$$

Combining Eqs. (39, 40, 41, and 42) into Eq. (38) yields

$$(E_z) \hat{z} - (v_y B_x) \hat{z} - (C\gamma (N)^{\gamma-2} \frac{\partial (N)}{\partial z}) \hat{z} = 0 . \quad (44)$$

Rewriting Eq. (44) so that the change of number density with height is on the left side of the equation, we are left with the following scalar expression:

$$\frac{\partial (N)}{\partial z} = (\frac{1}{C\gamma} (N)^{2-\gamma}) (E_z - v_y B_x) . \quad (45)$$

Since the values for the ion or electron number density are (transforming to dimensionless variables)

$$\begin{aligned} N_{Ions} &\rightarrow (+q)(n_1) = (+1)(n_1); \\ N_{Electrons} &\rightarrow (-q)(n_2) = (-1)(n_2); \end{aligned} \tag{46}$$

they can be substituted into Eq. (45), giving us an expression for the change of the ion number density across the magnetotail from the southern to the northern boundaries.

$$\frac{\partial (n_1)}{\partial z} = +\left(\frac{1}{C\gamma}(n_1)^{2-\gamma}\right)(E_z - v_y B_x). \tag{47}$$

Note that we have assumed the electron velocities are zero. Using the same steps described above, we can derive an expression for the change of the electron number density across the tail.

$$\frac{\partial (n_2)}{\partial z} = -\left(\frac{1}{C\gamma}(n_2)^{2-\gamma}\right)(E_z). \tag{48}$$

Therefore, we have a set of equilibrium equations (Eqs. (47) and (48)), derived from the force equation, which governs the change of ion and electron number densities across the tail for the model magnetotail. Summarizing, the force equilibrium equations are

$$\begin{aligned} \frac{\partial (n_1)}{\partial z} &= +\left(\frac{1}{C\gamma}(n_1)^{2-\gamma}\right)(E_z - v_y B_x); \\ \frac{\partial (n_2)}{\partial z} &= -\left(\frac{1}{C\gamma}(n_2)^{2-\gamma}\right)(E_z). \end{aligned} \tag{49}$$

At this point, we have a set of equilibrium equations which constrain the values of the terms within the total energy equation (Eq. (19)). We must now specify the boundary conditions. Additionally, we must add another condition which will prevent the particles (ions and electrons) contained within the model system from arbitrarily changing species. These conditions are discussed below.

Boundary Conditions

Equilibrium equations alone will not restrict the value range for each of the terms in the total energy equation (Eq. (19)). Their values face restrictions on the boundaries of the model system. Since the model system only has boundaries on the top and bottom, boundary conditions will only be applicable at these locations.

Number Density Boundary Conditions

For this model, it is assumed that charged particle density (ion or electron) outside the system is negligible compared to the number densities inside. Therefore, we can see that the particle number density inside the model must approach zero as one gets closer to the top or bottom boundaries of the model system. We must have a set of boundary conditions which depict this situation. Because boundary conditions on n_1 and n_2 are not specified, we must establish boundary conditions on the corresponding Lagrangian multipliers, which will be introduced and discussed later. These particular conditions are:

$$\begin{aligned} \lambda_1(0) &= 0; & \lambda_1(h) &= 0; \\ \lambda_2(0) &= 0; & \lambda_2(h) &= 0. \end{aligned} \tag{50}$$

Electric Field Boundary Conditions

Unlike the charged particle number densities, the model assumes there is no electric field outside the model system. This means that the electric field must equal zero at the boundaries of the system, which happens to be the top and bottom planes of the model system. The boundary conditions which restrict the equilibrium equations governing the model's electric field are depicted below.

$$E_z(0) = 0; \qquad E_z(h) = 0. \tag{51}$$

Magnetic Field Boundary Conditions

Unlike the charged particle number densities and the electric field, the model does assume a substantial magnetic field does exist outside the model system. Therefore, the magnetic field strength just inside the model's boundaries must equal whatever magnetic field strength lies just outside the boundary. The boundary conditions which depict this situation within the model are as follows:

$$B_x(0) = 0; \qquad B_x(h) = +B_{x_0}. \tag{52}$$

Particle Conservation Equations

These equations are used to ensure the number density of the individual species (ions and electrons) contained within the model magnetotail remains conserved. So far, we have had Maxwell's equations, which only guarantee that the sum total of the charged particles within the model system will remain conserved (Eq. (22)). In other words, a charged particle (proton or

electron) will not suddenly appear/disappear within the model system without advection. These equations ensure that individual particles within the model do not suddenly change species, that is, a proton becomes an electron or vice versa. Before we derive these particular conservation equations, we need to define the following variables.

$\overline{Q}$ = Total Flux of Charge Particles through the Surface of a Volume.
n_0 = Average Number of Charged Particles per Unit Volume.
$d\tau$ = Unit Volume.
da = Unit Surface Area.
l = Length of Model Volume.
w = Width of Model Volume.
h = Height of Model Volume.

We want to get an expression that shows the total sum of a particular particle (ion (n_1) or electron (n_2)) over a given volume is equal to the average number density (n_0) multiplied by the dimensions of the volume. These expressions are shown in Eqs. (53 and 54).

$$\int_V (n_1) \, d\tau = \int_V (n_0) \, d\tau = (n_0) \, h \, l \, w , \tag{53}$$

or,

$$\int_V (n_2) \, d\tau = \int_V (n_0) \, d\tau = (n_0) \, h \, l \, w . \tag{54}$$

Taking Eq. (53), let us arbitrarily state

$$n_1 = \frac{dQ}{dz} , \tag{55}$$

where Q is a variable defined by this equation and does not necessarily have any other physical meaning. Rewriting Eq. (53) in terms of Q gives us the following:

$$\begin{aligned}
\int_V (n_1) \, d\tau &= \int_V \left(\frac{dQ}{dz} \right) d\tau \, ; \\
&= \int_0^h \left(\frac{dQ}{dz} \right) l \, w \, dz \, : \\
&= l \, w \int_0^h (dQ) \, ; \\
&= l \, w \, [Q \,]_0^h \, ; \\
\therefore \int_V (n_1) \, d\tau &= l \, w \, [Q (h) - Q (0)] \, . \qquad (56)
\end{aligned}$$

Substituting Eq. (53) into Eq. (56) gives us the following:

$$\begin{aligned}
(n_0) \, h \, l \, w &= l \, w \, [Q (h) - Q (0)] \, ; \\
(n_0) \, h &= Q (h) - Q (0) \, . \qquad (57)
\end{aligned}$$

Assuming Q(h) and Q(0) have the same magnitudes, they must have the following values

$$\begin{aligned}
Q_z (h) &= + \frac{n_0 h}{2} \, ; \\
Q_z (0) &= 0 \, . \qquad (58)
\end{aligned}$$

The equations above, when used in conjunction with the other equilibrium equations, ensure that the particles contained within the model system do not suddenly change species.

Minimizing Model's Total Energy Equation

We now have a set of differential equations, derived from the appropriate equilibrium equations, which govern the values of each term within the total energy equation (Eq. (19)). In order to find which values establish a minimum total energy of the model system, we must solve these differential equations using the calculus of variations.

Calculus of Variations Calculations

The first thing we must do is adjoin the constraint equations using a set of Lagrangian multipliers. This is done by multiplying the constraint equations (written in the form 0 = ...) by a Lagrangian multiplier variable (Eqs. (59 - 64)), and adding the results to the total energy equation (Eq. (65 - 65e)). The constraint equations with their corresponding Lagrangian multipliers are

$$\lambda_{E_z} : \quad - \frac{dE_z}{dz} = n_1 - n_2 ; \tag{59}$$

$$\lambda_{B_x} : \quad - \frac{dB_x}{dz} = n_1 v_y ; \tag{60}$$

$$\lambda_1 : \quad - \frac{dn_1}{dz} = + \frac{1}{C_1 \gamma} n_1^{2-\gamma} (E_z - v_y B_x) ; \tag{61}$$

$$\lambda_2 : \quad - \frac{dn_2}{dz} = - \frac{1}{C_2 \gamma} n_2^{2-\gamma} (E_z) ; \tag{62}$$

$$\lambda_{Q_z} : \quad - \frac{dQ_z}{dz} = n_1 . \tag{63}$$

The modified energy equation is as follows:

$$\left(\frac{1}{xy}\right) U = \int_0^h \{ \left[\frac{E_z^2}{2} + \frac{B_x^2}{2} + \frac{n_1 v_x^2}{2} + C_1 n_1^{\gamma} + C_2 n_2^{\gamma} \right] \tag{64}$$

$$+ \lambda_{B_z} \left[-\frac{dE_z}{dz} + n_1 - n_2 \right] \tag{64a}$$

$$+ \lambda_{B_x} \left[-\frac{dB_x}{dz} + n_1 v_y \right] \tag{64b}$$

$$+ \lambda_1 \left[-\frac{dn_1}{dz} + \frac{1}{C_1 \gamma} n_1^{2-\gamma} \left(E_z - v_y B_x \right) \right] \tag{64c}$$

$$+ \lambda_2 \left[-\frac{dn_2}{dz} - \frac{1}{C_2 \gamma} n_2^{2-\gamma} E_z \right] \tag{64d}$$

$$+ \lambda_{Q_z} \left[-\frac{dQ_z}{dz} + n_1 \right] \} \, dz \tag{64e}$$

We now have the total energy equation (Eq. (19)) written as a function of a set of energy terms (E_z, B_x, n_1, n_2, Q_z, V_y, and Lagrangian multipliers and constants). In order to find the minimum total energy of the model system, we must find the particular set of values of the energy terms that, when plugged into the total energy equation (Eq. (19)), yield the lowest possible value for U.

We start the process by first assuming we know the value of U when the system is in a minimum total energy state. Then we look for the particular set of values that will give us assumed value of U. We do this by first expressing the dependent variables (E_z, B_x, n_1, n_2, Q_z, V_y) as a sum of a 'true' function and a 'variation' function. The 'variation' function itself is composed of an arbitrary component multiplied by an infinitesimal dimensionless parameter α.

The 'true' function is defined as having the value required to minimize Eq. (19) while the 'variation' function is defined as having any value.

				[Variation Function			]
Energy Term	=	True Function	+	[Dimensionless Parameter	×	Arbitrary Component	]
E_x	=	$\bar{E}_x$	+	[(α)	×	(δE_x)	] ;
B_x	=	$\bar{B}_x$	+	[(α)	×	(δB_x)	] ;
n_1	=	$\bar{n}_1$	+	[(α)	×	(δn_1)	] ;
n_2	=	$\bar{n}_2$	+	[(α)	×	(δn_2)	] ;
Q_x	=	$\bar{Q}_x$	+	[(α)	×	(δQ_x)	] ;
v_y	=	$\bar{v}_y$	+	[(α)	×	(δv_y)	] .

Expanding Eq. (64 -64e) in this form gives us Eq. (65 - 65e).

We can see that if we eliminate all the 'variation' functions from Eq. (65 - 65e) we would have the necessary values ('true' functions) of the energy terms to give us the minimum total energy or assumed value of U. Unfortunately, the 'variation' function can have any value due to its arbitrary component, so the only way we can eliminate it is to reduce the parameter α to zero. We can do this by taking the limit of Eq. (65 - 65e) as α goes to zero.

However, since we are looking for a minimum total energy condition of the model system when it is also in an equilibrium state, we must ensure the resulting expression depicts an equilibrium condition after we take the limit as α goes to zero. We saw from Chapter II of this thesis that an equilibrium condition exists when $d/d\alpha$ equals zero. Therefore, in order to maintain all the conditions of the model system that we want, we must also take the derivative of Eq. (65 - 65e), with respect to α at the same time that we take the limit as α goes to zero.

The results of performing these two mathematical operations yield Eq. (66 - 66e). Notice that the total energy of the model system is now expressed as a derivative with respect to α

$$\frac{1}{(xy)}U(\alpha) = \int_0^h \{[\frac{\bar{E}_z^2 + 2\bar{E}_z\alpha\delta E_z + \alpha^2\delta E_z^2}{2}$$

$$+ \frac{\bar{B}_x^2 + 2\bar{B}_x\alpha\delta B_x + \alpha^2\delta B_x^2}{2}$$

$$+ \frac{(\bar{n}_1 + \alpha\delta n_1)(\bar{v}_y^2 + 2\bar{v}_y\alpha\delta v_y + \alpha^2\delta v_y^2)}{2}$$

$$+ C_1(\bar{n}_1 + \alpha\delta n_1)^\gamma$$

$$+ C_2(\bar{n}_2 + \alpha\delta n_2)^\gamma] \qquad (65)$$

$$+ \lambda_{E_z}[-\frac{d(\bar{E}_z + \alpha\delta E_z)}{dz} + (\bar{n}_1 + \alpha\delta n_1) - (\bar{n}_2 + \alpha\delta n_2)] \qquad (65a)$$

$$+ \lambda_{B_x}[-\frac{d(\bar{B}_x + \alpha\delta B_x)}{dz} + (\bar{n}_1 + \alpha\delta n_1)(\bar{v}_y + \alpha\delta v_y)] \qquad (65b)$$

$$+ \lambda_1[-\frac{d(\bar{n}_1 + \alpha\delta n_1)}{dz} + \frac{(\bar{n}_1 + \alpha\delta n_1)^{2-\gamma}}{C_1\gamma}$$

$$\times \frac{(\bar{E}_z + \alpha\delta E_z) - (\bar{v}_y + \alpha\delta v_y)(\bar{B}_x + \alpha\delta B_x)}{C_1\gamma}] \qquad (65c)$$

$$+ \lambda_2[-\frac{d(\bar{n}_2 + \alpha\delta n_2)}{dz} - \frac{(\bar{n}_2 + \alpha\delta n_2)^{2-\gamma}}{C_2\gamma}$$

$$\times \frac{(\bar{E}_z + \alpha\delta E_z)}{C_2\gamma}] \qquad (65d)$$

$$+ \lambda_{Q_z}[-\frac{d(\bar{Q}_z + \alpha\delta Q_z)}{dz} + (\bar{n}_1 + \alpha\delta n_1)] \} dz . \qquad (65e)$$

$$\frac{1}{(xy)} \lim_{\alpha \to 0} \left(\frac{d}{d\alpha} U(\alpha) \right) = \int_0^h \{ [\bar{E}_z \delta E_z + \bar{B}_x \delta B_x + \frac{v_y^2 \delta n_1}{2} + \bar{n}_1 \bar{v}_y \delta v_y + C_1 \gamma \bar{n}_1^{\gamma-1} \delta n_1 + C_2 \gamma \bar{n}_2^{\gamma-1} \delta n_2] \tag{66}$$

$$+ \lambda_{B_z} [-\frac{d(\delta E_z)}{dz} + \delta n_1 - \delta n_2] \tag{66a}$$

$$+ \lambda_{B_x} [-\frac{d(\delta B_x)}{dz} + \bar{n}_1 \delta v_y + \bar{v}_y \delta n_2] \tag{66b}$$

$$+ \lambda_1 [-\frac{d(\delta n_1)}{dz} + \frac{\bar{n}_1^{2-\gamma} (\delta E_z - \bar{v}_y \delta B_x - \bar{B}_x \delta v_y)}{C_1 \gamma} + \frac{(2-\gamma) \bar{n}_1^{1-\gamma} \delta n_1 (E_z - \bar{v}_y \bar{B}_x)}{C_1 \gamma}] \tag{66c}$$

$$+ \lambda_2 [-\frac{d(\delta n_2)}{dz} - \frac{\bar{n}_2^{2-\gamma} \delta E_z}{C_2 \gamma} - \frac{(2-\gamma) \bar{n}_2^{1-\gamma} \delta n_2 E_z}{C_2 \gamma}] \tag{66d}$$

$$+ \lambda_{Q_z} [-\frac{d(\delta Q_z)}{dz} + \delta n_1] \} dz . \tag{66e}$$

$(dU/d\alpha)$. This expression depicts how much any function varies from the assumed minimum total energy value, U. When $dU/d\alpha$ equals zero, this variance will also be zero. Therefore, if we can solve Eq. (66 - 66e) so that $dU/d\alpha$ equals zero, we will find the values of the energy terms necessary to depict the minimum total energy state of the model system.

If we now reduce the value of the 'variation' function to zero, $dU/d\alpha$ will also become zero, thereby giving us a minimum total energy condition for the model system.

Taking a closer look at Eq. (66 - 66e) reveals that the value of $dU/d\alpha$ depends on the values of the arbitrary components (δE_x, δB_x, δn_1, δn_2, and δQ_x) of the 'variation' function. This poses a problem for us because the value of these arbitrary components can be anything. Therefore, we must somehow separate or factor out these arbitrary components from the rest of the equation so that we are left with only the part of the equation we need.

Integration by Parts

We use integration by parts to separate the arbitrary components from the rest of the expression in Eq. (66 - 66e) as shown here.

$$\text{Let } \delta X = \text{Any Arbitrary Component};$$

$$\begin{matrix}\text{Combined}\\ \text{Integral}\end{matrix} = \text{Endpoints} + \begin{matrix}\text{Separated}\\ \text{Integral}\end{matrix};$$

$$-\int \lambda \frac{d(\delta X)}{dz} = -\lambda(\delta X) + \int \frac{d(\lambda)}{dz}(\delta X). \qquad (67)$$

Notice the term outside the integral on the right-hand side of Eq. (67) depicts the endpoints or boundaries of a given function, λ in this case.

Applying integration by parts to Eq. (66 - 66e) gives us an equation Eq. (68 - 68e) in which the energy terms are written in the form as shown in Eq. (67). By doing this, we can solve the remaining part of the equation to find out what values of the energy terms will give us zero variance ($dU/d\alpha = 0$).

$$-\lambda_{E_z}\delta E_z + \int_0^h \left[\frac{d(\lambda_{E_z})}{dz}\delta E_z + \lambda_{E_z}\delta n_1 - \lambda_{E_z}\delta n_2\right] dz\ ; \tag{68a}$$

$$-\lambda_{B_x}\delta B_x + \int_0^h \left[\frac{d(\lambda_{B_x})}{dz}\delta B_x + \lambda_{B_x}\bar{n}_1\delta v_y + \lambda_{B_x}\bar{v}_y\delta n_1\right] dz\ ; \tag{68b}$$

$$-\lambda_1\delta n_1 + \int_0^h \left[\frac{d(\lambda_1)}{dz}\delta n_1 + \frac{\lambda_1\bar{n}_1^{\,2-\gamma}(\delta E_z - \bar{v}_y\delta B_x - \bar{B}_x\delta v_y)}{C_1\gamma} + \frac{(2-\gamma)\,\bar{n}_1^{\,1-\gamma}\,\delta n_1(E_z - \bar{v}_y\bar{B}_x)}{C_1\gamma}\right] dz\ ; \tag{68c}$$

$$-\lambda_2\delta n_2 + \int_0^h \left[\frac{d(\lambda_2)}{dz}\delta n_2 - \frac{\lambda_2\bar{n}_2^{\,2-\gamma}\delta E_z}{C_2\gamma} - \frac{\lambda_2(2-\gamma)\,\bar{n}_2^{\,1-\gamma}\delta n_2 E_z}{C_2\gamma}\right] dz\ : \tag{68d}$$

$$-\lambda_{Q_z}\delta Q_z + \int_0^h \left[\frac{d(\lambda_{Q_z})}{dz}\delta Q_z + \delta n_1\right] dz\ . \tag{68e}$$

Consolidating terms yields:

$$\frac{1}{(xy)}\frac{dU(\alpha)}{d\alpha} = -\left[\lambda_{B_z}\delta E_z + \lambda_{B_x}\delta B_x + \lambda_{n_1}\delta n_1 + \lambda_{n_2}\delta n_2 + \lambda_{Q_z}\delta Q_z\right]_0^h$$

$$+ \int_0^h \left\{ \left[E_z\delta E_z + B_x\delta B_x + \frac{V_y^2\delta n_1}{2} + n_1 V_y \delta V_y \right.\right.$$

$$\left. + C_1\gamma(n_1)^{\gamma-1}\delta n_1 + C_2\gamma(n_2)^{\gamma-1}\delta n_2 \right.$$

$$+ \frac{d(\lambda_{B_z})}{dz}\delta E_z + \lambda_{B_z}\delta n_1 - \lambda_{B_z}\delta n_2$$

$$+ \frac{d(\lambda_{B_x})}{dz}\delta B_x + \lambda_{B_x} n_1 \delta V_y + \lambda_{B_x} V_y \delta n_1$$

$$+ \frac{d(\lambda_1)}{dz}\delta n_1 + \frac{\lambda_1(n_1)^{2-\gamma}(\delta E_z - V_y\delta B_x - B_x\delta V_y)}{C_1\gamma}$$

$$+ \frac{\lambda_1(2-\gamma)(n_1)^{1-\gamma}(\delta n_1)(E_z - V_y B_x)}{C_1\gamma}$$

$$+ \frac{d(\lambda_2)}{dz}\delta n_2 - \frac{\lambda_2(n_2)^{2-\gamma}(\delta E_z)}{C_2\gamma}$$

$$- \frac{\lambda_2(2-\gamma)(n_2)^{1-\gamma}(\delta n_2)(E_z)}{C_2\gamma}$$

$$\left. + \frac{d(\lambda_{Q_z})}{dz}\delta Q_z + \lambda_{Q_z}\delta n_1 \right] \Big\}\, dz\,. \qquad (69)$$

It is important to note here that one of the constraints required by the calculus of variations is that the value of any function, "true" or "variation," must be the same at any defined endpoints of boundaries of a given system. Therefore, the first line of Eq. (69) will equal zero. In order for $dU/d\alpha$ to equal zero, the remaining differential equations in Eq. (69) must have the following forms:

$$\frac{d(\lambda_{B_z})}{dz} = -E_z - \frac{\lambda_1(n_1)^{2-\gamma}}{C_1\gamma} + \frac{\lambda_2(n_2)^{2-\gamma}}{C_2\gamma}; \tag{70}$$

$$\frac{d(\lambda_{B_x})}{dz} = -B_x + \frac{\lambda_1(n_1)^{2-\gamma}(V_y)}{C_1\gamma}; \tag{71}$$

$$\frac{d(\lambda_1)}{dz} = -\frac{V_y^2}{2} - (C_1\gamma)(n_1)^{\gamma-1} + \frac{\lambda_1(2-\gamma)(n_1)^{1-\gamma}(E_z - V_yB_x)}{C_1\gamma}$$

$$- \lambda_{E_z} - \lambda_{B_x}V_y - \lambda_{Q_z}; \tag{72}$$

$$\frac{d(\lambda_2)}{dz} = -(C_2\gamma)(n_2)^{\gamma-1} + \frac{\lambda_2(2-\gamma)(n_2)^{1-\gamma}(E_z)}{C_2\gamma} + \lambda_{E_z}; \tag{73}$$

$$\frac{d(\lambda_{Q_z})}{dz} = 0, \tag{74}$$

in order for $dU/d\alpha$ to equal zero. Additionally, the following velocity term must equal

$$V_y = +\frac{\lambda_1(n_1)^{1-\gamma}B_x}{C_1\gamma} - \lambda_{B_z}. \tag{75}$$

We now have a set of differential equations represented by Lagrangian multipliers (Eq. (70 - 74)) in addition to Eqs. (59 - 63) which, when solved, will provide us with the values of the energy terms that will minimize the minimum total energy equation (Eq. (19)). The next step is to solve this set of differential equations to find out what the value of the energy terms E_Z, B_X, n_1, n_2, Q_Z, and V_y should be in order to make $dU/d\alpha$ equal zero in Eq. (69). This is where a computer program becomes useful.

CHAPTER IV

MODEL PROGRAM

Program Description

As stated in Chapter III, we now have a set of ordinary differential equations (see Chapter III) which describe an idealized model of the earth's magnetotail. We want to solve these differential equations with boundary conditions to find a particular set of values of the energy terms (E_z, B_x, n_1, n_2, Q_z, and v_y) such that when put into the total energy equation (Eq. 19), they yield the lowest possible value for U. This then becomes the minimum total energy model for the magnetotail system. Attempting to solve these equations analytically would prove difficult, if not impossible. Therefore, we must use a computer program to solve these equations.

DVCPR Routine

In order to quickly and efficiently solve the differential equations derived in Chapter III, we have used an IMSL (International Mathematics Science Library) computer routine - DVCPR. The DVCPR program solves a system of ordinary differential equations with boundary conditions at two points, by using a variable order, variable step size, finite difference method with deferred corrections.

As stated above, the boundary conditions for the idealized magnetotail model occur at the top and bottom surfaces of the rectangular slab. Basically, the DVCPR tries to solve the differential equations by using the trapezoidal rule over the entire height of the magnetotail model. The accuracy of the programs calculations increases as the number of step sizes increases. These step sizes represent uniform horizontal slices within the model. The details of how this program works are shown in Appendix A.

Dimensional Transformation

We now have a program which will solve the system of dimensionless differential equations we derived in Chapter III. Before we enter these equations into the program, we must ensure the dimensionless forms of the energy terms relate to each other in the same manner as the dimensioned terms in Eq. (16) do. We do this with scaling quantities as shown in Eq. (76) below.

$$\text{Dimensioned Value} = \text{Dimensionless Value} \times \text{Scaling Quantity} . \tag{76}$$

In order to determine the values of the scaling quantities, we rewrite Eq. (16) and the constraint equations in the following form:

Energy Equation

$$u = \frac{m(n)(v_y^2)}{2} + \frac{(B_x^2)}{2\mu_0} + \frac{\epsilon_0 (E_z^2)}{2} + (C)(n^\gamma) . \tag{77}$$

(Note: $n = n_1$ or n_2 and $C = C_1$ or C_2.)

Maxwell's Equations

$$\frac{\partial (E_z)}{\partial (z)} = \frac{q(n_1)}{\epsilon_0} - \frac{q(n_2)}{\epsilon_0} , \tag{78}$$

and ,

$$\frac{\partial (B_x)}{\partial (z)} = -\mu_0 q(n_1)(v_y) . \tag{79}$$

Force Equations

$$\frac{\partial (n_1)}{\partial (z)} = \frac{(n_1)^{2-\gamma} (E_z - v_y B_x)}{(C_1) \gamma} , \tag{80}$$

and ,

$$\frac{\partial (n_2)}{\partial (z)} = \frac{(n_2)^{2-\gamma} (E_z)}{(C_2) \gamma} . \tag{81}$$

Charge Conservation Equation

$$\frac{\partial (Q_z)}{\partial (z)} = q (n_1) . \tag{82}$$

The next step is to multiply each of the equations above (Eq. (77 - 82)) by a corresponding scaling quantity.

Energy Equation

$$u = \frac{m (n n_s) (v_y v_{y_s})^2}{2} + \frac{(B_x B_{x_s})^2}{2\mu_0} + \frac{\epsilon_0 (E_z E_{z_s})^2}{2} + (C C_s) (n n_s)^\gamma . \tag{83}$$

Maxwell's Equations

$$\frac{\partial (E_z E_{z_s})}{\partial (z z_s)} = \frac{q (n_1 n_{1_s})}{\epsilon_0} - \frac{q (n_2 n_{2_s})}{\epsilon_0} , \tag{84}$$

and ,

$$\frac{\partial (B_z B_{z_s})}{\partial (z z_s)} = - \mu_0 q (n_1 n_{1_s}) (v_y v_{y_s}) . \tag{85}$$

Force Equations

$$\frac{\partial (n_1 n_{1_s})}{\partial (z z_s)} = \frac{(n_1 n_{1_s})^{2-\gamma} ((E_z E_{z_s}) - (v_y v_{y_s}) (B_x B_{x_s}))}{(C_1 C_{1_s}) \gamma} , \tag{86}$$

and ,

$$\frac{\partial (n_2 n_{2_s})}{\partial (z z_s)} = \frac{(n_2 n_{2_s})^{2-\gamma} (E_z E_{z_s})}{(C_2 C_{2_s}) \gamma} . \tag{87}$$

Charge Conservation Equation

$$\frac{\partial (Q_s Q_{z_s})}{\partial (z z_s)} = q (n_1 n_{1_s}) . \tag{88}$$

In Eqs. (84 - 88), we can collect all the non-scaled energy terms on the left side of the equation(s) and set them equal to any arbitrary value we want. In this case, we will set them equal to one. Now we set the remaining constants and scaled quantities on the right side of the equations equal to the left side of the equations to get the following equations:

Maxwell's Equations

$$1 = + \frac{q}{\epsilon_0} \frac{(n_{1_s}) (z_s)}{(E_{z_s})} ;$$

$$1 = - \frac{q}{\epsilon_0} \frac{(n_{2_s}) (z_s)}{(E_{z_s})} ; \tag{89}$$

and ,

$$1 = - \mu_0 q \frac{(n_{1_s}) (v_{y_s}) (z_s)}{(B_{z_s})} . \tag{90}$$

Force Equations

$$1 = + \frac{1}{\gamma} \frac{(n_{1_s})^{2-\gamma} (E_{x_s})}{(C_{1_s})} ;$$

$$1 = - \frac{1}{\gamma} \frac{(v_{y_s})(B_{z_s})}{(C_{1_s})} ; \quad (91)$$

and ,

$$1 = + \frac{1}{\gamma} \frac{(n_{2_s})^{2-\gamma} (E_{x_s})}{(C_{2_s})} . \quad (92)$$

Charge Conservation Equation

$$1 = + q \frac{(n_{1_s})(z_s)}{(Q_{z_s})} . \quad (93)$$

We basically perform the same type of operation for the energy equation (Eq. (83)) with a slight twist. The first thing we do is factor the constants and scaled variables from the first term on the right side of Eq. (83). We then divide the rest of the terms on the right-hand side of the equation by the same factor as shown in Eq. (94).

Energy Equation

$$u = \frac{(mn_s v_{y_s}^2)(\frac{1}{2} n v_y^2)}{(mn_s v_{y_s}^2)} + \frac{(\frac{B_{x_s}^2}{2\mu_0})(\frac{1}{2} B_x^2)}{(mn_s v_{y_s}^2)} + \frac{(\epsilon_0 E_{z_s}^2)(\frac{1}{2} E_z^2)}{(mn_s v_{y_s}^2)} + \frac{(C_s n_s^{\gamma})(C n^{\gamma})}{(mn_s v_{y_s}^2)} . \quad (94)$$

But since,

$$\frac{\left(\frac{1}{2}nv_y^2\right)}{\left(mn_s v_{y_s}^2\right)} = \frac{\left(\frac{1}{2}B_x^2\right)}{\left(mn_s v_{y_s}^2\right)} = \frac{\left(\frac{1}{2}E_z^2\right)}{\left(mn_s v_{y_s}^2\right)} = \frac{\left(Cn^\gamma\right)}{\left(mn_s v_{y_s}^2\right)} = \frac{1}{\left(mn_s v_{y_s}^2\right)}, \tag{95}$$

we can say,

$$m\, n_s\, v_{y_s}^2 = \frac{B_{x_s}^2}{2\mu_0} = \epsilon_0 E_{z_s}^2 = C_s\, n_s^\gamma . \tag{96}$$

At this point we have eight scaling equations (Eqs. (89 - 93, 96)) made up of five constants (ϵ_0, μ_0, γ, e, and m) and seven unknown scaling variables (E_{z_s}, B_{x_s}, n_s, z_s, Q_{z_s}, C_s, and v_{y_s}). It is important to note that we are talking about scaling quantities here, not scaled quantities. In the thesis, "scaling" quantities are used to generate dimensioned parameters by multiplying them with a given dimensionless number, and are not to be confused with a "scale" height or length that represents an interval in which some parameter changes by a factor of e.

Setting one of the unknown scaling variables to a specific value with units (i.e. $v_s = 3.0 \times 10^8$ m/s), we can begin rewriting the remaining unknown scaling variables in terms of constants and one unknown variable, which we arbitrarily pick to be n. Since we are choosing v_s to be equal to the speed of light, we will denote it as a constant c, from now on.

Therefore, we begin to solve for the values of the scaling quantities by starting with

$$E_{x_s} = c \times B_{z_s} . \tag{97}$$

We can see from Eq. (90) that

$$B_{x_s} = \sqrt{\mu_0 n_s c^2 m}\,. \tag{98}$$

At this point, we can solve for any of the scaling quantities from Eqs. (89 - 93). We arbitrarily solve for the scaling height z_s, from Eq. (89). Also using Eqs. (97) and (98), we see that

$$z_s = \frac{\epsilon_0 (E_{x_s})}{q n_s} = \frac{\epsilon_0 [c (B_{x_s})]}{q n_s} = \frac{\epsilon_0 [c (\sqrt{\mu_0 n_s c^2 m})]}{q n_s}\,. \tag{99}$$

If we now square Eq. (99) and factor out $c = (\mu_0 \epsilon_0)^{-\frac{1}{2}}$, we get

$$z_s^2 = \frac{m}{\mu_0 q^2 n_s}\,. \tag{100}$$

Taking the square root of Eq. (100) yields

$$z_s = \sqrt{\frac{m}{\mu_0 q^2 n_s}}\,, \tag{101}$$

which is written in terms of constants and one scaling quantity, n_s. We are now at a point where we can rewrite the remaining scaling variables in terms of n_s, z_s, c, and other known constants. They are as follows:

$$
\begin{aligned}
E_{z_s} &= \frac{q}{\epsilon_0}\,(n_s z_s)\,; \\
B_{z_s} &= \frac{1}{c}\,(E_{z_s})\,; \\
Q_{z_s} &= e\,(n_s z_s)\,: \\
C_s &= \frac{q}{\epsilon_0 \gamma}\,(n_s^{2-\gamma} z_s^{2})\,.
\end{aligned}
\tag{102}
$$

We now have all the scaling quantities written in terms of constants and two scaling quantities, n_S and z_S. Since the scaling height, z_S, is also written in terms of the scaling number density, n_S, all the scaling quantities are related to each other. Choosing a value for n_S will set the values for the other scaling quantities accordingly. At this point, we are able to use the dimensionless forms of the energy terms within the minimum total energy program and use DVCPR routine. The details of the minimum total program are shown in Appendix B.

Model Output

By picking a suitable scaling number density, we can generate appropriate values for the remaining scaling quantities. Multiplying these scaling quantities by dimensionless numbers provides the input for the DVCPR program to begin solving the dimensionless differential equations we derived in Chapter III. The program then divides the model's N-S profile into a number of segments and comes up with dimensionless values for each of the energy variables for each segment. These values can then be plotted on a graph to come up with dimensionless N-S profiles of the energy variables. The profiles generated by this program only depict the region between the bottom surface of the model, or neutral sheet, to the top surface or the plasma sheet boundary layer. Although the southern half of the central plasma sheet is not depicted in

this model, the profiles should by symmetrical from north to south for the number densities, ion velocities, and ion temperatures. Due to the nature of the magnetotail, the electric and magnetic fields would have asymmetrical profiles.

By setting the dimensionless number density of the model magnetotail to one and setting the scaling number density to 1.0×10^6 particles per cubic meter (typical value observed within the central plasma sheet of the earth's magnetotail), we come up with the following scaling quantities for the other model energy parameters.

Scaling Quantities

n_s -> (1.0×10^6 [m^{-3}])
z_s -> (2.28×10^5 [m])
E_s -> (4.12×10^3 [V/m])
B_s -> (1.37×10^{-5} [t])
C_s -> (1.5×10^{-14} [(kg)(m^4)/(A)(s^2)])

Next, we multiply these scaling quantities by one to come up with the following model energy parameters, with units.

Raw Data	=	Dimensionless Value	X	Scaling Quantity
n_{RAW} -> 1.0×10^6 [m^{-3}]	=	(1.0)	X	(1.0×10^6 [m^{-3}])
z_{RAW} -> 2.28×10^5 [m]	=	(1.0)	X	(2.28×10^5 [m])
E_{RAW} -> 4.12×10^3 [V/m]	=	(1.0)	X	(4.12×10^3 [V/m])
B_{RAW} -> 1.37×10^{-5} [t]	=	(1.0)	X	(1.37×10^{-5} [t])
C_{RAW} -> 1.5×10^{-14} [kgm^4/A^3]	=	(1.0)	X	(1.5×10^{-14} [kgm^4/A^3])

These numbers, when entered into the minimum total energy program (Appendix B), generate integrated numerical data (Appendix C) and a dimensionless N-S profile as shown in Fig. 24.

Notice that the ion and electron number densities both increase as they get closer to the model magnetotail's neutral sheet, which is what we would expect to see in the earth's magnetotail. Also note that the magnetic field strength goes to zero at the model magnetotail's neutral sheet--again what we would expect to see in the earth's magnetotail.

Figures 25 through 28 show how the dimensionless energy parameters vary as the height of the model increases from 0.01, a very thin slab, to 95 scaling heights, a thick slab (numerical data are in Appendix C). It is interesting to note that all the parameter changes occur within three (6.84×10^5 m) or four scale heights (9.12×10^5 m), no matter how high we make the profile. In order to ensure the results generated by the minimum energy model are not inconsistent with the laws of classical physics, we compare the height in which the parameter changes take place to the Debye length and the Larmor radius of an ion used within the model. The equations for finding an ion's Debye length and Larmor radius are

$$\text{Debye Length} = \lambda_D = 69.0 \left(\frac{T_{ion}}{n_{ion}} \right)^{1/2};$$

$$\text{Larmor Radius} = r = \frac{(m_{ion})(v_{ion})}{(q)(B)}.$$

Using the numerical data from Appendix C, we see that the ion Debye length is approximately 1542 m while the Larmor radius ranges in value from 2.29×10^5 - 5.62×10^6 m. We can ignore the Debye length since it is smaller than the Larmor radius. Looking at the Larmor radius, however, we can see that its values have the same order of magnitude as the height in which the parameters change in the model profiles. This result shows that the minimum energy model is not inconsistent with the laws of classical physics.

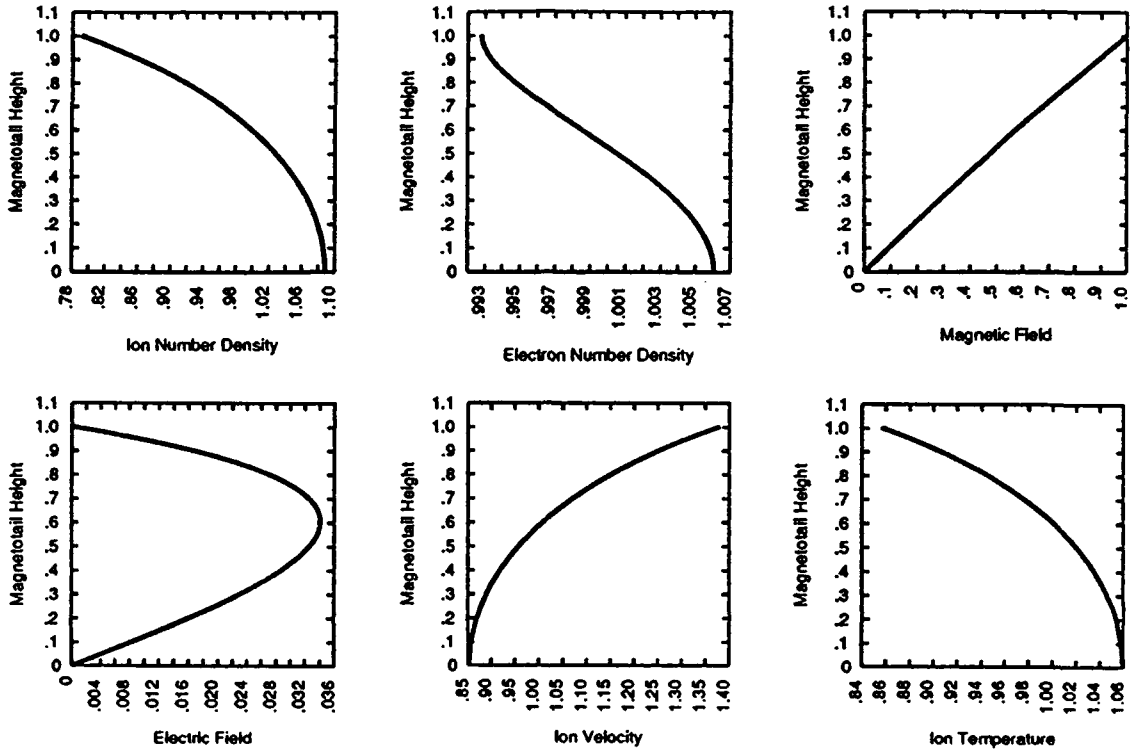

FIG. 24. N-S profiles of number densities (n_1 and n_2), x-component of the magnetic field (B_x), and the z-component of the electric field (E_z) generated from the minimum total energy program.

TABLE II. Scaling Data Corresponding to Fig. (24).

Scaling Quantity	Number of Scaling Quantities
n_s (Number Density)	= 1.0 ;
z_s (Model Magnetotail Height)	= 1.0 ;
E_s (Z-component of the Electric Field)	= 1.0 ;
B_s (X-component of the Magnetic Field)	= 1.0 ;
C_s (Magnetotail Adiabatic Constant)	= 1.0 .

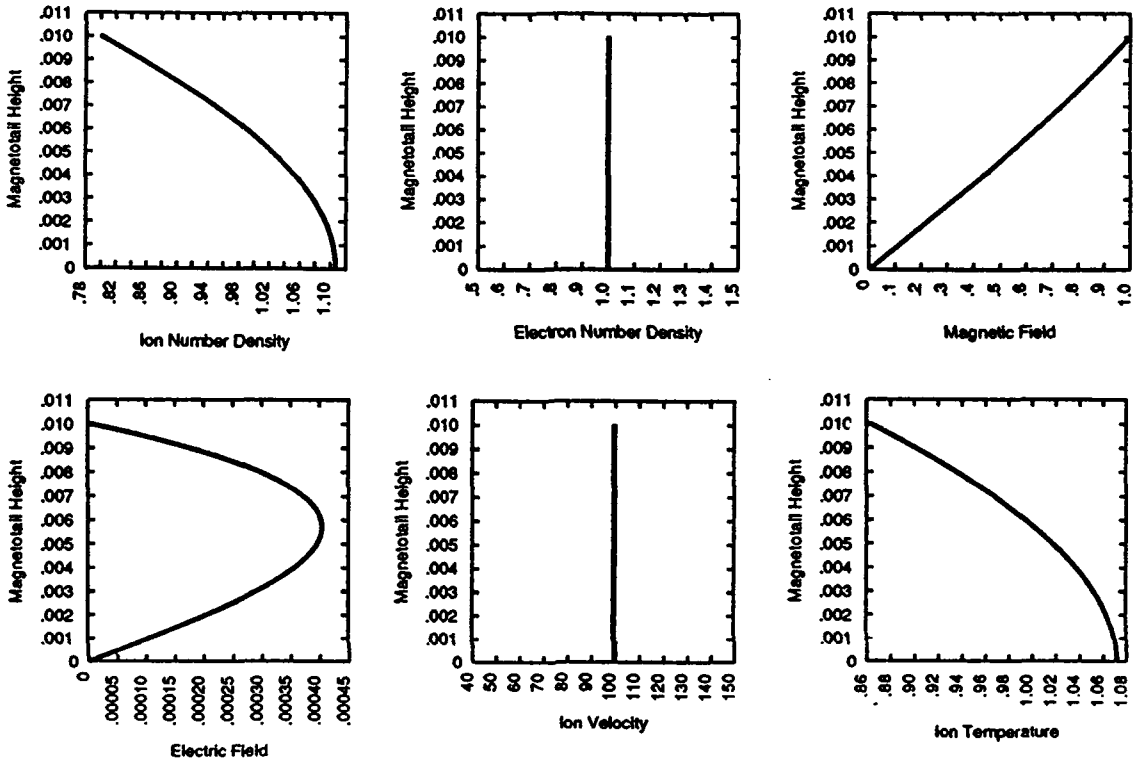

FIG. 25. N-S profiles of number densities (n_1 and n_2), x-component of the magnetic field (B_x), and the z-component of the electric field (E_z) generated from the minimum total energy program.

TABLE III. Scaling Data Corresponding to Fig. (25).

Scaling Quantity	Number of Scaling Quantities
n_s (Number Density)	= 1.0 ;
z_s (Model Magnetotail Height)	= 0.01 ;
E_s (Z-component of the Electric Field)	= 1.0 ;
B_s (X-component of the Magnetic Field)	= 1.0 ;
C_s (Magnetotail Adiabatic Constant)	= 1.0 .

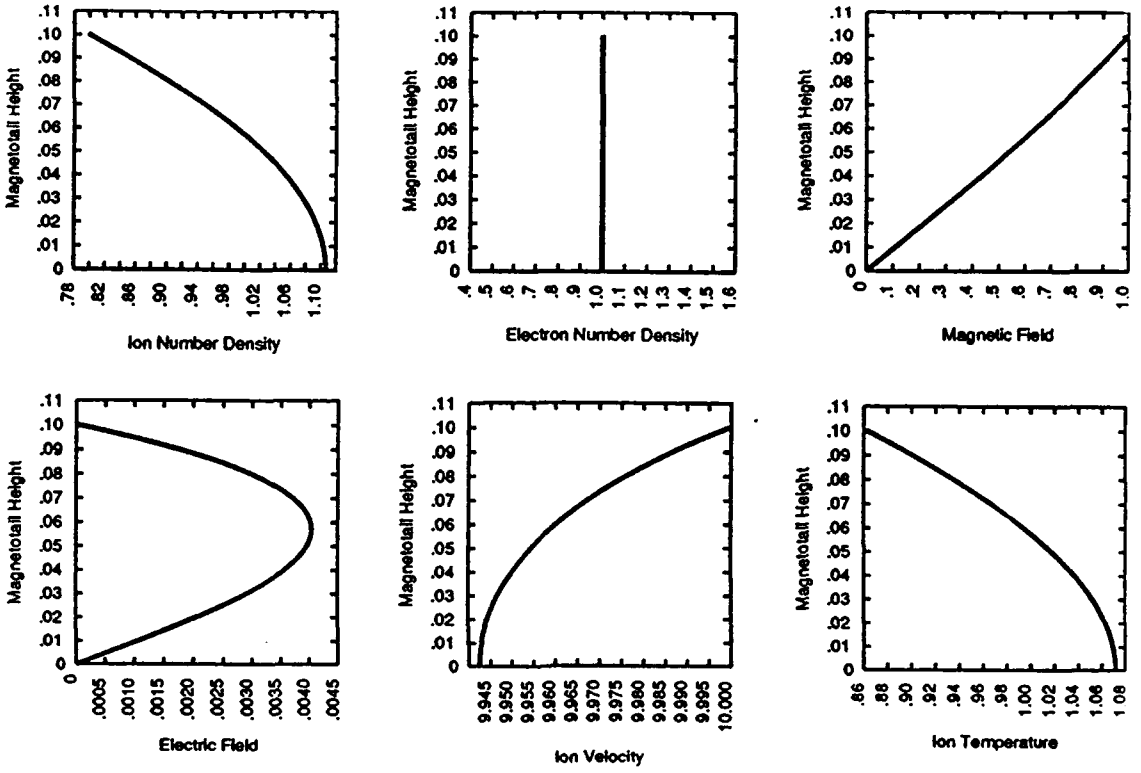

FIG. 26. N-S profiles of number densities (n_1 and n_2), x-component of the magnetic field (B_x), and the z-component of the electric field (E_z) generated from the minimum total energy program.

TABLE IV. Scaling Data Corresponding to Fig. (26).

Scaling Quantity	Number of Scaling Quantities
n_s (Number Density)	= 1.0 ;
z_s (Model Magnetotail Height)	= 0.1 ;
E_s (Z-component of the Electric Field)	= 1.0 ;
B_s (X-component of the Magnetic Field)	= 1.0 ;
C_s (Magnetotail Adiabatic Constant)	= 1.0 .

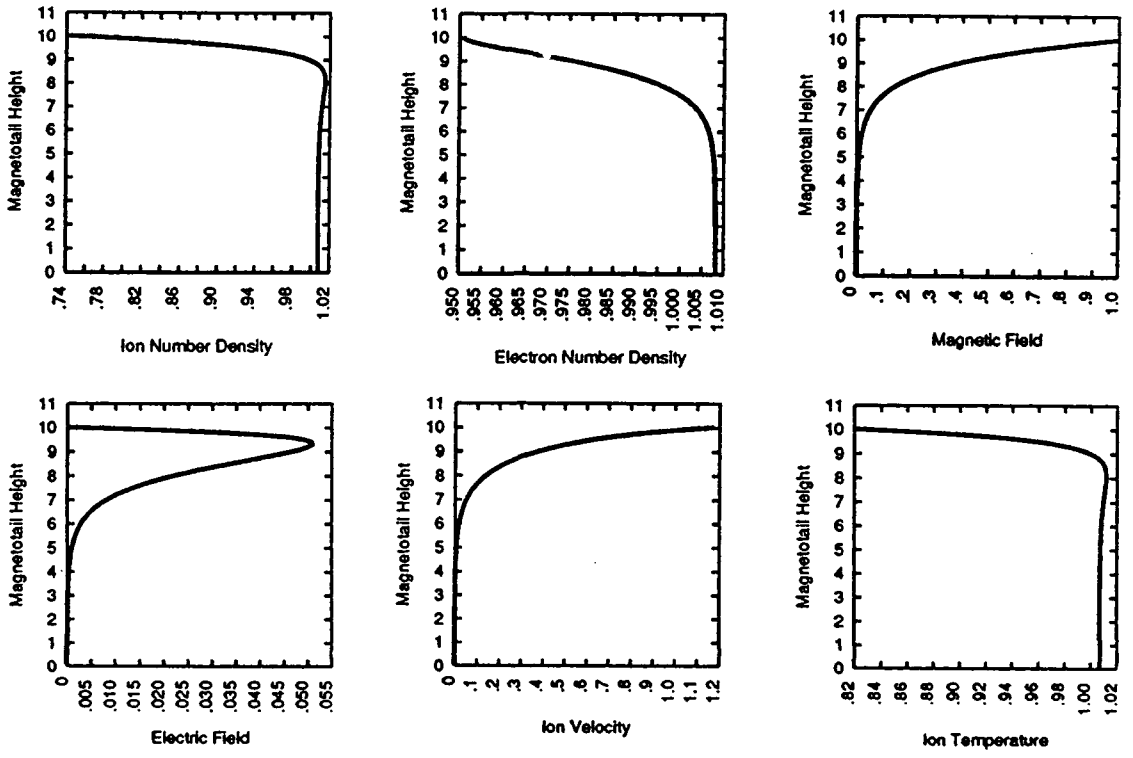

FIG. 27. N-S profiles of number densities (n_1 and n_2), x-component of the magnetic field (B_x), and the z-component of the electric field (E_z) generated from the minimum total energy program.

TABLE V. Scaling Data Corresponding to Fig. (27).

Scaling Quantity	Number of Scaling Quantities
n_s (Number Density)	= 1.0 ;
z_s (Model Magnetotail Height)	= 10.0 ;
E_s (Z-component of the Electric Field)	= 1.0 ;
B_s (X-component of the Magnetic Field)	= 1.0 ;
C_s (Magnetotail Adiabatic Constant)	= 1.0 .

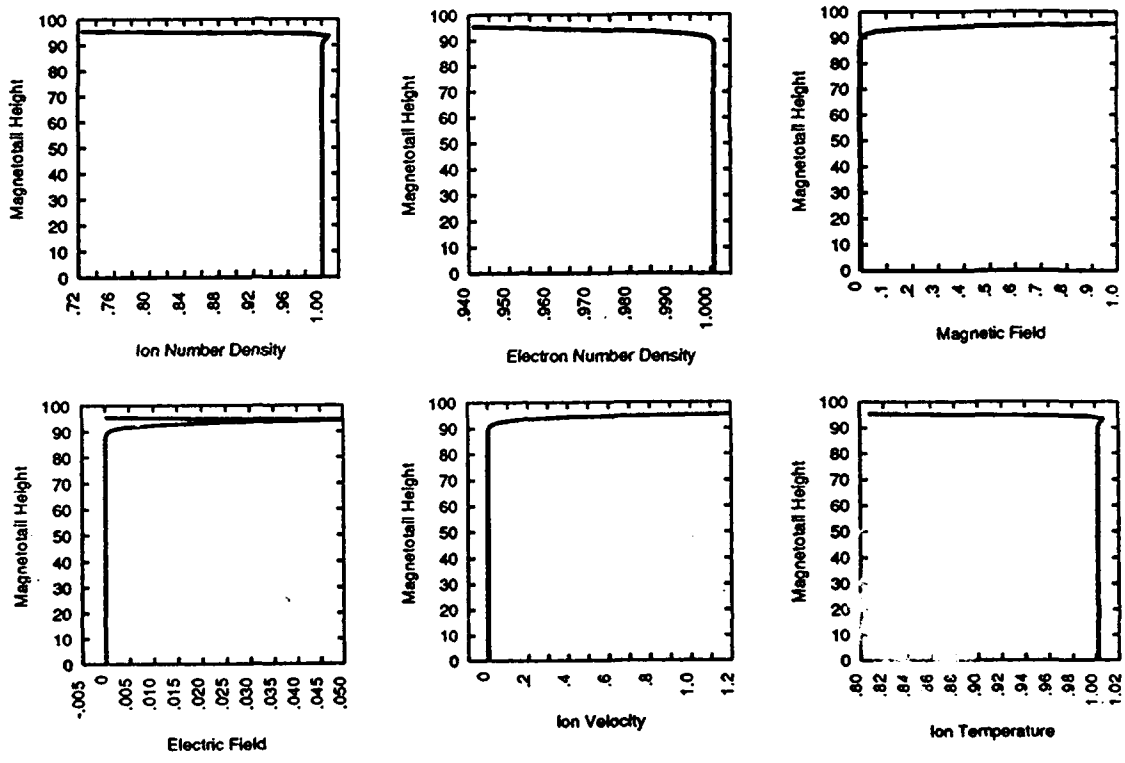

FIG. 28. N-S profiles of number densities (n_1 and n_2), x-component of the magnetic field (B_x), and the z-component of the electric field (E_z) generated from the minimum total energy program.

TABLE VI. Scaling Data Corresponding to Fig. (28).

Scaling Quantity	Number of Scaling Quantities
n_s (Number Density)	= 1.0 ;
z_s (Model Magnetotail Height)	= 95.0 ;
E_s (Z-component of the Electric Field)	= 1.0 ;
B_s (X-component of the Magnetic Field)	= 1.0 ;
C_s (Magnetotail Adiabatic Constant)	= 1.0 .

In order to come up with real values that represent typical values of the earth's magnetotail, we would have to multiply the scaling quantities by the following dimensionless values.

Raw Data	=	Dimensionless Value	X	Scaling Quantity
n_{RAW} -> 1.0×10^{6} $[m^{-3}]$	=	(1.0)	X	(1.0×10^{6} $[m^{-3}]$)
z_{RAW} -> 2.96×10^{7} [m]	=	(1.30×10^{2})	X	(2.28×10^{5} [m])
E_{RAW} -> 1.5×10^{-5} [V/m]	=	(3.64×10^{-9})	X	(4.12×10^{3} [V/m])
B_{RAW} -> 2.0×10^{-8} [t]	=	(1.46×10^{-3})	X	(1.37×10^{-5} [t])
C_{RAW} -> 6.9×10^{-19} $[kgm^4/A^3]$	=	(4.59×10^{-5})	X	(1.5×10^{-14} $[kgm^4/A^3]$)

Unfortunately, the minimum total energy program is unable to handle these numbers because the system height (1.30×10^{2} scale heights) is much larger than the scaling height z_s. However, by starting with a small height, unity for example, and increasing it until the program can no longer handle the input values, we can look at the trends in the numerical data (Appendix C) and profiles (Figs. 29 - 34) and draw conclusions from them.

Remember, the top and bottom values of each of these profiles are constrained by the following boundary conditions:

$$\lambda_1(0) = 0; \qquad \lambda_1(h) = 0;$$

$$\lambda_2(0) = 0; \qquad \lambda_2(h) = 0;$$

$$E_z(0) = 0; \qquad E_z(h) = 0;$$

$$B_x(0) = 0; \qquad B_x(h) = +B_{x_0}.$$

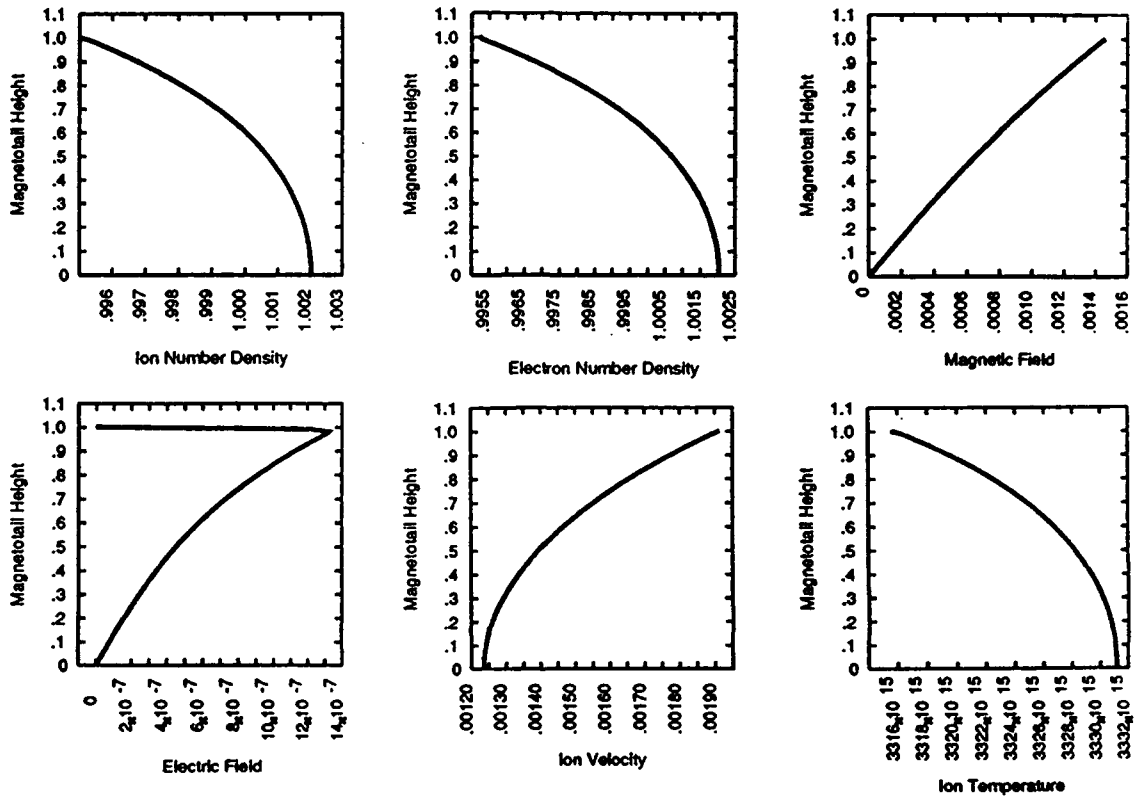

FIG. 29. N-S profiles of number densities (n_1 and n_2), x-component of the magnetic field (B_x), and the z-component of the electric field (E_z) generated from the minimum total energy program.

TABLE VII. Scaling Data Corresponding to Fig. (29).

Dimensioned Parameter	=	Dimensionless Unit	X	Scaling Quantity
n_{RAW} -> 1.0 X 10^{6} [m^{-3}]	=	(1.0)	X	(1.0 X 10^{6} [m^{-3}])
z_{RAW} -> 2.28 X 10^{5} [m]	=	(1.0)	X	(2.28 X 10^{5} [m])
E_{RAW} -> 1.5 X 10^{-5} [V/m]	=	(3.64 X 10^{-9})	X	(4.12 X 10^{3} [V/m])
B_{RAW} -> 2.0 X 10^{-8} [t]	=	(1.46 X 10^{-3})	X	(1.37 X 10^{-5} [T])
C_{RAW} -> 6.9 X 10^{-19} [kgm^4/A^3]	=	(4.59 X 10^{-5})	X	(1.5 X 10^{-14} [kgm^4/A^3])

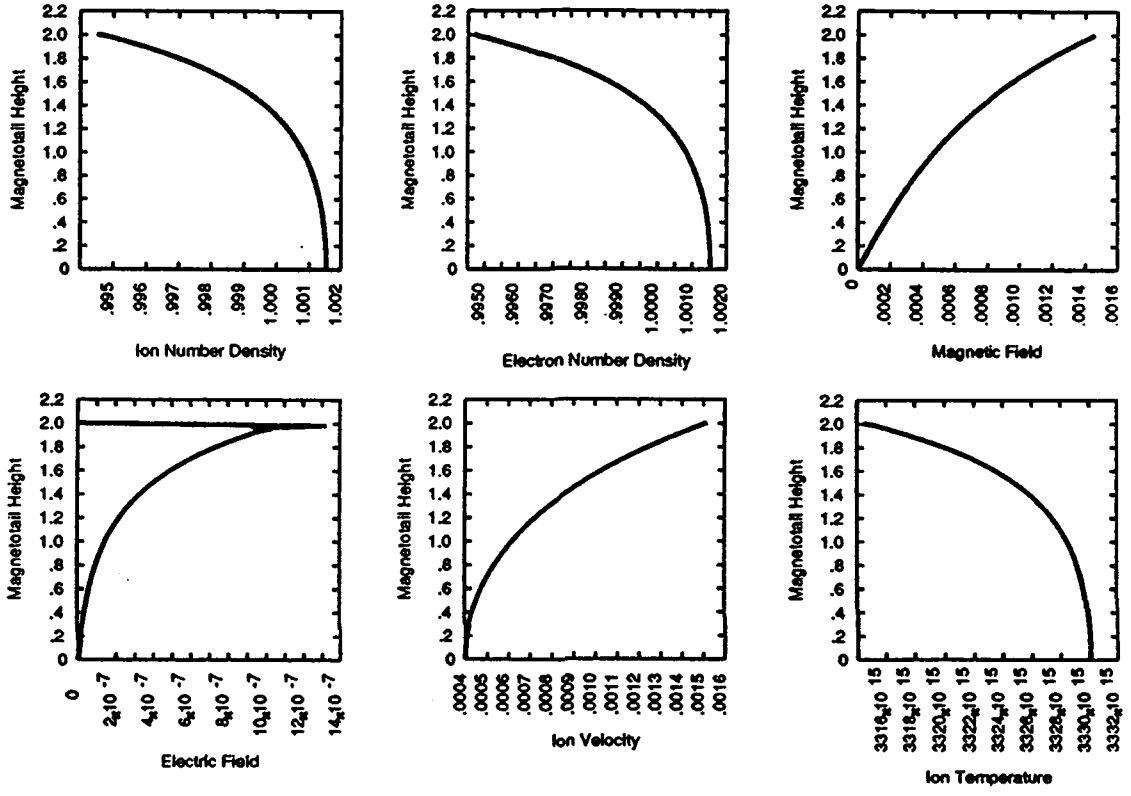

FIG. 30. N-S profiles of number densities (n_1 and n_2), x-component of the magnetic field (B_x), and the z-component of the electric field (E_z) generated from the minimum total energy program.

TABLE VIII. Scaling Data Corresponding to Fig. (30).

Dimensioned Parameter	=	Dimensionless Unit	X	Scaling Quantity
n_{RAW} -> 1.0 X 10^{6} [m^{-3}]	=	(1.0)	X	(1.0 X 10^{6} [m^{-3}])
z_{RAW} -> 4.56 X 10^{5} [m]	=	(2.0)	X	(2.28 X 10^{5} [m])
E_{RAW} -> 1.5 X 10^{-5} [V/m]	=	(3.64 X 10^{-9})	X	(4.12 X 10^{3} [V/m])
B_{RAW} -> 2.0 X 10^{-8} [t]	=	(1.46 X 10^{-3})	X	(1.37 X 10^{-5} [t])
C_{RAW} -> 6.9 X 10^{-19} [kgm^4/A^3]	=	(4.59 X 10^{-5})	X	(1.5 X 10^{-14} [kgm^4/A^3])

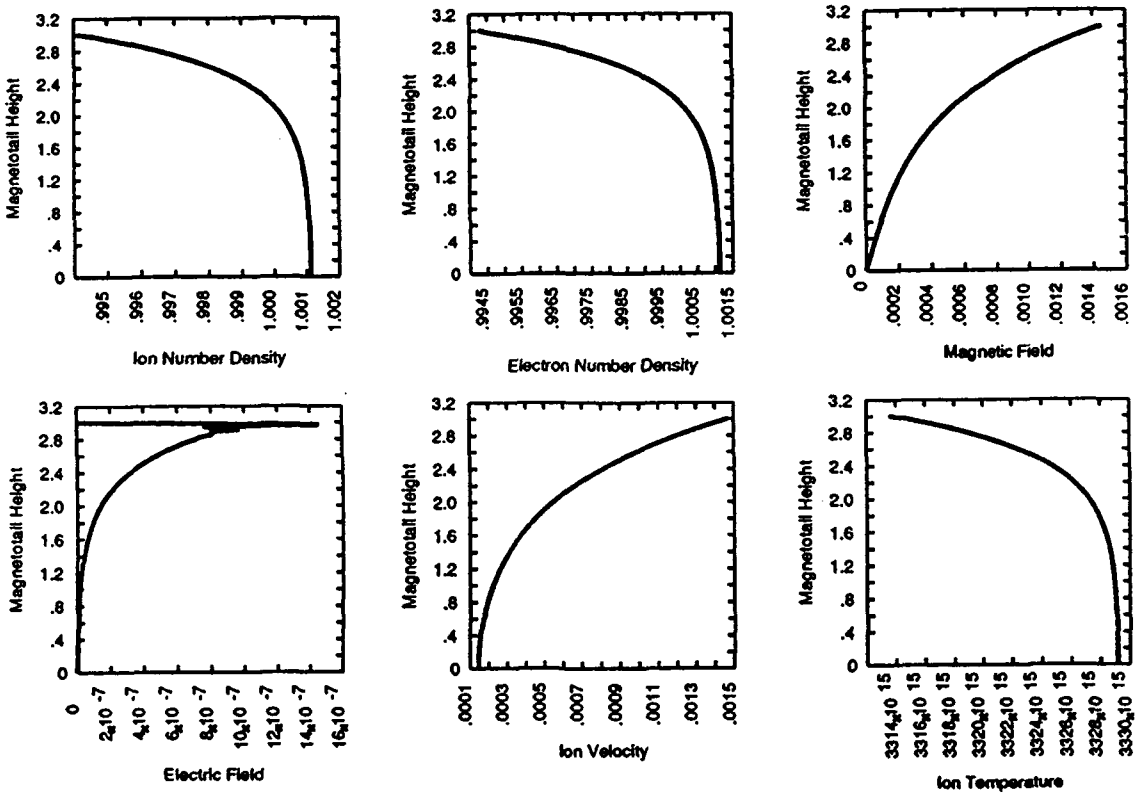

FIG. 31. N-S profiles of number densities (n_1 and n_2), x-component of the magnetic field (B_x), and the z-component of the electric field (E_z) generated from the minimum total energy program.

TABLE IX. Scaling Data Corresponding to Fig. (31).

Dimensioned Parameter	=	Dimensionless Unit	X	Scaling Quantity
n_{RAW} -> 1.0 X 10^{6} [m^{-3}]	=	(1.0)	X	(1.0 X 10^{6} [m^{-3}])
z_{RAW} -> 6.84 X 10^{5} [m]	=	(3.0)	X	(2.28 X 10^{5} [m])
E_{RAW} -> 1.5 X 10^{-5} [V/m]	=	(3.64 X 10^{-9})	X	(4.12 X 10^{3} [V/m])
B_{RAW} -> 2.0 X 10^{-8} [t]	=	(1.46 X 10^{-3})	X	(1.37 X 10^{-5} [t])
C_{RAW} -> 6.9 X 10^{-19} [kgm^4/A^3]	=	(4.59 X 10^{-5})	X	(1.5 X 10^{-14} [kgm^4/A^3])

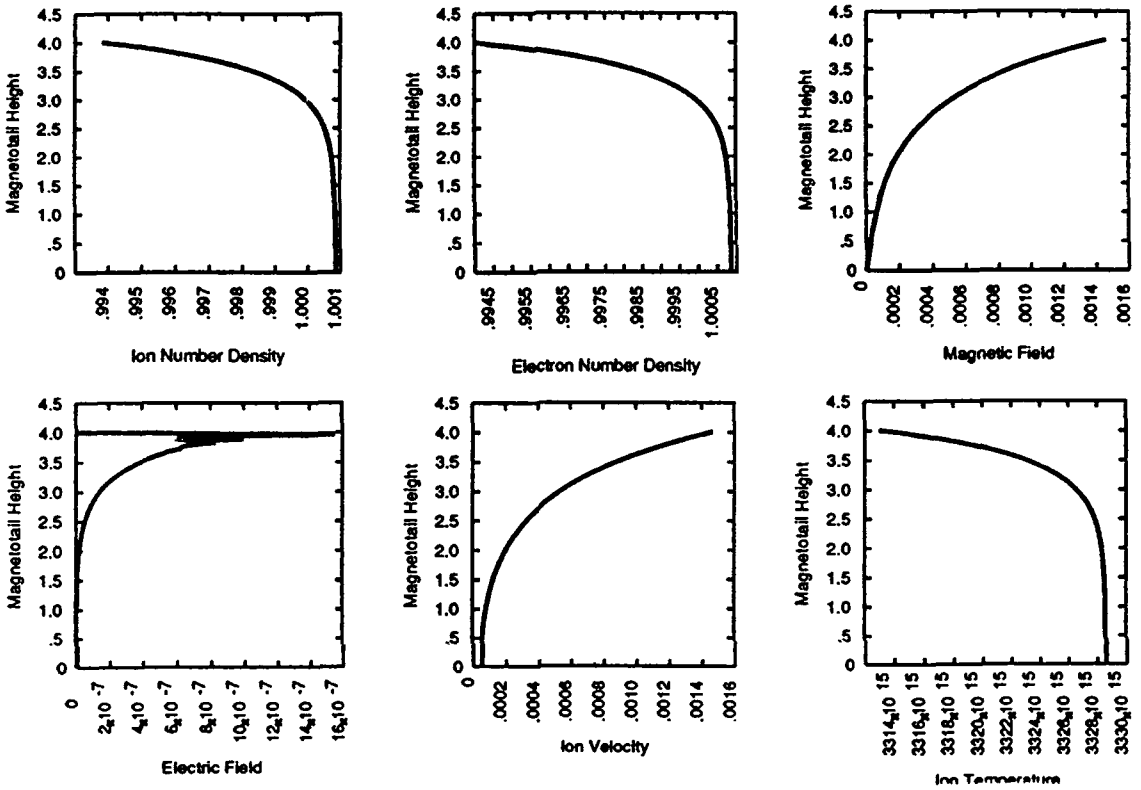

FIG. 32. N-S profiles of number densities (n_1 and n_2), x-component of the magnetic field (B_x), and the z-component of the electric field (E_z) generated from the minimum total energy program.

TABLE X. Scaling Data Corresponding to Fig. (32).

Dimensioned Parameter	=	Dimensionless Unit	X	Scaling Quantity
n_{RAW} -> 1.0 X 10^{6} [m^{-3}]	=	(1.0)	X	(1.0 X 10^{6} [m^{-3}])
z_{RAW} -> 9.12 X 10^{5} [m]	=	(4.0)	X	(2.28 X 10^{5} [m])
E_{RAW} -> 1.5 X 10^{-5} [V/m]	=	(3.64 X 10^{-9})	X	(4.12 X 10^{3} [V/m])
B_{RAW} -> 2.0 X 10^{-8} [t]	=	(1.46 X 10^{-3})	X	(1.37 X 10^{-5} [t])
C_{RAW} -> 6.9 X 10^{-19} [kgm^4/A^3]	=	(4.59 X 10^{-5})	X	(1.5 X 10^{-14} [kgm^4/A^3])

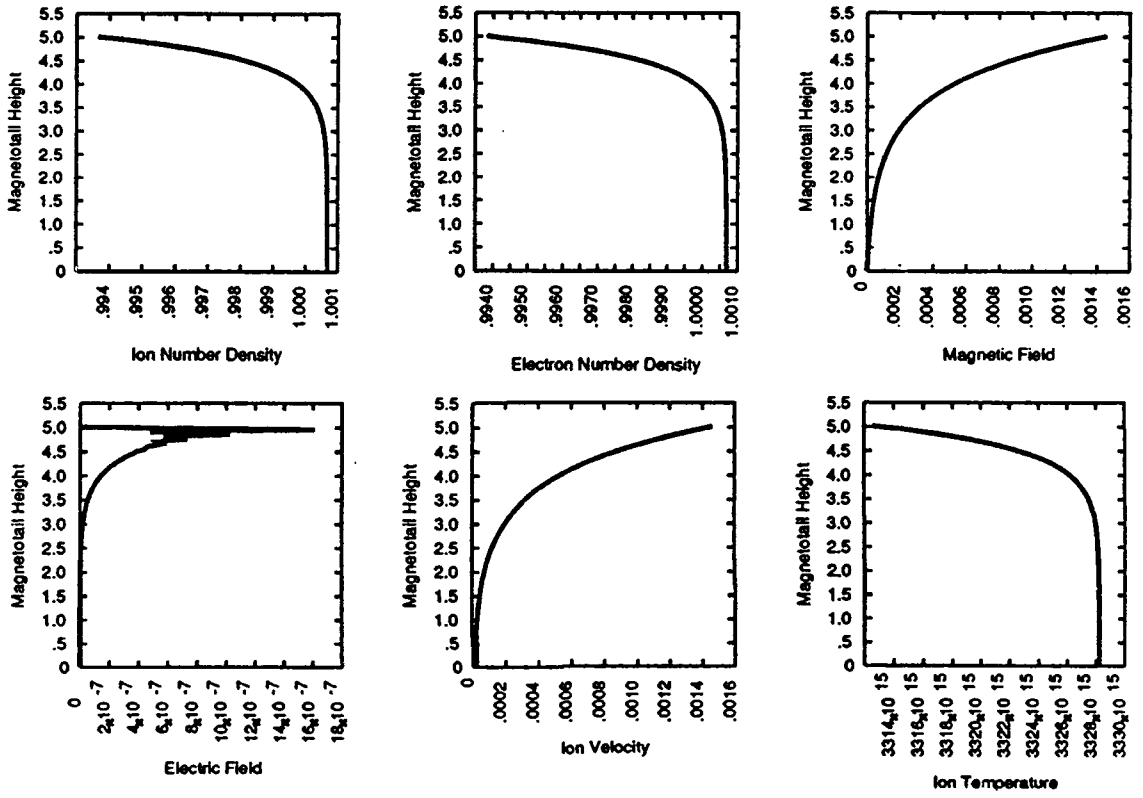

FIG. 33. N-S profiles of number densities (n_1 and n_2), x-component of the magnetic field (B_x), and the z-component of the electric field (E_z) generated from the minimum total energy program.

TABLE XI. Scaling Data Corresponding to Fig. (33).

Dimensioned Parameter	=	Dimensionless Unit	X	Scaling Quantity
n_{RAW} -> 1.0 X 10^{6} [m^{-3}]	=	(1.0)	X	(1.0 X 10^{6} [m^{-3}])
z_{RAW} -> 1.14 X 10^{6} [m]	=	(5.0)	X	(2.28 X 10^{5} [m])
E_{RAW} -> 1.5 X 10^{-5} [V/m]	=	(3.64 X 10^{-9})	X	(4.12 X 10^{3} [V/m])
B_{RAW} -> 2.0 X 10^{-8} [t]	=	(1.46 X 10^{-3})	X	(1.37 X 10^{-5} [t])
C_{RAW} -> 6.9 X 10^{-19} [kgm^4/A^3]	=	(4.59 X 10^{-5})	X	(1.5 X 10^{-14} [kgm^4/A^3])

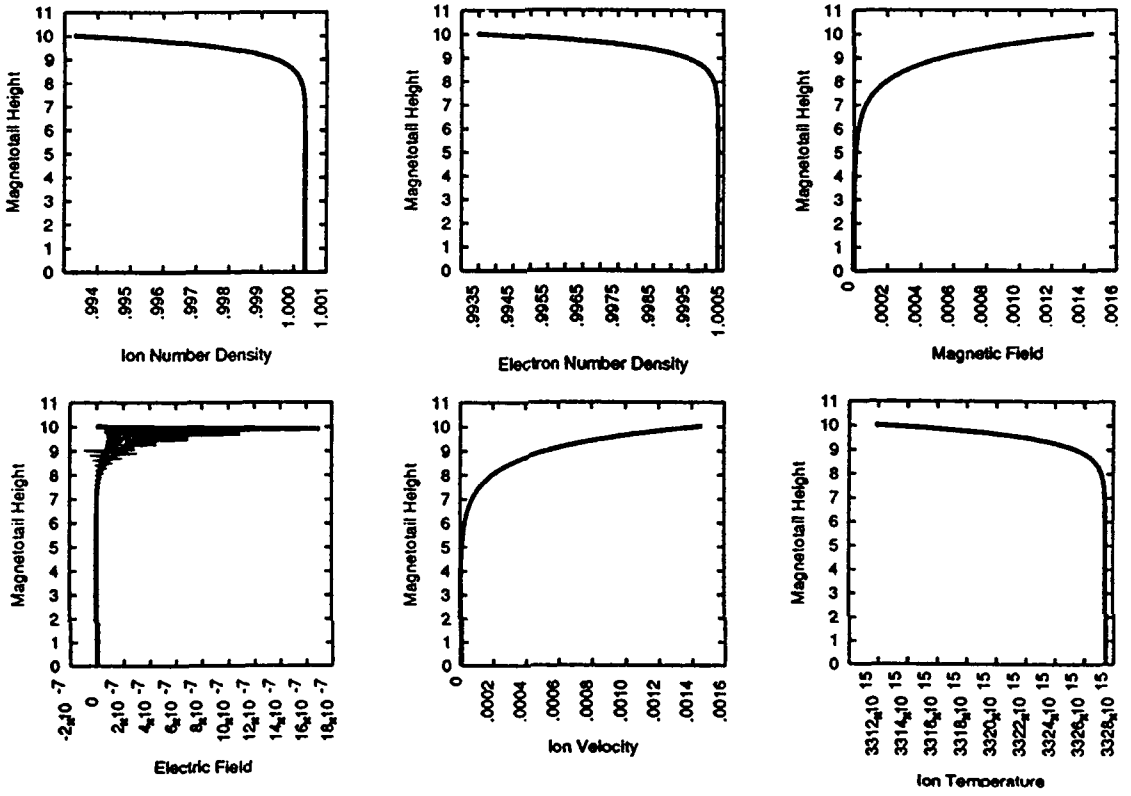

FIG. 34. N-S profiles of number densities (n_1 and n_2), x-component of the magnetic field (B_x), and the z-component of the electric field (E_z) generated from the minimum total energy program.

TABLE XII. Scaling Data Corresponding to Fig. (34).

Dimensioned Parameter	=	Dimensionless Unit	X	Scaling Quantity
n_{RAW} -> 1.0 X 10^{6} [m^{-3}]	=	(1.0)	X	(1.0 X 10^{6} [m^{-3}])
z_{RAW} -> 2.28 X 10^{6} [m]	=	(10.0)	X	(2.28 X 10^{5} [m])
E_{RAW} -> 1.5 X 10^{-5} [V/m]	=	(3.64 X 10^{-9})	X	(4.12 X 10^{3} [V/m])
B_{RAW} -> 2.0 X 10^{-8} [t]	=	(1.46 X 10^{-3})	X	(1.37 X 10^{-5} [t])
C_{RAW} -> 6.9 X 10^{-19} [kgm^4/A^3]	=	(4.59 X 10^{-5})	X	(1.5 X 10^{-14} [kgm^4/A^3])

Comparison of these calculated N-S profiles to those observed in the earth's magnetotail, as well as the overall assessment of the energy minimizing technique presented in this thesis, will be discussed in the next chapter.

CHAPTER V

DATA ANALYSIS

Observed Magnetotail Parameters

The ultimate goal of executing the minimum total energy program (see Appendix 2) is to come up with values for the ion and electron number densities (n_1 and n_2) and for the electric (E_z) and magnetic (B_x) field strengths over the height of the model magnetotail system. Plotting these on a graph yields N-S profiles of these model parameters. By comparing the model's calculated profiles with those obtained from typical values of the earth's magnetotail, we should be able to determine how effective the minimum total energy model is at defining a minimum total energy state of the earth's magnetotail.

Figure 35 depicts a N-S profile of some key parameters typical of the near earth's magnetotail (20 - 30 R_e) during solar quiet times and with a southward interplanetary magnetic field (IMF). In order to compare the profiles in Fig. (35) to the ones generated by the minimum energy model, we must first linearize the logarithmic scales for the number density, flow speed, and ion temperatures (Figs. 36 - 38). Since this N-S profile does not change dramatically for a northward pointing IMF (Lui, 1987), we will assume that the minimum energy model depicts this situation also.

Comparison to Model Output

At first glance, the model generated profiles do not compare very well to the profiles obtained from averaged parameters observed in the earth's magnetotail, but there are some similarities. Looking at the model generated profiles using typical magnetotail values (Figs. 29 - 34), except for height, and noting that we are only looking at the central plasma sheet region, we can make some comparisons between the two profiles. Notice that in both profiles, model generated and

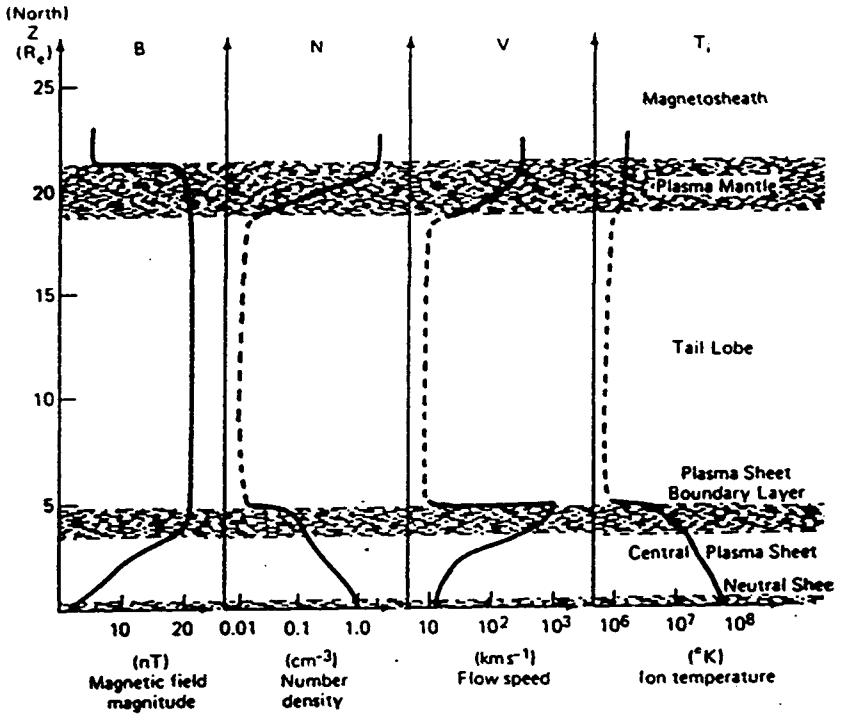

FIG. 35. North-south profiles of magnetic field (B), number density (n), plasma bulk flow speed (v), and ion temperature (T_i) in the midnight region of the magnetotail [Lui, 1987].

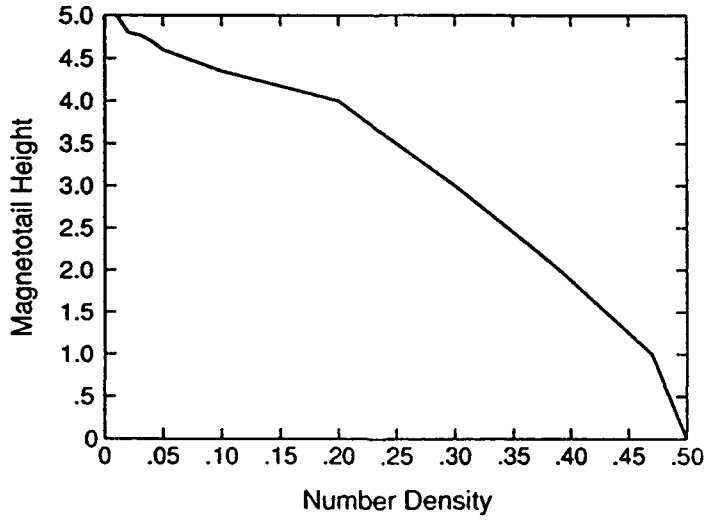

FIG. 36. Number density (n) profile from Fig. (35) using a linear number density scale.

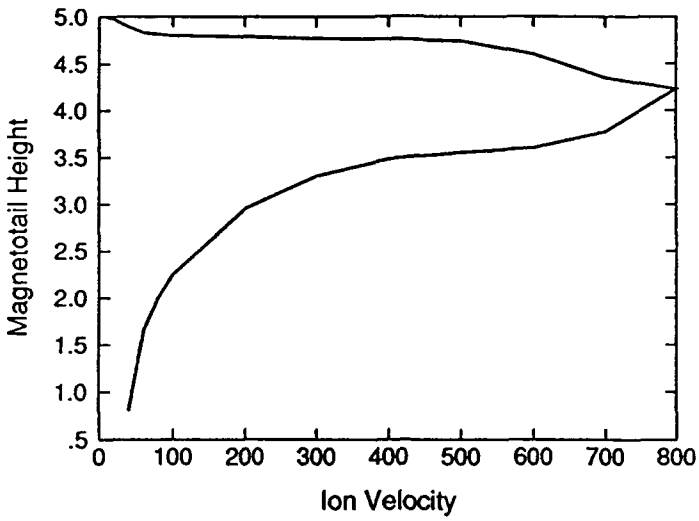

FIG. 37. Plasma bulk flow speed (v) profile from Fig. (35) using a linear velocity scale.

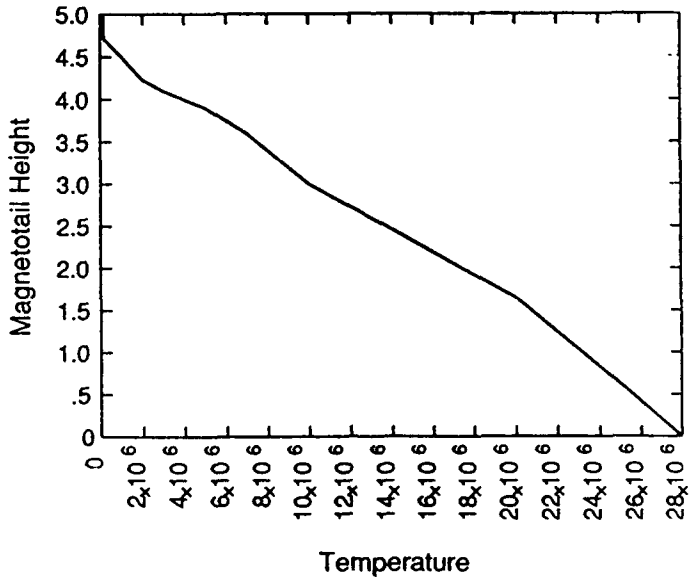

FIG. 38. Ion temperature (T_i) profile from Fig. (35) using a linear temperature scale.

observed, the ion and electron number densities increase rapidly near the upper edges of the boundary (plasma sheet boundary layer for the observed profile). The number densities then increase less rapidly as they approach the center or bottom boundary (neutral sheet) of each profile. The model differs from the observed values in that there is no significant increase in the number densities towards the center of the system (or neutral sheet).

Another similarity occurs in the magnetic field strength profiles. The observed magnetic field strength appears to lose strength more quickly in the top half of the central plasma sheet (3 - 5 R_e) than in the lower half (0 - 3 R_e). The same situation occurs in the model magnetotail, but the magnetic field strength rate changes more rapidly in the upper half of the model and less so (if at all) in the lower half of the profile. This difference becomes more dramatic with increased scale height (Figs 33 - 34).

The velocity and temperature trends for both the magnetotail and model profiles also show some similarities. For instance, both systems have their maximum velocities at their upper boundaries, which decrease until they reach their minimum at the lower boundaries. The temperature trends, on the other hand, show the opposite trend for both systems. Both systems have their lowest temperatures at the upper boundaries, which increase to a maximum at the lower boundaries.

Finally, both the magnetotail and the model systems both display a degree of diamagnetism. In other words, both systems have a tendency to try to get rid of the magnetic field energy from their centers. Looking at the profiles for both systems shows that the magnetic energy is at a minimum near the bottom boundary or center of each system. In the magnetotail system, this magnetic field energy increases slowly away from the center, then about halfway (3 R_e) between the neutral sheet and the plasma sheet boundary layer, the magnetic field strength increases more rapidly. The same thing happens in the model system, but the rate of magnetic field energy strength is more dramatic with increased profile height. The comparisons between the

magnetotail and model systems are summarized in Table XIII.

As mentioned earlier, all the energy parameter changes appear to be confined to the top of all the N-S profiles as the model system's height becomes greater than ten scaling heights ($z = 10 \times z_s$). It appears that any further increases in the profile heights will only stretch the bottom regions of each profile whose values already remain relatively constant at higher heights. This phenomenon seems to suggest that the model is depicting a situation where the majority of the energy changes or action takes place within the outer boundaries or sheaths of the region being

Table XIII. Profile Comparison Summary Between Model and Magnetotail Systems.

Observed	Model
Number density increases rapidly at the Plasma Sheet Boundary Layer, less so near the Neutral Sheet.	Number density increases rapidly at the top boundary, less rapidly at the bottom boundary.
Magnetic field strength decreases quickly near the Plasma Sheet Boundary Layer, less so near the Neutral Sheet.	Magnetic field strength decreases quickly near the top boundary, less so near the bottom boundary.
Plasma bulk flow speeds are greatest near the Plasma Sheet Boundary Layer, lowest near the Neutral Sheet.	Ion velocities are greatest near the top boundary of the model, lowest near the bottom boundary.
Ion temperatures are lowest at the Plasma Sheet Boundary Layer, highest at the Neutral Sheet.	Ion temperatures are lowest at the top boundary of the model, highest at the bottom boundary.
Magnetic field displays some degree of diamagnetism.	Magnetic field displays some degree of diamagnetism.
Height of the top half of the Central Plasma Sheet is about 3.19×10^7 m.	Maximum height of the model is about 2.28×10^6 m.

modeled. Closer inspection of the observed energy profiles in Fig. 35 shows similar trends within or near the Plasma Sheet Boundary Layer just as the model seems to indicate.

There appear to be many reasons to explain the differences observed between the two profiles, and one of the more obvious may be the geometry of the model system. Although the Central Plasma Sheet of the earth's magnetotail can be approximated by a rectangular slab, its height-to-width proportions are not infinite as depicted by the model system. While making the model's length and width dimensions infinite helped keep calculations simple, it did not accurately portray the magnetotail system.

The boundary conditions placed on the model system may also have restricted it too much to accurately depict the magnetotail system. For instance, the model system constrains the z component of the electric field to be zero at both the bottom and top boundaries. Although this constraint keeps the model simple, it may not reflect what is actually observed within the neutral sheet and plasma sheet boundary layer. Some of the boundary conditions may have been too simple due to some of the assumptions made. For example, the model assumes that the z component of the magnetic field equals zero at the bottom boundary (or neutral sheet), which may not be true in the magnetotail. Similar arguments can be made for the other boundary conditions used in the model.

Another possible reason for the differences observed between the two profiles may be that the model may have been oversimplified and does not depict actual magnetotail conditions. For example, the model described in this thesis used only an x component of the magnetic field (no y component). This was done for two reasons. The first was to simplify the calculations required for the minimum total energy program. The second reason was that for a first approximation, the region that the model was trying to depict (the midnight region of the central plasma sheet) the y component of the magnetic field appeared to be negligible compared to the x component. We cannot say the same thing about the z component of the magnetic

field. Because the Central Plasma Sheet is the likely site where anti-parallel magnetic field lines would connect between the northern and southern tail lobes, the z component of the magnetic field does exist within the earth's magnetotail. This z component of the magnetic field would probably have an appreciable effect on the outcome of the model's output.

Another model oversimplification was that it only allowed one species of particles, ions, to move about within the model system. Again, this assumption was used to keep the calculations for the minimum total energy simple. This assumption may have affected the electron number density profile. Given the same initial parameters in the computer program, the electron number density profiles should have looked like the ion number density profiles.

Finally, the model system was assumed to be in a steady-state condition. Observations of the earth's magnetotail suggest that it is rarely, if ever, in a steady-state condition. Therefore, we have a situation where we are trying to compare a steady-state model system to a non steady-state magnetotail. If it were possible to get some profiles of the earth's magnetotail parameters while it experienced a steady-state condition, however briefly, we might see some additional correlations between the model and actual magnetotail systems.

CHAPTER V

CONCLUSIONS

Although the minimum total energy model presented in this thesis is able to depict many of the trends observed within the central plasma sheet of the earth's magnetotail, it is evident that it does not have the sufficient detail to depict it accurately. One similarity that the model does have with the earth's magnetotail, however, is that almost all of the parameter changes occur near the outer or top boundary of the model system. The same thing is true in the earth's central plasma sheet in that the greatest parameter changes also occur near the outer boundary or plasma sheet boundary layer. Another similarity between the model and the earth's central plasma sheet is that both systems show diamagnetic qualities. In other words, both systems show indications of trying to rid their centers of magnetic field energy.

Therefore, the model seems to suggest that in order for the central plasma sheet in the earth's magnetotail to reach a minimum total energy state, it must attempt to eliminate as much energy from the center of its system as possible. The model demonstrates this fact very well with the magnetic field energy. It appears that the model system attempts to reach a minimum total energy state by keeping the magnetic field energy to a minimum near the center, and allowing its energy to increase near the outer boundary. There is some indication that the earth's magnetotail system also shows some indication of trying to keep the magnetic field strength near the neutral sheet to a minimum.

These similarities seem to indicate that although the model may be oversimplified in its present form, it does have a handle on the basic physics governing the energies located within the central plasma sheet. However, it is also evident that further modifications are still needed to make this minimum total energy model useful.

Areas for Future Studies

One of the first steps to improving this model may be to eliminate or modify some of the assumptions used, specifically those discussed in Chapter V. Other areas of improvement include:

a) changing the geometry of the model to better correspond to the shape of the central plasma sheet located within the earth's magnetotail.

b) using boundary conditions that more accurately depict conditions observed within the plasma sheet boundary layer.

c) adding a z component of the magnetic field into the model system.

d) adding a capability into the model to include a gradient up and down the x-axis of magnetotail model. In this way, the model would be able to take into account the processes occurring up and down the magnetotail axis.

e) including additional processes observed within the earth's magnetotail into the model.

f) comparing model output with profiles generated from the earth's magnetotail during northward IMF.

Although this model, in its present form, does not precisely depict the earth's magnetotail system, it may represent, to a first approximation, other systems in non-thermodynamic equilibriums (i.e. radiating systems).

REFERENCES

Adkins, C. J., *Equilibrium Thermodynamics*, Second Edition, McGraw-Hill Book Company (UK) Limited, Maidenhead, England, 1968.

Akasofu, S. I., *Polar and Magnetospheric Substorms*, Springer-Verlag, New York, 1968.

Akasofu, S. I., "Energy Coupling Between the Solar Wind and the Magnetosphere," *Space Sci. Rev.*, 28, 121-190, 1981.

Akasofu, S. I., "Concluding Remarks," in *Magnetospheric Physics*, 429-433, edited by Lui, A. T. Y., John Hopkins University Press, Baltimore, 1987.

Axford, W. I., "Tail of the Magnetosphere," *J. Geophys. Res.*, 70, 1231, 1965.

Carovillano, R. L., J. F. McClay, and H. R. Radoski, "Physics of the Magnetosphere," Springer-Verlag New York Inc., New York, 1967.

Clauer, C. R. and R. L. McPherron, "Mapping the Local Time-Universal Time Development of Magnetospheric Substorms Using Mid-latitude Magnetic Observations," *J. Geophys. Res.*, 79(19), 2811-2820, 1974.

Cowley, S. W. H. and D. J. Southwood, "Some Properties of a Steady-State Geomagnetic Tail," *J. Geophys. Res. Ltrs.*, 7(10), 833-836, 1980.

Eastman, T. E., L. A. Frank, and C. Y. Huang, "The Boundary Layer as the Primary Transport Regions of the Earth's Magnetotail," *J. Geophys. Res.*, 90, 9541, 1985.

Goldstein, H., *Classical Mechanics*, Second Edition, Addison-Wesley Publishing Co., Reading, Massachusetts, 1980.

Gosling, J. T., D. N. Baker, and E. W. Hones, Jr., "Journeys of a Spacecraft," *Los Alamos Science*, 33-53, 1984.

Heikkila, W. J., "Impulsive Plasma Transport through the Magnetotpause," *Geophys. Res. Lett.*, 9, 877, 1982

Hones, E. W. Jr., "The Earth's Magnetotail," *Scientific American*, 40-47, 1986.

Lanzerotti, L. J. and Krimigis, S. M., "Comparative Magnetospheres," *Physics Today*, 24-34, 1985.

Lui, A. T. Y., "Observations on the Fluid Aspects of Magnetotail Dynamics," in *Magnetospheric Physics*, edited by Lui, A. T. Y., Chapter 3, 101-118, John Hopkins University Press, Baltimore, 1987.

Lui, A. T. Y., "Road Map to Magnetotail Domains," in *Magnetospheric Physics*, edited by Lui, A. T. Y., Chapter 1, 3-9, John Hopkins University Press, Baltimore, 1987.

Lundin, R., I. Sandahl, and J. Woch, "The Contribution of the Boundary Layer EMF to Magnetospheric Substorms," in *Magnetospheric Substorms*, Geophysical Monograph 64, edited by Kan, J. R., Potemra, T. A., Kokubun S., and Iijima T., American Geophysical Union, Washington D.C., 1991.

McPherron, R. L., "Physical Process Producing Magnetospheric Substorms and Magnetic Storms," in *Geomagnetism*, Vol 4, edited by J. A. Jacobs, Chapter 7, Academic Press, London, 1991.

National Research Council, *Solar-Terrestrial Research for the 1980's*, National Academy Press, 1981.

Pilipp W. and G. Morfill, "The Plasma Mantle as the Origin of the Plasma Sheet," in *Magnetospheric Particles and Fields*, edited by B. M. McCormac, 55, D. Reidel Publ. Co., Dordrecht, Holland, 1974.

Pippard, A. B., *The Elements of Classical Thermodynamics*, Cambridge, London, 1957.

Sibeck, D. G., "Evidence for Flux Ropes in the Earth's Magnetotail," in *Physics of Magnetic Flux Ropes*, Geophysical Monograph 58, edited by Russell, C. T., Priest, E. R., Lee, L. C., 637-646, American Geophysical Union, Washington D.C., 1990.

Tascione, Thomas F., "Magnetosphere," in *Introduction to the Space Environment*, Chapter 5, Orbit Book Company, Malabar, Florida, 1988.

Williams, D. J., "Ring Current and Radiation Belts," *Rev. of Geophys.* 25(3), 570-578, 1987.

APPENDIXES

APPENDIX A: IMSL DVCPR Program Information

IMSL ROUTINE NAME - DVCPR
(As reproduced from IMSL Library
FORTRAN Subroutines for Mathematics and Statistics)

PURPOSE - Solve a system of ordinary differential equations with boundary conditions at two points, using a variable order, variable step size finite difference method with deferred corrections.

USAGE - Call DVCPR (N, FCNI, FCNJ, FCNB, XA, XB, NGMAX, NGRID, IP, IR, TOL, X, Y, IY, ABT, PAR, WORK, IWORK, IER).

ARGUMENTS - N - Number of differential equations (INPUT).

FCNI - Name of subroutine for evaluating derivatives (INPUT). The subroutine itself must also be provided by the user and it should be of the following form:

```
SUBROUTINE FCNI (N, X, Y, YPRIME)
REAL Y(N), YPRIME(N) ...
```

FCNI should evaluate YPRIME(1) ... YPRIME(N) given N, X, and Y(1) ... Y(N). YPRIME(I) is the derivative of Y(I) with respect to X.

FCNI must appear in an external statement in the calling program.

FCNJ - Name of the subroutine for evaluating the N by N Jacobian matrix of partial derivatives (INPUT). The subroutine itself must also be provided by the user and it should be of the following form:

```
SUBROUTINE FCNJ (N, X, Y, PD)
REAL Y(N), PD(N, N) ...
```

FCNJ should evaluate PD(I, J) for I, J = 1, N, given N, X, and Y(1) ... Y(N). PD(I, j) is the partial derivative of YPRIME(I) with respect to Y(J).

FCNJ must appear in an external statement in the calling program.

FCNB - Name of the subroutine for evaluating the boundary conditions (INPUT). The subroutine itself must also be provided by the user and it should be of the following form:

```
SUBROUTINE FCNB (N, YA, YB, F)
REAL YA(N), YB(N), F(N) ...
```

FCNB should evaluate F(1) ... F(N) given YA(1) ... YA(N), YB(1) ... YB(N). YA(I) and YB(I) are the values of Y(I) at XA and XB, respectively, and the boundary conditions are defined by F(I) = 00.0, I = 1, N. The initial conditions must be defined first, then the coupled conditions, and then the final conditions.

FCNB must appear in an external statement in the calling program.

XA, XB - Two points where boundary conditions are given (INPUT). XA must be less than XB.

NGMAX - Maximum number of grid points to be allowed (INPUT).

NGRID - Number of points in the input grid (counting endpoints). NGRID must be greater than 3. On output, NGRID will contain the final number of grid points (INPUT/OUTPUT).

IP - Number of initial conditions (INPUT). IP must be greater than or equal to 0 and less than N.

IR - Number of coupled boundary conditions (INPUT). IP + IR must be greater than 0 but less than or equal to N.

TOL - Relative error control parameter (INPUT). The computations stop when ABS (ERROR (J, I))/AMAX1 (ABS (Y(J, I), 1.0) is less than TOL for all J = 1 ... N, I = 1 ... NGRID, where ERROR (J, I) is the estimated error in Y(J, I).

X - Vector of length NGMAX containing the final grid. If PAR(4) = 0, the program initialize X to a uniform mesh of NGRID points. Otherwise the user must supply the initial grid on input (INPUT/OUTPUT).

Y - Matrix of dimension N by NGMAX containing the computed solution on the final grid. Y(J, I) will return an approximation to the Jth solution component at X(I). If PAR(4) = 0, the program initialize Y to zero. Otherwise the user must supply initial values for Y (INPUT/OUTPUT).

IY - Row dimension of matrix Y, exactly as specified in the dimension statement (INPUT). IY must be greater than or equal to N.

ABT - Vector of length N containing, in its Jth component, an estimate of the maximum absolute error over the grid points for the Jth solution component (OUTPUT).

PAR - Options vector of length 5 (INPUT). If PAR(1) = 0 the default options are used and the remaining components are ignored. If PAR(1) = 1, all remaining components of PAR must be given a

value. The default value of PAR(I) in each case is zero.

PAR(2) greater than 0 implies that continuation is to be done for this highly nonlinear problem. It is assumed that the user has embedded his problem in a one parameter family

DY/DX = YPRIME (X, Y, EPSNU)
F(Y(A), Y(B), EPSNU) = 0

such that for EPSNU = 0, the problem is simple (e.g. linear), and for EPSNU = 1, the original problem is recovered. The program will automatically attempt to go from EPSNU = 0 to EPSNU = 1. PAR(2) is the starting step in the continuation. The step may be varied by DVCPR but a lower bound the stepsize of 0.01 is imposed. The following common block should appear in subroutines FCNI, FCNJ, and FCNB -

```
COMMON / C1 / EPSNU, CONT
REAL EPSNU
LOGICAL CONT
```

If CONT = .TRUE. vectors YPRIME in subroutine FCNI and F in subroutine FCNB should be defined by

YPRIME(I) = D(YPRIME(I))/D(EPSNU)
F(I) = D(F(I))/D(EPSNU)

and when CONT = .FALSE., YPRIME and F should have their normal definitions.

PAR(3) = 1, implies that intermediate output is to be printed (for debugging purposes).

PAR(4) = 1, implies that initial values for X and Y are supplied by the user.

PAR(5) = 1, implies that the differential equations and boundary conditions are linear, and the algorithm should take advantage of this fact.

WORK - Real work vector of length

N*(3*N*NGMAX+4*N+1)+NGMAX*(7*N+2)

IWORK - Integer work vector of length

2*N*NGMAX+N+NGMAX

IER - Error parameter (OUTPUT).
Terminal error

IER = 129 Illegal values for N, NGRID, IP, or IP.
IER = 130 More than NGMAX grid points are needed to solve the problem.
IER = 131 Newton's iteration diverged.
IER = 132 Newton's iteration reached roundoff error level. If requested precision is not attained, this means that TOL is too small.

APPENDIX B: Minimum Total Energy Program

MINIMUM TOTAL ENERGY PROGRAM

```
REAL Z(1001), K(10, 1001), WORK(384824), ZA, ZB, PAR(5), ABT(3), TOL, U(1001),
  ENERGY(1001), VX(1001), ZBR(1001), N1R(1001), N2R(1001), EZR(1001), BYR(1001),
  QR(1001)

REAL MRAW, QRAW, NRAW, ZRAW, ERAW, BRAW, CRAW, VLIGHT, EPSILON, MU, NS, ZS, ES,
   BS, QS, CS, VS, MQN, BOLT, TRAW

INTEGER IWORK(21031), N, IK, IER, NGMAX, NGRID, IP, IR

INTEGER I, MRATIO

COMMON/XXX/VAR, C, C1, C2, GAM, G1, G2, ZA, ZB, DENSITY, B0, N0

EXTERNAL FCNI, FCNJ, FCNB

**********************************************************************************
**                              OPEN DATA FILES                                 **
**********************************************************************************

OPEN (1, FILE = 'FILENAME.DAT',  STATUS = 'NEW')   [This part of the program opens files
OPEN (2, FILE = 'PLOT-N1.PLT',   STATUS = 'NEW')    storing numerical and plotting data]
OPEN (3, FILE = 'PLOT-N2.PLT',   STATUS = 'NEW')
OPEN (4, FILE = 'PLOT-EFLD.PLT', STATUS = 'NEW')
OPEN (5, FILE = 'PLOT-BFLD.PLT', STATUS = 'NEW')
OPEN (6, FILE = 'PLOT-Q.PLT',    STATUS = 'NEW')

**********************************************************************************
**                    INPUT INITIAL VALUES (HAVING DIMENSIONS)                  **
**********************************************************************************

WRITE (*, *) 'Enter number density (in particles per cubic meter)'      [measured n1
READ  (*, *)  NRAW                                                      or n2]

WRITE (*, *) 'Enter height of magnetotail (in meters)'                  [measured z]
READ  (*, *)  ZRAW

WRITE (*, *) 'Enter z-component of the electric field (in volts per meter)'   [measured Ez]
READ  (*, *)  ERAW

WRITE (*, *) 'Enter x-component of the magnetic field (in teslas)'      [measured Bx]
READ  (*, *)  BRAW

WRITE (*, *) 'Enter magnetotail temperature (in degrees Kelvin)'        [measured T]
READ  (*, *)  TRAW
```

****
** CONSTANTS **
****

VLIGHT	= 3.0×10^{8}	[Velocity of Light]
GAM	= 5.0 / 3.0	[Gamma = Ratio of Specific Heats]
EPSILON	= 8.85×10^{-12}	[Permittivity of Free Space]
MU	= 1.257×10^{-6}	[Permeability of Free Space]
BOLT	= 1.381×10^{-23}	[Boltzmann Constant]
M_{RAW}	= 1.67×10^{-27}	[Mass of Ion in kgs]
Q_{RAW}	= 1.602×10^{-19}	[Electron Charge]
C_{RAW}	= (BOLT) * (T_{RAW})*$(N_{RAW} \times 10^{(1-GAM)})$	[Calculated Adiabatic Constant]

****
** SCALING QUANTITIES **
****

N_{RAW}	= Inputted from above	[Measured Number Density]
N_S	= N_{RAW}	[Scaled num den = measured num den]
Z_S	= Sqrt $(M_{RAW} / (MU * N_{RAW} * Q_{RAW}^2))$	[Scaled magnetotail ht]
E_S	= $(Q_{RAW} * N_S * Z_S) / (EPSILON)$	[Scaled E fld strength]
B_S	= $(E_S) / (VLIGHT)$	[Scaled B fld strength]
Q_S	= $(Q_{RAW} * N_S * Z_S)$	[Scaled Chg conserve term]
C_S	= $(VLIGHT^2) * N_S^{(1 - GAM)} * M_{RAW}$	[Scaled adiabatic constant]

****
** DIMENSIONLESS VALUES **
****

Z_{RAW}	= Inputted from above (measured magnetotail height in meters)
E_{RAW}	= Inputted from above (measured electric field in volts per meter)
B_{RAW}	= Inputted from above (measured magnetic field in teslas)
C_{RAW}	= Calculated from above (adiabatic constant)

N_0	= N_{RAW} / N_S	[Num den w/ units]
Z_0	= Z_{RAW} / Z_S	[Magnetotail ht w/ units]
E_0	= E_{RAW} / E_S	[E fld w/ units]
B_0	= B_{RAW} / B_S	[B fld w/ units]
C_0	= C_{RAW} / C_S	[Adiabatic constant w/ units]
C_1	= C_0	[Adiabatic constant for ions]
C_2	= C_0	[Adiabatic constant for electrons]
G_1	= $1 / (C_1 * GAM)$	
G_2	= $1 / (C_2 * GAM)$	

```
**********************************************************************************************
**                                  DVCPR ARGUMENT SETUP                                    **
**********************************************************************************************

N          = 10                    [Number of variables]
Z_A        = 0                     [Height of bottom surface of model]
Z_B        = Z0                    [Height of top surface of model]
NGMAX      = 1001                  [Number of grid points}
NGRID      = 100                   [Number of horizontal slices in model]
IP         = 5                     [Number of initial conditions]
IR         = 0                     [Number of coupled boundary conds]
IK         = 10                    [Number of output columns]
TOL        = 0.01                  [Relative error parameter]
PAR(1)     = 1                     [No defaults]
PAR(2)     = 0
PAR(3)     = 0                     [No printed output for debugging]
PAR(4)     = 1                     [Values for X and Y supplied by user]
PAR(5)     = 0                     [Diff Eqs. and B.C.s are not linear]

**********************************************************************************************
**                                  INITIAL GUESS                                           **
**********************************************************************************************

RMM1       = NGRID - 1             [This part of the program divides the
                                    magnetotail into evenly spaced Z(I)
DO 10 I    = 1, NGRID              horizontal planes]
RIM1       = I - 1
Z(I)       = ZA + RIM1/RMM1 * (ZB - ZA)

K(1, I)    = N0                    [Estimated ion num density (N) at ht I]
K(2, I)    = N0                    [Estimated electron num density at ht I]
K(3, I)    = 0                     [Estimated electric field at ht I]
K(4, I)    = Z(I) * (B_0 / Z_B)    [Estimated magnetic field at ht I]
K(5, I)    = Z(I) * (N_0 * Z_B) / Z_B  [Estimated charge conservation at ht I]
K(6, I)    = 0                     [Lagrangian equiv of n_1 at ht I]
K(7, I)    = 0                     [Lagrangian equiv of n_2 at ht I]
K(8, I)    = 0                     [Lagrangian equiv of E_z at ht I]
K(9, I)    = 0                     [Lagrangian equiv of B_x at ht I]
K(10, I)   = 0                     [Lagranfian equiv of Q_z at ht I]

10 CONTINUE
```

```
**********************************************************************************************
**                        CALL THE IMSL SUBROUTINE DVCPR                                    **
**********************************************************************************************

CALL DVCPR (N, FCNI, FCNJ, FCNB, ZA, ZB, NGMAX, NGRID, IP, IR, TOL, Z, K, IK, ABT, PAR,
            WORK, IWORK, IER)

IF (IER .GT. 100) GOTO 200

**********************************************************************************************
**                  TRANSFORM DIMENSIONLESS VARIABLE TO REAL VALUES                         **
**********************************************************************************************

DO 800 I    = 1, NGRID                          [Real Value = Dimensionless value
                                                          x scaled quantity]
Z_BR(I)     = Z(I)    * Z_S                     [Yields real magnetotail ht at ht I]
N_1R(I)     = K(1, I) * N_RAW                   [Yields real ion num density at ht I]
N_2R(I)     = K(2, I) * N_RAW                   [Yields real elect num density at ht I]
E_ZR(I)     = K(3, I) * E_S                     [Yields real E fld strength at ht I]
B_YR(I)     = K(4, I) * B_S                     [Yields real B fld strength at ht I]
Q_R(I)      = K(5, I) * Q_S

800 CONTINUE

**********************************************************************************************
**                          FORMAT THE DVCPR OUTPUT                                       **
**********************************************************************************************
```

Once the system of ordinary differential equations are calculated by this program we want the out put to be formatted as follows:

Interval	Value of Z at Ht (I)	Value of n_1 at Ht (I)	Value of n_2 at Ht (I)	Value of E_z at Ht (I)	Value of B_x at Ht (I)
Z (I)	K (1, I)	K (2, I)	K (3, I)	K (4, I)	K (5, I)
.	.	.	.	.	.
.	.	.	.	.	.

Interval	Value of Q_z at Ht (I)	Value of λ_1 at Ht (I)	Value of λ_2 at Ht (I)	Value of λ_z at Ht (I)	Value of λ_x at Ht (I)
Z (I)	K (5, I)	K (6, I)	K (7, I)	K (8, I)	K (9, I)
.	.	.	.	.	.
.	.	.	.	.	.

(This data can be transferred into a plotting routine in order to make N-S profiles of the desired parameters).

```
**********************************************************************************************
**          CALCULATING THE MINIMUM TOTAL ENERGY (U) OF THE MAGNETOTAIL                     **
**********************************************************************************************

DO 141      = 1, NGRID

V_y(I)      = [-K(6, I) / C_1 * GAM)] * [ K(1, I)^(1-GAM)] * B_x + K(9, I)
```

$$\text{or} \qquad \left[V_y = -\frac{\lambda_1}{C_1 \gamma} (n_1)^{1-\gamma} (B_x) + \lambda_{B_x} \right]$$

```
U(I)        = 0.5 * K(1, I) * [(V_y(I))^2] + 0.5 * K(3, I)^2 + 0.5 * K(4, I)^2 + C_1 * K(1, I)^GAM +
              C_2 * K(2, I)^GAM
```

$$\text{or} \qquad \left[U (I) = \frac{n_1 v_y^2}{2} + \frac{E_x^2}{2} + \frac{B_x^2}{2} + C_1 (n_1)^{\gamma} + C_2 (n_2)^{\gamma} \right]$$

```
ENERGY(I) = U(I)
WRITE (1, 145) 'Energy at Ht [z(I)] is [ENERGY(I)]'

SUM       = 0
DO 160 I  = 1, NGRID
SUMNEXT   = ENERGY(I) + SUM
SUM       = SUMNEXT
UTOTAL    = SUMNEXT
```

$$\text{or} \quad \left[U (\text{TOTAL}) = \sum_{Z_A}^{Z_B} \left\{ \frac{n_1 v_y^2}{2} + \frac{E_x^2}{2} + \frac{B_x^2}{2} + C_1 (n_1)^{\gamma} + C_2 (n_2)^{\gamma} \right\} \right]$$

```
WRITE (1, 170) 'The minimum value of U with a magnetotail ht of [Z_B] is [UTOTAL]'

200  TYPE *, 'Run terminated because IER = [IER]'

END
```

```
**********************************************************************************************
**                  SUBROUTINE FOR CALCULATING THE DIFFERENTIAL EQUATIONS                    **
**********************************************************************************************

SUBROUTINE FCNI (N, Z, K, KPRIME)
REAL X, K(N), KPRIME(N), n1, n2, Ez, Bx, Qz, λ1, λ2, λE, λB, λQ, vy
INTEGER N
COMMON/XXX/VAR, C, C1, C2, GAM, G1, G2, ZA, ZB, DENSITY, B0, N0

n1      = K(1)
n2      = K(2)
Ez      = K(3)
Bx      = K(4)
Qz      = K(5)
λ1      = K(6)
λ2      = K(7)
λz      = K(8)
λx      = K(9)
λz      = K(10)

vy      = [ +λ1 * G1 * ( n1 )^1-GAM * Bx - λx ]   or [ vy = + λ1 ( n1 )^1-γ ( Bx ) / C1γ - λBx ];

KPRIME(1) = [ G1 * ( n1 )^2-GAM ]
          * [ Ez - ( vy * Bx ) ]                   or [ ∂n1/∂z = + ( n1 )^2-γ( Ez - vyBx ) / C1γ ];

KPRIME(2) = [ -G2 * ( n2 )^2-GAM ] * [ Ez ]        or [ ∂n2/∂z = - ( n2 )^2-γ( Ez ) / C2γ ];

KPRIME(3) = [ n1 - n2 ]                            or [ ∂Ez/∂z = + ( n1 - n2 ) ];

KPRIME(4) = [ n1 * vy ]                            or [ ∂Bx/∂z = + ( n1vy ) ];

KPRIME(5) = [ n1 ]                                 or [ ∂Qz/∂z = + ( n1 ) ];
```

KPRIME(6) = [(-.5 * v_y^2) - (C_1 * GAM * (n_1)$^{GAM-1}$)
+ (λ_1 * G_1 * (2 - GAM) * (n_1)$^{1-GAM}$
* (- E_z + (v_y * B_x)) - λ_E
- (λ_x * v_y) - λ_Q

or [$\frac{\partial \lambda_1}{\partial z} = -\frac{v_y^2}{2} - C_1 \gamma (n_1)^{\gamma-1}$
$+ \frac{\lambda_1 (2-\gamma)(n_1)^{1-\gamma}}{C_1\gamma}$
$\times (- E_z + v_y B_x) - \lambda_{B_z}$
$- (\lambda_{B_z} v_y) - \lambda_{Q_z}$];

KPRIME(7) = [$-C_2$ * GAM * (n_2)$^{GAM-1}$]
+ [λ_2 * G_2 * (2 - GAM)
* (n_2)$^{1-GAM}$ * E_z]
+ λ_E

or [$\frac{\partial \lambda_2}{\partial z} = - C_2 \gamma (n_2)^{\gamma-1}$
$+ \frac{\lambda_2 (2-\gamma)}{C_2\gamma}$
$\times (n_2)^{1-\gamma} (E_z)$
$+ \lambda_{B_z}$];

KPRIME(8) = [$-E_z$ - λ_1 * G_1 * (n_1)$^{2-GAM}$]
+ [λ_2 * G_2 * (n_2)$^{2-GAM}$]

or [$\frac{\partial \lambda_{B_z}}{\partial z} = - E_z - \frac{\lambda_1 (n_1)^{2-\gamma}}{C_1\gamma}$
$+ \frac{\lambda_2 (n_2)^{2-\gamma}}{C_2\gamma}$];

KPRIME(9) = [$-B_x + \lambda_1$ * G_1 * (n_1)$^{2-GAM}$ * v_y]

or [$\frac{\partial \lambda_{B_x}}{\partial z} = - B_x + \frac{\lambda_1 (n_1)^{2-\gamma} (v_y)}{C_1\gamma}$];

KPRIME(10) = [0]

or [$\frac{\partial Q_z}{\partial z} = (0)$];

RETURN
END

****
** SUBROUTINE FOR CALCULATING THE JACOBIAN MATRIX **
****

SUBROUTINE FCNJ (N, Z, K, PD)

REAL Z, K(N), PD(N,N), n_1, n_2, E_z, B_x, Q_z, λ_1, λ_2, λ_E, λ_B, λ_Q, v_y, $\frac{\partial v_y}{\partial n_1}$, $\frac{\partial v_y}{\partial \lambda_1}$, $\frac{\partial v_y}{\partial B_x}$

INTEGER N

COMMON/XXX/VAR, C, C_1, C_2, GAM, G_1, G_2, Z_A, Z_B, DENSITY, B_0, N_0

n_1 = K(1)
n_2 = K(2)
E_z = K(3)
B_x = K(4)
Q_z = K(5)
λ_1 = K(6)
λ_2 = K(7)
λ_z = K(8)
λ_x = K(9)
λ_z = K(10)

v_y = [$+\lambda_1 * G_1 * (n_1)^{2-GAM} * B_x - \lambda_x$] or [$v_y = + \frac{\lambda_1 (n_1)^{1-\gamma} (B_x)}{C_1 \gamma} - \lambda_{B_x}$];

DO 300 I = 1, 10
DO 310 J = 1, 10
PD(I, J) = 0.0
310 CONTINUE
300 CONTINUE

$\frac{\partial v_y}{\partial n_1}$ = [$+G_1 * \lambda_1 * (1 - GAM)$] $* [(1 / (n_1)^{GAM}) * B_x]$ or [$\frac{\partial v_y}{\partial n_1} = + \frac{\lambda_1 (1 - \gamma) (B_x)}{C_1 \gamma (n_1)^{\gamma}}$];

$\frac{\partial v_y}{\partial B_x}$ = [$1 + G_1 * \lambda_1 * (n_1)^{1-GAM}$] or [$\frac{\partial v_y}{\partial B_x} = 1 + \frac{\lambda_1 (n_1)^{1-\gamma}}{C_1 \gamma}$];

$\frac{\partial v_y}{\partial \lambda_1}$ = [$+G_1 * (n_1)^{1-GAM} * B_y$] or [$\frac{\partial v_y}{\partial \lambda_1} = + \frac{(n_1)^{1-\gamma} (B_x)}{C_1 \gamma}$];

$\frac{\partial v_y}{\partial \lambda_{B_x}}$ = [-1.0] or [$\frac{\partial v_y}{\partial \lambda_{B_x}} = - (1.0)$];

$$PD(1,1) = [\, G_1 * (2 - GAM) * (n_1)^{1-GAM} * (E_z - v_y * B_x) \,] - [\, G_1 * (n_1)^{2-GAM} * (\frac{\partial v_y}{\partial n_1} * B_x) \,] \quad \text{or} \quad [\, \frac{\partial n_1}{\partial n_1} = \frac{(2-\gamma)(n_1)^{1-\gamma}}{C_1\gamma} \times (E_z - v_y B_x) - \frac{(n_1)^{2-\gamma}(\frac{\partial v_y}{\partial n_1} B_x)}{C_1\gamma} \,];$$

$$PD(1,3) = [\, G_1 * (n_1)^{2-GAM} \,] \quad \text{or} \quad [\, \frac{\partial n_1}{\partial E_z} = \frac{(n_1)^{2-\gamma}}{C_1\gamma} \,];$$

$$PD(1,4) = [\, -G_1 * (n_1)^{2-GAM} * (B_x * \frac{\partial v_y}{\partial B_x} + v_y) \,] \quad \text{or} \quad [\, \frac{\partial n_1}{\partial B_x} = -\frac{(n_1)^{2-\gamma}}{C_1\gamma} \times (B_x)(\frac{\partial v_y}{\partial B_x}) + v_y \,];$$

$$PD(1,6) = [\, -G_1 * (n_1)^{2-GAM} * (B_x * \frac{\partial v_y}{\partial \lambda_1}) \,] \quad \text{or} \quad [\, \frac{\partial n_1}{\partial \lambda_1} = -\frac{(n_1)^{2-\gamma}(B_x)(\frac{\partial v_y}{\partial \lambda_1})}{C_1\gamma} \,];$$

$$PD(1,9) = [\, -G_1 * (n_1)^{2-GAM} * (B_x * \frac{\partial v_y}{\partial \lambda_{B_x}}) \,] \quad \text{or} \quad [\, \frac{\partial n_1}{\partial \lambda_{B_x}} = -\frac{(n_1)^{2-\gamma}(B_x)(\frac{\partial v_y}{\partial \lambda_{B_x}})}{C_1\gamma} \,];$$

$$PD(2,2) = [\, -G_2 * (2 - GAM) * (n_2)^{1-GAM} * (E_z) \,] \quad \text{or} \quad [\, \frac{\partial n_2}{\partial n_2} = -\frac{(2-\gamma)(n_2)^{1-\gamma}(E_z)}{C_2\gamma} \,];$$

$$PD(2,3) = [\, -G_2 * (n_2)^{2-GAM} \,] \quad \text{or} \quad [\, \frac{\partial n_2}{\partial E_z} = -\frac{(n_2)^{2-\gamma}}{C_2\gamma} \,];$$

$PD(3, 1) = [+1.0]$ or $[\frac{\partial E_z}{\partial n_1} = +(1.0)];$

$PD(3, 2) = [-1.0]$ or $[\frac{\partial E_z}{\partial n_2} = -(1.0)];$

$PD(4, 1) = [(n_1 * \frac{\partial v_y}{\partial n_1}) + v_y]$ or $[\frac{\partial B_x}{\partial n_1} = (n_1)(\frac{\partial v_y}{\partial n_1}) + v_y];$

$PD(4, 4) = [n_1 * \frac{\partial v_y}{\partial B_x}]$ or $[\frac{\partial B_x}{\partial B_x} = (n_1)(\frac{\partial v_y}{\partial B_x})];$

$PD(4, 6) = [n_1 * \frac{\partial v_y}{\partial \lambda_1}]$ or $[\frac{\partial B_x}{\partial \lambda_1} = (n_1)(\frac{\partial v_y}{\partial \lambda_1})];$

$PD(4, 9) = [n_1 * \frac{\partial v_y}{\partial \lambda_{B_x}}]$ or $[\frac{\partial B_x}{\partial \lambda_{B_x}} = (n_1)(\frac{\partial v_y}{\partial \lambda_{B_x}})];$

$PD(5, 1) = [+1.0]$ or $[\frac{\partial Q_x}{\partial n_1} = +(1.0)];$

$$PD(6,1) = \left[\left(-v_y * \frac{\partial v_y}{\partial n_1} \right) \right. \quad \text{or} \quad \left[\frac{\partial \lambda_1}{\partial n_1} = -\left(v_y \right)\left(\frac{\partial v_y}{\partial n_1} \right) \right.$$

$$- (1/G_1) * (GAM - 1) * (n_1)^{GAM-2} \qquad - (C_1\gamma)(\gamma - 1)(n_1)^{\gamma-2}$$

$$+ (G_1 * \lambda_1 * (2 - GAM)) \qquad + \frac{\lambda_1 (2 - \gamma)}{C_1\gamma}$$

$$* ((1 - GAM) * (n_1)^{-GAM} \qquad \times (1 - \gamma)(n_1)^{-\gamma}$$

$$* (-E_z + vy * Bx)) \qquad \times (-E_z + v_y B_x)$$

$$+ L1 * (G_1 * (n_1)^{1-GAM} * \left(\frac{\partial v_y}{\partial n_1} * B_x \right) \qquad + \lambda_1 (n_1)^{1-\gamma} \left(\frac{\partial v_y}{\partial n_1} \right)(B_x)$$

$$* (2 - GAM) - \left(\lambda_{B_x} * \frac{\partial v_y}{\partial n_1} \right)] \qquad \times (2 - \gamma) - \lambda_{B_x} \left(\frac{\partial v_y}{\partial n_1} \right)];$$

$$PD(6,3) = [-G_1 * \lambda_1 * (2 - GAM) \qquad \text{or} \quad \left[\frac{\partial \lambda_1}{\partial E_z} = -\frac{\lambda_1 (2 - \gamma)(n_1)^{1-\gamma}}{C_1\gamma} \right];$$

$$* (n_1)^{1-GAM}]$$

$$PD(6,4) = \left[\left(-v_y * \frac{\partial v_y}{\partial B_x} \right) \right. \quad \text{or} \quad \left[\frac{\partial \lambda_1}{\partial B_x} = -\left(v_y \right)\left(\frac{\partial v_y}{\partial B_x} \right) \right.$$

$$+ (G_1 * \lambda_1 * (2 - GAM) \qquad + \frac{\lambda_1 (2 - \gamma)}{C_1\gamma}$$

$$* (n_1)^{1-GAM} * \frac{\partial v_y}{\partial B_x} * B_x) \qquad \times (n_1)^{1-\gamma} \left(\frac{\partial v_y}{\partial B_x} \right)(B_x)$$

$$- \left(\lambda_{B_x} * \frac{\partial v_y}{\partial B_x} \right) \qquad - \lambda_{B_x} \left(\frac{\partial v_y}{\partial B_x} \right)$$

$$+ (G_1 * \lambda 1 * (n_1)^{1-GAM} * v_y)] \qquad + \frac{\lambda_1 (2 - \gamma)(n_1)^{1-\gamma}(v_y)}{C_1\gamma}];$$

$$PD(6,6) = [\,(-v_y * \frac{\partial v_y}{\partial \lambda_1}) + (G_1 * \lambda_1 * (2 - GAM) * (n_1)^{1-GAM} * \frac{\partial v_y}{\partial \lambda_1} * B_x) - (G_1 * (2 - GAM)) * (n_1)^{1-GAM} * (-E_z + v_y * B_x) - (\lambda_{B_z} * \frac{\partial v_y}{\partial \lambda_1})\,]$$

$$\text{or } [\,\frac{\partial \lambda_1}{\partial \lambda_1} = -(v_y)(\frac{\partial v_y}{\partial \lambda_1}) + \frac{\lambda_1 (2 - \gamma)}{C_1 \gamma} \times (n_1)^{1-\gamma}(\frac{\partial v_y}{\partial \lambda_1})(B_x) - \frac{(2 - \gamma)}{C_1 \gamma} \times (n_1)^{1-\gamma}(-E_z + v_y B_x) - \lambda_{B_z}(\frac{\partial v_y}{\partial \lambda_1})\,];$$

$$PD(6,8) = [\,-1.0\,]$$

$$\text{or } [\,\frac{\partial \lambda_1}{\partial \lambda_{B_z}} = -(1.0)\,];$$

$$PD(6,9) = [\,(-v_y * \frac{\partial v_y}{\partial \lambda_{B_z}}) + (G_1 * \lambda_1 * (2 - GAM) * (n_1)^{1-GAM} * \frac{\partial v_y}{\partial \lambda_{B_z}} * B_x) - (\lambda_{B_z} * \frac{\partial v_y}{\partial \lambda_{B_z}}) - v_y\,]$$

$$\text{or } [\,\frac{\partial \lambda_1}{\partial \lambda_{B_z}} = -(v_y)(\frac{\partial v_y}{\partial \lambda_{B_z}}) + \frac{\lambda_1 (2 - \gamma)}{C_1 \gamma} \times (n_1)^{1-\gamma}(\frac{\partial v_y}{\partial B_z})(B_z) - \lambda_{B_z}(\frac{\partial v_y}{\partial B_z}) - v_y\,];$$

$$PD(6,10) = [\,-1.0\,]$$

$$\text{or } [\,\frac{\partial \lambda_1}{\partial \lambda_{Q_z}} = -(1.0)\,];$$

$$PD(7,2) = [\,(-1/G_2) * (GAM-1) * (n_2)^{GAM-2} + (\lambda_2 * G_2) * (2-GAM) * (1-GAM) * (n_2)^{-GAM} * E_z\,]$$

$$\text{or } [\,\frac{\partial \lambda_2}{\partial n_2} = -(C_2\gamma)(\gamma-1) \times (n_2)^{\gamma-2} + \frac{\lambda_2}{C_2\gamma} \times (2-\gamma)(1-\gamma) \times (n_2)^{-\gamma}(E_z)\,];$$

$$PD(7,3) = [\,G_2 * \lambda_2 * (2-GAM) * (n_2)^{1-GAM}\,]$$

$$\text{or } [\,\frac{\partial \lambda_2}{\partial E_z} = \frac{\lambda_2 (2-\gamma)(n_2)^{1-\gamma}}{C_2\gamma}\,];$$

$$PD(7,7) = [\,G_2 * (2-GAM) * (n_2)^{1-GAM} * E_z\,]$$

$$\text{or } [\,\frac{\partial \lambda_2}{\partial \lambda_2} = \frac{(2-\gamma)(n_2)^{1-\gamma}(E_z)}{C_2\gamma}\,];$$

$$PD(7,8) = [\,+1.0\,]$$

$$\text{or } [\,\frac{\partial \lambda_2}{\partial \lambda_{E_z}} = +(1.0)\,];$$

$$PD(8,1) = [\, -G_1 * \lambda_1 * (2 - GAM) * (n_1)^{1-GAM} \,] \quad \text{or} \quad \left[\frac{\partial \lambda_{E_z}}{\partial n_1} = - \frac{\lambda_1 (2 - \gamma)(n_1)^{1-\gamma}}{C_1 \gamma} \right];$$

$$PD(8,2) = [\, G_2 * \lambda_2 * (2 - GAM) * (n_2)^{1-GAM} \,] \quad \text{or} \quad \left[\frac{\partial \lambda_{E_z}}{\partial n_2} = + \frac{\lambda_2 (2 - \gamma)(n_2)^{1-\gamma}}{C_2 \gamma} \right];$$

$$PD(8,3) = [\, -1.0 \,] \quad \text{or} \quad \left[\frac{\partial \lambda_{E_z}}{\partial E_z} = - (1.0) \right];$$

$$PD(8,6) = [\, -G_1 * (n_1)^{2-GAM} \,] \quad \text{or} \quad \left[\frac{\partial \lambda_{E_z}}{\partial \lambda_{n_1}} = - \frac{(n_1)^{2-\gamma}}{C_1 \gamma} \right];$$

$$PD(8,7) = [\, G_2 * (n_2)^{2-GAM} \,] \quad \text{or} \quad \left[\frac{\partial \lambda_{E_z}}{\partial \lambda_{n_2}} = + \frac{(n_2)^{2-\gamma}}{C_2 \gamma} \right];$$

$$PD(9,1) = [\, G_1 * \lambda_1 * (n_1)^{2-GAM} * \left(\frac{\partial v_y}{\partial n_1} \right) + G_1 * \lambda_1 * (2 - GAM) * (n_1)^{1-GAM} * v_y \,]$$

$$\text{or} \quad \left[\frac{\partial \lambda_{E_z}}{\partial n_1} = + \frac{\lambda_1 (n_1)^{2-\gamma} \left(\frac{\partial v_y}{\partial n_1} \right)}{C_1 \gamma} + \frac{\lambda_1 (2 - \gamma)(n_1)^{1-\gamma} (v_y)}{C_1 \gamma} \right];$$

$$PD(9,4) = [\,-1 + G_1 * \lambda_1 * (n_1)^{2\text{-}GAM} * \left(\frac{\partial v_y}{\partial n_1}\right)\,] \quad \text{or} \quad \left[\frac{\partial \lambda_{B_x}}{\partial B_x} = -1 + \frac{\lambda_1 (n_1)^{2-\gamma} \left(\frac{\partial v_y}{\partial B_x}\right)}{C_1 \gamma}\right];$$

$$PD(9,6) = [\,G_1 * (n_1)^{2\text{-}GAM} * \left(\lambda_1 * \frac{\partial v_y}{\partial \lambda_1} + v_y\right)\,] \quad \text{or} \quad \left[\frac{\partial \lambda_{B_x}}{\partial \lambda_1} = + \frac{\lambda_1 (n_1)^{2-\gamma} \left(\frac{\partial v_y}{\partial \lambda_1}\right)}{C_1 \gamma} + \frac{(n_1)^{2-\gamma} (v_y)}{C_1 \gamma}\right];$$

$$PD(9,9) = [\,G_1 * \lambda_1 * (n_1)^{2\text{-}GAM} * \frac{\partial v_y}{\partial \lambda_{B_x}}\,] \quad \text{or} \quad \left[\frac{\partial \lambda_{B_x}}{\partial \lambda_{B_x}} = + \frac{\lambda_1 (n_1)^{2-\gamma} \left(\frac{\partial v_y}{\partial \lambda_{B_x}}\right)}{C_1 \gamma}\right];$$

RETURN

END

```
**********************************************************************************************
**                  SUBROUTINE FOR ENTERING BOUNDARY CONDITIONS                             **
**********************************************************************************************

SUBROUTINE FCNB (N, KA, KB, F)
REAL KA(N), KB(N), F(N)
INTEGER N
COMMON/XXX/VAR, C, C1, C2, GAM, G1, G2, ZA, ZB, DENSITY, B0, N0


F(1)      = KA(6)                 or [ B.C. at sfc A is   λ1  = 0 ];
F(2)      = KA(7)                 or [ B.C. at sfc A is   λ2  = 0 ];
F(3)      = KA(3)                 or [ B.C. at sfc A is   Ey  = 0 ];
F(4)      = KA(4)                 or [ B.C. at sfc A is   Bx  = 0 ];
F(5)      = KA(5)                 or [ B.C. at sfc A is   Qz  = 0 ];
F(6)      = KB(6)                 or [ B.C. at sfc B is   λ1  = 0 ];
F(7)      = KB(7)                 or [ B.C. at sfc B is   λ2  = 0 ];
F(8)      = KB(3)                 or [ B.C. at sfc B is   Ey  = 0 ];
F(9)      = KB(4) - B0            or [ B.C. at sfc B is   Bx  = + Bx0 ];
F(10)     = KB(5) - ( N0 * ZB )   or [ B.C. at sfc B is   Qz  = + ( n0zB )];
```

(Note: Surface A is the bottom surface of the model magnetotail which in this particular case represents the center or neutral sheet of the earth's magnetotail. Surface B is the top of the model magnetotail and represents the upper boundary of the earth's magnetotail.)

```
RETURN

END
```

APPENDIX C: Model Data

Multiplying Scaling Quantities by One.

These tables show the calculated values of each energy variable in the minimum total energy equation. The value of each variable is added to the values calculated from the previous scaling height.

1. For $n_0 = 1.0$; $z_0 = 1.0$; $Ez_0 = 1.0$; $Bx_0 = 1.0$; $C_0 = 1.0$.

Integrating Energy Parameters from 0.0 to 1.0.

I	z(I)	U(I)	n_1(I)	n_2(I)	E_z(I)	B_x(I)	V_y(I)	Temp(I)
1	0.00	2.56	1.09	1.01	0.00	0.00	0.85	1.06
5	0.04	12.81	5.44	5.03	0.01	0.09	4.27	5.30
10	0.09	25.63	10.88	10.06	0.04	0.42	8.55	10.59
20	0.19	51.33	21.71	20.12	0.16	1.79	17.17	21.16
30	0.29	77.21	32.46	30.16	0.35	4.10	25.95	31.66
40	0.39	103.34	43.06	40.19	0.61	7.38	34.99	42.08
50	0.50	129.82	53.47	50.21	0.92	11.64	44.37	52.36
60	0.60	156.72	63.62	60.20	1.25	16.90	54.19	62.48
70	0.70	184.12	73.43	70.18	1.59	23.17	64.60	72.37
80	0.80	212.07	82.83	80.13	1.89	30.49	75.73	81.98
90	0.90	240.57	91.70	90.07	2.11	38.89	87.77	91.23
100	1.00	269.56	99.94	99.99	2.19	48.37	100.97	100.03

2. For $n_0 = 1.0$; $z_0 = 0.01$; $Ez_0 = 1.0$; $Bx_0 = 1.0$; $C_0 = 1.0$.

Integrating Energy Parameters from 0.0 to 0.01.

I	z(I)	U(I)	n_1(I)	n_2(I)	E_z(I)	B_x(I)	V_y(I)	Temp(I)
1	0.00	5491	1.11	1.00	0.00	0.00	99.58	1.07
5	0.0004	27452	5.53	5.00	0.0001	0.11	497.91	5.36
10	0.0009	54866	11.06	10.00	0.0005	0.50	995.82	10.71
20	0.0019	109406	22.05	20.00	0.0020	2.11	1991.44	21.38
30	0.0029	163278	32.92	30.00	0.0045	4.83	2987.46	31.96
40	0.0039	216150	43.58	40.00	0.0077	8.63	3983.29	42.41
50	0.0050	267703	53.97	50.00	0.0115	13.50	4979.12	52.69
60	0.0060	317633	64.03	60.00	0.0156	19.39	5974.95	62.75
70	0.0070	365657	73.71	70.00	0.0195	26.28	6970.80	72.55
80	0.0080	411516	82.96	80.00	0.0228	34.13	7966.65	81.05
90	0.0090	454976	91.72	90.00	0.0252	42.88	8962.50	91.22
100	0.0100	495832	99.95	100.00	0.0260	52.49	9958.38	100.02

3. For $n_0 = 1.0$; $z_0 = 0.1$; $Ez_0 = 1.0$; $Bx_0 = 1.0$; $C_0 = 1.0$.

Integrating Energy Parameters from 0.0 to 1.0.

I	z(I)	U(I)	n_1(I)	n_2(I)	E_z(I)	B_x(I)	V_y(I)	Temp(I)
1	0.00	56.90	1.11	1.00	0.00	0.00	9.94	1.07
5	0.004	284.44	5.53	5.00	0.001	0.11	49.71	5.36
10	0.009	568.51	11.06	10.00	0.005	0.50	99.43	10.71
20	0.019	1133.92	22.05	20.00	0.020	2.11	198.86	21.37
30	0.029	1692.96	32.91	30.00	0.045	4.82	298.32	31.96
40	0.039	2242.46	43.57	40.00	0.077	8.62	397.80	42.41
50	0.050	2779.35	53.96	50.00	0.115	13.48	497.32	52.69
60	0.060	3300.67	64.03	60.00	0.155	19.36	596.89	62.74
70	0.070	3803.63	73.71	70.00	0.194	26.24	696.53	72.55
80	0.080	4285.63	82.96	80.00	0.228	34.09	796.25	82.05
90	0.090	4744.31	91.72	90.00	0.251	42.83	896.06	91.22
100	0.100	5177.52	99.95	100.00	0.260	52.44	996.00	100.02

4. For $n_0 = 1.0$; $z_0 = 10.0$; $Ez_0 = 1.0$; $Bx_0 = 1.0$; $C_0 = 1.0$.

Integrating Energy Parameters from 0.0 to 10.0.

I	z(I)	U(I)	n_1(I)	n_2(I)	E_z(I)	B_x(I)	V_y(I)	Temp(I)
1	0.00	2.03	1.01	1.01	0.00	0.00	9.6×10^{-5}	1.01
5	0.405	10.15	5.04	5.04	9.0×10^{-6}	9.9×10^{-5}	4.9×10^{-4}	5.03
10	0.911	20.30	10.08	10.08	4.4×10^{-5}	4.7×10^{-4}	1.1×10^{-3}	10.07
20	1.923	40.61	20.16	20.16	2.4×10^{-4}	2.5×10^{-3}	3.4×10^{-3}	20.14
30	2.935	60.91	30.25	30.24	8.8×10^{-4}	8.5×10^{-3}	9.3×10^{-3}	30.21
40	3.947	81.21	40.33	40.32	2.8×10^{-3}	2.5×10^{-2}	2.6×10^{-2}	40.28
50	4.960	101.52	50.41	50.40	8.6×10^{-3}	7.0×10^{-2}	7.0×10^{-2}	50.35
60	5.972	121.82	60.50	60.48	2.6×10^{-2}	1.9×10^{-1}	1.9×10^{-1}	60.43
70	6.984	142.13	70.61	70.53	7.8×10^{-2}	5.3×10^{-1}	5.2×10^{-1}	70.51
80	7.996	162.50	80.75	80.53	2.2×10^{-1}	1.46	1.43	80.62
90	9.009	183.28	90.85	90.38	5.7×10^{-1}	4.00	3.93	90.70
100	10.021	206.51	99.88	99.98	9.5×10^{-1}	10.00	11.14	100.05

5. For $n_0 = 1.0$; $z_0 = 95.0$; $Ez_0 = 1.0$; $Bx_0 = 1.0$; $C_0 = 1.0$.

Integrating Energy Parameters from 0.0 to 95.0.

I	z(I)	U(I)	n_1(I)	n_2(I)	E_z(I)	B_x(I)	V_y(I)	Temp(I)
1	0.00	2.01	1.01	1.01	0.00	0.00	6.4×10^{-18}	1.00
5	3.85	10.03	5.00	5.00	4.4×10^{-11}	4.1×10^{-12}	4.0×10^{-12}	5.01
10	8.67	20.06	10.01	10.01	5.8×10^{-12}	2.1×10^{-11}	3.5×10^{-12}	10.02
20	18.30	40.12	20.02	20.02	8.2×10^{-11}	1.4×10^{-10}	8.7×10^{-12}	20.04
30	27.94	60.18	30.03	30.03	-7.7×10^{-11}	4.7×10^{-10}	8.3×10^{-11}	30.06
40	37.57	80.24	40.04	40.04	9.6×10^{-11}	1.2×10^{-9}	2.5×10^{-10}	40.08
50	47.21	100.30	50.05	50.05	1.2×10^{-11}	2.4×10^{-9}	5.9×10^{-10}	50.12
60	56.84	120.36	60.05	60.05	-4.9×10^{-11}	4.4×10^{-9}	1.8×10^{-9}	60.13
70	66.47	140.42	70.06	70.06	-7.7×10^{-10}	8.4×10^{-9}	5.5×10^{-9}	70.15
80	76.11	160.48	80.07	80.07	-2.0×10^{-9}	1.1×10^{-8}	3.8×10^{-9}	80.17
90	85.74	180.54	90.08	90.08	1.0×10^{-5}	1.1×10^{-4}	1.1×10^{-4}	90.19
100	95.37	201.24	99.81	99.97	9.0×10^{-2}	1.66	1.84	100.01

Typical Magnetotail Values.

6. a) For $n_0 = 1.0$; $z_0 = 1.0$; $Ez_0 = 3.64\text{x}10^{-9}$; $Bx_0 = 1.46\text{x}10^{-3}$; $C_0 = 4.59\text{x}10^{-5}$.

Integrating Energy Terms from 0.0 to 1.0.

I	z(I)	U(I)	n_1(I)	n_2(I)	E_z(I)	B_x(I)	V_y(I)	Temp(I)
1	0.00	$9.3\text{x}10^{-5}$	1.00	1.00	0.00	0.00	$1.2\text{x}10^{-3}$	$4.6\text{x}10^{-5}$
5	0.04	$4.6\text{x}10^{-4}$	5.01	5.01	$7.8\text{x}10^{-8}$	$1.3\text{x}10^{-4}$	$6.2\text{x}10^{-3}$	$2.3\text{x}10^{-4}$
10	0.09	$9.3\text{x}10^{-4}$	10.02	10.02	$3.5\text{x}10^{-7}$	$5.6\text{x}10^{-4}$	$1.2\text{x}10^{-2}$	$4.6\text{x}10^{-4}$
20	0.19	$1.9\text{x}10^{-3}$	20.04	20.04	$1.5\text{x}10^{-6}$	$2.4\text{x}10^{-3}$	$2.5\text{x}10^{-2}$	$9.2\text{x}10^{-4}$
30	0.29	$2.8\text{x}10^{-3}$	30.06	30.05	$3.5\text{x}10^{-6}$	$5.5\text{x}10^{-3}$	$3.8\text{x}10^{-2}$	$1.4\text{x}10^{-3}$
40	0.39	$3.7\text{x}10^{-3}$	40.07	40.07	$6.4\text{x}10^{-6}$	$9.9\text{x}10^{-3}$	$5.1\text{x}10^{-2}$	$1.8\text{x}10^{-3}$
50	0.50	$4.6\text{x}10^{-3}$	50.08	50.08	$1.0\text{x}10^{-5}$	$1.6\text{x}10^{-2}$	$6.4\text{x}10^{-2}$	$2.3\text{x}10^{-3}$
60	0.60	$5.6\text{x}10^{-3}$	60.08	60.08	$1.5\text{x}10^{-5}$	$2.3\text{x}10^{-2}$	$7.9\text{x}10^{-2}$	$2.8\text{x}10^{-3}$
70	0.70	$6.5\text{x}10^{-3}$	70.08	70.07	$2.2\text{x}10^{-5}$	$3.2\text{x}10^{-2}$	$9.4\text{x}10^{-2}$	$3.2\text{x}10^{-3}$
80	0.80	$7.5\text{x}10^{-3}$	80.07	80.07	$3.0\text{x}10^{-5}$	$4.2\text{x}10^{-2}$	$1.1\text{x}10^{-1}$	$3.7\text{x}10^{-3}$
90	0.90	$8.4\text{x}10^{-3}$	90.04	90.04	$4.1\text{x}10^{-5}$	$5.4\text{x}10^{-2}$	$1.3\text{x}10^{-1}$	$4.1\text{x}10^{-3}$
100	1.00	$9.3\text{x}10^{-3}$	99.99	99.99	$5.2\text{x}10^{-5}$	$6.7\text{x}10^{-2}$	$1.5\text{x}10^{-1}$	$4.6\text{x}10^{-3}$

b) For

$$U(I) = \sum_{0}^{I} \frac{n_1 v_y^2}{2} + \frac{E_z^2}{2} + \frac{B_x^2}{2} + Cn_1^{\gamma} + Cn_2^{\gamma} .$$

Energy Variables' Percentage of U(I).

I	z(I)	U(I)	$n_1V_y^2/2$ (%)	$E_z^2/2$ (%)	$B_x^2/2$ (%)	Cn_1^{γ} (%)	Cn_2^{γ} (%)
1	0.00	$9.29\text{x}10^{-5}$	0.08	0.00	0.00	0.50	0.50
5	0.04	$4.65\text{x}10^{-4}$	0.08	$1.94\text{x}10^{-12}$	$5.08\text{x}10^{-6}$	0.50	0.50
10	0.09	$9.30\text{x}10^{-4}$	0.08	$9.29\text{x}10^{-12}$	$2.41\text{x}10^{-5}$	0.50	0.50
20	0.19	$1.86\text{x}10^{-3}$	0.08	$4.12\text{x}10^{-11}$	$1.05\text{x}10^{-4}$	0.50	0.50
30	0.29	$2.79\text{x}10^{-3}$	0.08	$9.90\text{x}10^{-11}$	$2.45\text{x}10^{-4}$	0.50	0.50
40	0.39	$3.72\text{x}10^{-3}$	0.09	$1.88\text{x}10^{-10}$	$4.48\text{x}10^{-4}$	0.50	0.50
50	0.50	$4.65\text{x}10^{-3}$	0.09	$3.19\text{x}10^{-10}$	$7.18\text{x}10^{-4}$	0.50	0.50
60	0.60	$5.59\text{x}10^{-3}$	0.09	$5.04\text{x}10^{-10}$	$1.06\text{x}10^{-3}$	0.49	0.49
70	0.70	$6.52\text{x}10^{-3}$	0.10	$7.62\text{x}10^{-10}$	$1.49\text{x}10^{-3}$	0.49	0.49
80	0.80	$7.45\text{x}10^{-3}$	0.10	$1.12\text{x}10^{-9}$	$2.01\text{x}10^{-3}$	0.49	0.49
90	0.90	$8.39\text{x}10^{-3}$	0.11	$1.63\text{x}10^{-9}$	$2.63\text{x}10^{-3}$	0.49	0.49
100	1.00	$9.33\text{x}10^{-3}$	0.12	$2.21\text{x}10^{-9}$	$3.38\text{x}10^{-3}$	0.49	0.49

The value for the minimum total energy of this model system is $9.33\text{x}10^{-3}$.

Typical Magnetotail Values.

7. a) For $n_0 = 1.0$; $z_0 = 2.0$; $Ez_0 = 3.64\times10^{-9}$; $Bx_0 = 1.46\times10^{-3}$; $C_0 = 4.59\times10^{-5}$.

Integrating Energy Terms from 0.0 to 2.0.

I	z(I)	U(I)	n_1(I)	n_2(I)	E_z(I)	B_x(I)	V_y(I)	Temp(I)
1	0.00	9.2×10^{-5}	1.00	1.00	0.00	0.00	4.0×10^{-4}	4.6×10^{-5}
5	0.08	4.6×10^{-4}	5.01	5.01	1.6×10^{-8}	8.1×10^{-5}	2.0×10^{-3}	2.3×10^{-4}
10	0.18	9.2×10^{-4}	10.02	10.02	7.4×10^{-8}	3.7×10^{-4}	4.0×10^{-3}	4.6×10^{-4}
20	0.38	1.8×10^{-3}	20.03	20.03	3.2×10^{-7}	1.6×10^{-3}	8.2×10^{-3}	9.2×10^{-4}
30	0.59	2.8×10^{-3}	30.04	30.04	7.9×10^{-7}	3.6×10^{-3}	1.3×10^{-2}	1.4×10^{-3}
40	0.79	3.7×10^{-3}	40.06	40.06	1.6×10^{-6}	6.7×10^{-3}	1.8×10^{-2}	1.8×10^{-3}
50	0.99	4.6×10^{-3}	50.07	50.07	2.7×10^{-6}	1.1×10^{-2}	2.3×10^{-2}	2.3×10^{-3}
60	1.19	5.5×10^{-3}	60.07	60.07	4.6×10^{-6}	1.6×10^{-2}	3.0×10^{-2}	2.8×10^{-3}
70	1.40	6.5×10^{-3}	70.07	70.07	7.3×10^{-6}	2.3×10^{-2}	3.8×10^{-2}	3.2×10^{-3}
80	1.60	7.4×10^{-3}	80.06	80.06	1.1×10^{-5}	3.2×10^{-2}	4.8×10^{-2}	3.7×10^{-3}
90	1.80	8.3×10^{-3}	90.04	90.04	1.8×10^{-5}	4.2×10^{-2}	5.9×10^{-2}	4.1×10^{-3}
100	2.00	9.2×10^{-3}	99.99	99.99	2.6×10^{-5}	5.6×10^{-2}	7.3×10^{-2}	4.6×10^{-3}

b) For

$$U(I) = \sum_{0}^{I} \frac{n_1 v_y^2}{2} + \frac{E_z^2}{2} + \frac{B_x^2}{2} + Cn_1^{\gamma} + Cn_2^{\gamma} .$$

Energy Variables' Percentage of U(I).

I	z(I)	U(I)	$n_1V_y^2/2$ (%)	$E_z^2/2$ (%)	$B_x^2/2$ (%)	Cn_1^{γ} (%)	Cn_2^{γ} (%)
1	0.00	9.29×10^{-5}	8.7×10^{-4}	0.00	0.00	0.50	0.50
5	0.08	4.61×10^{-4}	8.7×10^{-4}	8.63×10^{-14}	2.14×10^{-6}	0.50	0.50
10	0.18	9.22×10^{-4}	8.8×10^{-4}	4.19×10^{-13}	1.02×10^{-5}	0.50	0.50
20	0.38	1.84×10^{-3}	9.1×10^{-4}	1.99×10^{-12}	4.55×10^{-5}	0.50	0.50
30	0.59	2.77×10^{-3}	9.8×10^{-4}	5.41×10^{-12}	1.09×10^{-4}	0.50	0.50
40	0.79	3.69×10^{-3}	1.1×10^{-3}	1.21×10^{-11}	2.08×10^{-4}	0.50	0.50
50	0.99	4.61×10^{-3}	1.2×10^{-3}	2.53×10^{-11}	3.52×10^{-4}	0.50	0.50
60	1.19	5.53×10^{-3}	1.4×10^{-3}	5.11×10^{-11}	5.56×10^{-4}	0.50	0.50
70	1.40	6.46×10^{-3}	1.7×10^{-3}	1.02×10^{-10}	8.42×10^{-4}	0.50	0.50
80	1.60	7.39×10^{-3}	2.1×10^{-3}	2.05×10^{-10}	1.24×10^{-3}	0.50	0.50
90	1.80	8.31×10^{-3}	2.7×10^{-3}	4.14×10^{-10}	1.80×10^{-3}	0.50	0.50
100	2.00	9.24×10^{-3}	3.4×10^{-3}	8.05×10^{-10}	2.57×10^{-3}	0.50	0.50

The value for the minimum total energy of this model system is 9.24×10^{-2}.

Typical Magnetotail Values.

8. a) For $n_0 = 1.0$; $z_0 = 3.0$; $Ez_0 = 3.64\text{x}10^{-9}$; $Bx_0 = 1.46\text{x}10^{-3}$; $C_0 = 4.59\text{x}10^{-5}$.

Integrating Energy Terms from 0.0 to 3.0.

I	z(I)	U(I)	n_1(I)	n_2(I)	E_z(I)	B_x(I)	V_y(I)	Temp(I)
1	0.00	$9.2\text{x}10^{-5}$	1.00	1.00	0.00	0.00	$1.4\text{x}10^{-4}$	$4.6\text{x}10^{-5}$
5	0.12	$4.6\text{x}10^{-4}$	5.01	5.01	$3.2\text{x}10^{-9}$	$4.4\text{x}10^{-5}$	$7.3\text{x}10^{-4}$	$2.3\text{x}10^{-4}$
10	0.27	$9.2\text{x}10^{-4}$	10.01	10.01	$1.5\text{x}10^{-8}$	$2.0\text{x}10^{-4}$	$1.5\text{x}10^{-3}$	$4.6\text{x}10^{-4}$
20	0.58	$1.8\text{x}10^{-3}$	20.02	20.02	$6.8\text{x}10^{-8}$	$8.6\text{x}10^{-4}$	$3.1\text{x}10^{-3}$	$9.2\text{x}10^{-4}$
30	0.88	$2.8\text{x}10^{-3}$	30.03	30.03	$1.8\text{x}10^{-7}$	$2.0\text{x}10^{-3}$	$4.9\text{x}10^{-3}$	$1.4\text{x}10^{-3}$
40	1.18	$3.7\text{x}10^{-3}$	40.04	40.04	$3.9\text{x}10^{-7}$	$3.9\text{x}10^{-3}$	$7.3\text{x}10^{-3}$	$1.8\text{x}10^{-3}$
50	1.49	$4.6\text{x}10^{-3}$	50.05	50.05	$7.9\text{x}10^{-7}$	$6.5\text{x}10^{-3}$	$1.0\text{x}10^{-2}$	$2.3\text{x}10^{-3}$
60	1.79	$5.5\text{x}10^{-3}$	60.06	60.06	$1.5\text{x}10^{-6}$	$1.0\text{x}10^{-2}$	$1.4\text{x}10^{-2}$	$2.8\text{x}10^{-3}$
70	2.10	$6.4\text{x}10^{-3}$	70.06	70.06	$2.8\text{x}10^{-6}$	$1.5\text{x}10^{-2}$	$1.9\text{x}10^{-2}$	$3.2\text{x}10^{-3}$
80	2.40	$7.4\text{x}10^{-3}$	80.06	80.06	$5.3\text{x}10^{-6}$	$2.2\text{x}10^{-2}$	$2.6\text{x}10^{-2}$	$3.7\text{x}10^{-3}$
90	2.70	$8.3\text{x}10^{-3}$	90.04	90.04	$9.8\text{x}10^{-6}$	$3.1\text{x}10^{-2}$	$3.6\text{x}10^{-2}$	$4.1\text{x}10^{-3}$
100	3.00	$9.2\text{x}10^{-3}$	99.99	99.99	$1.7\text{x}10^{-5}$	$4.4\text{x}10^{-2}$	$4.9\text{x}10^{-2}$	$4.6\text{x}10^{-3}$

b) For

$$U(I) = \sum_{0}^{I} \frac{n_1 v_y^2}{2} + \frac{E_z^2}{2} + \frac{B_x^2}{2} + Cn_1^{\gamma} + Cn_2^{\gamma} .$$

Energy Variables' Percentage of U(I).

I	z(I)	U(I)	$n_1V_y^2/2$ (%)	$E_z^2/2$ (%)	$B_x^2/2$ (%)	Cn_1^{γ} (%)	Cn_2^{γ} (%)
1	0.00	$9.21\text{x}10^{-5}$	$1.1\text{x}10^{-4}$	0.00	0.00	0.50	0.50
5	0.12	$4.60\text{x}10^{-4}$	$1.1\text{x}10^{-4}$	$3.34\text{x}10^{-15}$	$6.32\text{x}10^{-7}$	0.50	0.50
10	0.27	$9.21\text{x}10^{-4}$	$1.2\text{x}10^{-4}$	$1.67\text{x}10^{-14}$	$3.04\text{x}10^{-6}$	0.50	0.50
20	0.58	$1.84\text{x}10^{-3}$	$1.3\text{x}10^{-4}$	$8.96\text{x}10^{-14}$	$1.39\text{x}10^{-5}$	0.50	0.50
30	0.88	$2.76\text{x}10^{-3}$	$1.5\text{x}10^{-4}$	$2.94\text{x}10^{-13}$	$3.51\text{x}10^{-5}$	0.50	0.50
40	1.18	$3.68\text{x}10^{-3}$	$1.9\text{x}10^{-4}$	$8.54\text{x}10^{-13}$	$7.17\text{x}10^{-5}$	0.50	0.50
50	1.49	$4.60\text{x}10^{-3}$	$2.5\text{x}10^{-4}$	$2.43\text{x}10^{-12}$	$1.33\text{x}10^{-4}$	0.50	0.50
60	1.79	$5.53\text{x}10^{-3}$	$3.5\text{x}10^{-4}$	$6.94\text{x}10^{-12}$	$2.33\text{x}10^{-4}$	0.50	0.50
70	2.09	$6.45\text{x}10^{-3}$	$5.1\text{x}10^{-4}$	$2.02\text{x}10^{-11}$	$3.99\text{x}10^{-4}$	0.50	0.50
80	2.40	$7.37\text{x}10^{-3}$	$7.9\text{x}10^{-4}$	$5.96\text{x}10^{-11}$	$6.74\text{x}10^{-4}$	0.50	0.50
90	2.70	$8.30\text{x}10^{-3}$	$1.3\text{x}10^{-3}$	$1.79\text{x}10^{-10}$	$1.13\text{x}10^{-3}$	0.50	0.50
100	3.00	$9.22\text{x}10^{-3}$	$2.0\text{x}10^{-3}$	$5.28\text{x}10^{-10}$	$1.91\text{x}10^{-3}$	0.50	0.50

The value for the minimum total energy of this model system is $9.22\text{x}10^{-3}$.

Typical Magnetotail Values.

9. a) For $n_0 = 1.0$; $z_0 = 4.0$; $Ez_0 = 3.64\text{x}10^{-9}$; $Bx_0 = 1.46\text{x}10^{-3}$; $C_0 = 4.59\text{x}10^{-5}$.

Integrating Energy Terms from 0.0 to 4.0.

I	z(I)	U(I)	n_1(I)	n_2(I)	E_z(I)	B_x(I)	V_y(I)	Temp(I)
1	0.00	$9.2\text{x}10^{-5}$	1.00	1.00	0.00	0.00	$5.3\text{x}10^{-5}$	$4.6\text{x}10^{-5}$
5	0.16	$4.6\text{x}10^{-4}$	5.00	5.00	$5.8\text{x}10^{-10}$	$2.2\text{x}10^{-5}$	$2.7\text{x}10^{-4}$	$2.3\text{x}10^{-4}$
10	0.36	$9.2\text{x}10^{-4}$	10.01	10.01	$2.7\text{x}10^{-9}$	$9.8\text{x}10^{-5}$	$5.4\text{x}10^{-4}$	$4.6\text{x}10^{-4}$
20	0.77	$1.8\text{x}10^{-3}$	20.02	20.02	$1.3\text{x}10^{-8}$	$4.3\text{x}10^{-4}$	$1.2\text{x}10^{-3}$	$9.2\text{x}10^{-4}$
30	1.17	$2.8\text{x}10^{-3}$	30.03	30.03	$3.9\text{x}10^{-8}$	$1.1\text{x}10^{-3}$	$2.0\text{x}10^{-3}$	$1.4\text{x}10^{-3}$
40	1.58	$3.7\text{x}10^{-3}$	40.03	40.03	$9.8\text{x}10^{-8}$	$2.1\text{x}10^{-3}$	$3.1\text{x}10^{-3}$	$1.8\text{x}10^{-3}$
50	1.98	$4.6\text{x}10^{-3}$	50.04	50.04	$2.3\text{x}10^{-7}$	$3.6\text{x}10^{-3}$	$4.8\text{x}10^{-3}$	$2.3\text{x}10^{-3}$
60	2.39	$5.5\text{x}10^{-3}$	60.05	60.05	$5.3\text{x}10^{-7}$	$6.0\text{x}10^{-3}$	$7.2\text{x}10^{-3}$	$2.8\text{x}10^{-3}$
70	2.79	$6.4\text{x}10^{-3}$	70.05	70.05	$1.2\text{x}10^{-6}$	$9.6\text{x}10^{-3}$	$1.1\text{x}10^{-2}$	$3.2\text{x}10^{-3}$
80	3.20	$7.4\text{x}10^{-3}$	80.05	80.05	$2.7\text{x}10^{-6}$	$1.5\text{x}10^{-2}$	$1.6\text{x}10^{-2}$	$3.7\text{x}10^{-3}$
90	3.60	$8.3\text{x}10^{-3}$	90.04	90.04	$6.1\text{x}10^{-6}$	$2.3\text{x}10^{-2}$	$2.5\text{x}10^{-2}$	$4.1\text{x}10^{-3}$
100	4.00	$9.2\text{x}10^{-3}$	99.99	99.99	$1.3\text{x}10^{-5}$	$3.5\text{x}10^{-2}$	$3.7\text{x}10^{-2}$	$4.6\text{x}10^{-3}$

b) For

$$U(I) = \sum_{0}^{I} \frac{n_1 v_y^2}{2} + \frac{E_z^2}{2} + \frac{B_x^2}{2} + Cn_1^{\gamma} + Cn_2^{\gamma} .$$

Energy Variables' Percentage of U(I).

I	z(I)	U(I)	$n_1V_y^2/2$ (%)	$E_z^2/2$ (%)	$B_x^2/2$ (%)	Cn_1^{γ} (%)	Cn_2^{γ} (%)
1	0.00	$9.20\text{x}10^{-5}$	$1.5\text{x}10^{-5}$	0.00	0.00	0.50	0.50
5	0.16	$4.60\text{x}10^{-4}$	$1.5\text{x}10^{-5}$	$1.09\text{x}10^{-16}$	$1.51\text{x}10^{-7}$	0.50	0.50
10	0.36	$9.20\text{x}10^{-4}$	$1.6\text{x}10^{-5}$	$5.65\text{x}10^{-16}$	$7.35\text{x}10^{-7}$	0.50	0.50
20	0.77	$1.84\text{x}10^{-3}$	$1.9\text{x}10^{-5}$	$3.56\text{x}10^{-15}$	$3.50\text{x}10^{-6}$	0.50	0.50
30	1.17	$2.76\text{x}10^{-3}$	$2.5\text{x}10^{-5}$	$1.51\text{x}10^{-14}$	$9.47\text{x}10^{-6}$	0.50	0.50
40	1.58	$3.68\text{x}10^{-3}$	$3.7\text{x}10^{-5}$	$6.07\text{x}10^{-14}$	$2.13\text{x}10^{-5}$	0.50	0.50
50	1.98	$4.60\text{x}10^{-3}$	$6.0\text{x}10^{-5}$	$2.49\text{x}10^{-13}$	$4.43\text{x}10^{-5}$	0.50	0.50
60	2.39	$5.52\text{x}10^{-3}$	$1.0\text{x}10^{-4}$	$1.05\text{x}10^{-12}$	$8.96\text{x}10^{-5}$	0.50	0.50
70	2.79	$6.44\text{x}10^{-3}$	$2.0\text{x}10^{-4}$	$4.56\text{x}10^{-12}$	$1.80\text{x}10^{-4}$	0.50	0.50
80	3.20	$7.36\text{x}10^{-3}$	$3.8\text{x}10^{-4}$	$2.01\text{x}10^{-11}$	$3.60\text{x}10^{-4}$	0.50	0.50
90	3.60	$8.29\text{x}10^{-3}$	$7.5\text{x}10^{-4}$	$9.04\text{x}10^{-11}$	$7.27\text{x}10^{-4}$	0.50	0.50
100	4.00	$9.22\text{x}10^{-3}$	$1.5\text{x}10^{-3}$	$4.15\text{x}10^{-10}$	$1.48\text{x}10^{-3}$	0.50	0.50

The value for the minimum total energy of this model system is $9.22\text{x}10^{-3}$.

Typical Magnetotail Values.

10. a) For $n_0 = 1.0$; $z_0 = 5.0$; $Ez_0 = 3.64\text{x}10^{-9}$; $Bx_0 = 1.46\text{x}10^{-3}$; $C_0 = 4.59\text{x}10^{-5}$.

Integrating Energy Terms from 0.0 to 5.0.

I	z(I)	U(I)	n_1(I)	n_2(I)	E_z(I)	B_x(I)	V_y(I)	Temp(I)
1	0.00	$9.2\text{x}10^{-5}$	1.00	1.00	0.00	0.00	$1.9\text{x}10^{-5}$	$4.6\text{x}10^{-5}$
5	0.20	$4.6\text{x}10^{-4}$	5.00	5.00	$9.7\text{x}10^{-11}$	$9.9\text{x}10^{-6}$	$9.8\text{x}10^{-5}$	$2.3\text{x}10^{-4}$
10	0.46	$9.2\text{x}10^{-4}$	10.01	10.01	$4.7\text{x}10^{-10}$	$4.5\text{x}10^{-5}$	$2.0\text{x}10^{-4}$	$4.6\text{x}10^{-4}$
20	0.96	$1.8\text{x}10^{-3}$	20.02	20.02	$2.5\text{x}10^{-9}$	$2.0\text{x}10^{-4}$	$4.5\text{x}10^{-4}$	$9.2\text{x}10^{-4}$
30	1.47	$2.8\text{x}10^{-3}$	30.03	30.03	$8.4\text{x}10^{-9}$	$5.1\text{x}10^{-4}$	$8.2\text{x}10^{-4}$	$1.4\text{x}10^{-3}$
40	1.97	$3.7\text{x}10^{-3}$	40.03	40.03	$2.5\text{x}10^{-8}$	$1.1\text{x}10^{-3}$	$1.4\text{x}10^{-3}$	$1.8\text{x}10^{-3}$
50	2.48	$4.6\text{x}10^{-3}$	50.04	50.04	$6.9\text{x}10^{-8}$	$2.0\text{x}10^{-3}$	$2.3\text{x}10^{-3}$	$2.3\text{x}10^{-3}$
60	2.99	$5.5\text{x}10^{-3}$	60.05	60.05	$1.9\text{x}10^{-7}$	$3.5\text{x}10^{-3}$	$3.9\text{x}10^{-3}$	$2.8\text{x}10^{-3}$
70	3.49	$6.4\text{x}10^{-3}$	70.05	70.05	$5.3\text{x}10^{-7}$	$6.1\text{x}10^{-3}$	$6.5\text{x}10^{-3}$	$3.2\text{x}10^{-3}$
80	4.00	$7.4\text{x}10^{-3}$	80.05	80.05	$1.5\text{x}10^{-6}$	$1.0\text{x}10^{-2}$	$1.1\text{x}10^{-2}$	$3.7\text{x}10^{-3}$
90	4.50	$8.3\text{x}10^{-3}$	90.04	90.04	$4.0\text{x}10^{-6}$	$1.7\text{x}10^{-2}$	$1.8\text{x}10^{-2}$	$4.1\text{x}10^{-3}$
100	5.01	$9.2\text{x}10^{-3}$	99.99	99.99	$1.0\text{x}10^{-5}$	$2.9\text{x}10^{-2}$	$3.0\text{x}10^{-2}$	$4.6\text{x}10^{-3}$

b) For

$$U(I) = \sum_{0}^{I} \frac{n_1 v_y^2}{2} + \frac{E_z^2}{2} + \frac{B_x^2}{2} + Cn_1^{\gamma} + Cn_2^{\gamma} .$$

Energy Variables' Percentage of U(I).

I	z(I)	U(I)	$n_1V_y^2/2$ (%)	$E_z^2/2$ (%)	$B_x^2/2$ (%)	Cn_1^{γ} (%)	Cn_2^{γ} (%)
1	0.00	$9.20\text{x}10^{-5}$	$2.1\text{x}10^{-6}$	0.00	0.00	0.50	0.50
5	0.20	$4.60\text{x}10^{-4}$	$2.1\text{x}10^{-6}$	$3.21\text{x}10^{-18}$	$3.19\text{x}10^{-8}$	0.50	0.50
10	0.46	$9.20\text{x}10^{-4}$	$2.2\text{x}10^{-6}$	$1.72\text{x}10^{-17}$	$1.57\text{x}10^{-7}$	0.50	0.50
20	0.96	$1.84\text{x}10^{-3}$	$2.8\text{x}10^{-6}$	$1.33\text{x}10^{-16}$	$7.89\text{x}10^{-7}$	0.50	0.50
30	1.47	$2.76\text{x}10^{-3}$	$4.4\text{x}10^{-6}$	$7.64\text{x}10^{-16}$	$2.33\text{x}10^{-6}$	0.50	0.50
40	1.97	$3.68\text{x}10^{-3}$	$8.0\text{x}10^{-6}$	$4.45\text{x}10^{-15}$	$5.93\text{x}10^{-6}$	0.50	0.50
50	2.48	$4.60\text{x}10^{-3}$	$1.6\text{x}10^{-5}$	$2.69\text{x}10^{-14}$	$1.42\text{x}10^{-5}$	0.50	0.50
60	2.99	$5.52\text{x}10^{-3}$	$3.6\text{x}10^{-5}$	$1.70\text{x}10^{-13}$	$3.39\text{x}10^{-5}$	0.50	0.50
70	3.49	$6.44\text{x}10^{-3}$	$8.4\text{x}10^{-5}$	$1.10\text{x}10^{-12}$	$8.13\text{x}10^{-5}$	0.50	0.50
80	3.99	$7.36\text{x}10^{-3}$	$2.0\text{x}10^{-4}$	$7.30\text{x}10^{-12}$	$1.97\text{x}10^{-4}$	0.50	0.50
90	4.50	$8.28\text{x}10^{-3}$	$4.9\text{x}10^{-4}$	$4.90\text{x}10^{-11}$	$4.84\text{x}10^{-4}$	0.50	0.50
100	5.00	$9.21\text{x}10^{-3}$	$1.2\text{x}10^{-3}$	$3.54\text{x}10^{-10}$	$1.20\text{x}10^{-3}$	0.50	0.50

The value for the minimum total energy of this model system is $9.20\text{x}10^{-3}$.

Typical Magnetotail Values.

11. a) For $n_0 = 1.0$; $z_0 = 10.0$; $Ez_0 = 3.64\text{x}10^{-9}$; $Bx_0 = 1.46\text{x}10^{-3}$; $C_0 = 4.59\text{x}10^{-5}$.

Integrating Energy Terms from 0.0 to 10.0.

I	z(I)	U(I)	n_1(I)	n_2(I)	E_z(I)	B_x(I)	V_y(I)	Temp(I)
1	0.00	$9.2\text{x}10^{-5}$	1.00	1.00	0.00	0.00	$1.3\text{x}10^{-7}$	$4.6\text{x}10^{-5}$
5	0.40	$4.6\text{x}10^{-4}$	5.00	5.00	$3.8\text{x}10^{-13}$	$1.3\text{x}10^{-7}$	$6.7\text{x}10^{-7}$	$2.3\text{x}10^{-4}$
10	0.91	$9.2\text{x}10^{-4}$	10.01	10.01	$4.1\text{x}10^{-13}$	$6.3\text{x}10^{-7}$	$1.5\text{x}10^{-6}$	$4.6\text{x}10^{-4}$
20	1.92	$1.8\text{x}10^{-3}$	20.02	20.02	$1.7\text{x}10^{-12}$	$3.4\text{x}10^{-6}$	$4.6\text{x}10^{-6}$	$9.2\text{x}10^{-4}$
30	2.94	$2.8\text{x}10^{-3}$	30.03	30.03	$4.7\text{x}10^{-12}$	$1.1\text{x}10^{-5}$	$1.3\text{x}10^{-5}$	$1.4\text{x}10^{-3}$
40	3.95	$3.7\text{x}10^{-3}$	40.03	40.03	$2.0\text{x}10^{-11}$	$3.3\text{x}10^{-5}$	$3.5\text{x}10^{-5}$	$1.8\text{x}10^{-3}$
50	4.96	$4.6\text{x}10^{-3}$	50.04	50.04	$2.1\text{x}10^{-10}$	$9.4\text{x}10^{-5}$	$9.6\text{x}10^{-5}$	$2.3\text{x}10^{-3}$
60	5.97	$5.5\text{x}10^{-3}$	60.05	60.05	$1.7\text{x}10^{-9}$	$2.6\text{x}10^{-4}$	$2.6\text{x}10^{-4}$	$2.8\text{x}10^{-3}$
70	6.98	$6.4\text{x}10^{-3}$	70.05	70.05	$1.3\text{x}10^{-8}$	$7.2\text{x}10^{-4}$	$7.2\text{x}10^{-4}$	$3.2\text{x}10^{-3}$
80	8.00	$7.4\text{x}10^{-3}$	80.05	80.05	$9.6\text{x}10^{-8}$	$2.0\text{x}10^{-3}$	$2.0\text{x}10^{-3}$	$3.7\text{x}10^{-3}$
90	9.00	$8.3\text{x}10^{-3}$	90.04	90.04	$7.1\text{x}10^{-7}$	$5.5\text{x}10^{-3}$	$5.5\text{x}10^{-3}$	$4.1\text{x}10^{-3}$
100	10.02	$9.2\text{x}10^{-3}$	99.99	99.99	$5.2\text{x}10^{-6}$	$1.5\text{x}10^{-2}$	$1.5\text{x}10^{-2}$	$4.6\text{x}10^{-3}$

b) For

$$U(I) = \sum_{0}^{I} \frac{n_1 v_y^2}{2} + \frac{E_z^2}{2} + \frac{B_x^2}{2} + Cn_1^{\gamma} + Cn_2^{\gamma} .$$

Energy Variables' Percentage of U(I).

I	z(I)	U(I)	$n_1V_y^2/2$ (%)	$E_z^2/2$ (%)	$B_x^2/2$ (%)	Cn_1^{γ} (%)	Cn_2^{γ} (%)
1	0.00	$9.20\text{x}10^{-5}$	$9.1\text{x}10^{-11}$	0.00	0.00	0.50	0.50
5	0.40	$4.60\text{x}10^{-4}$	$9.6\text{x}10^{-11}$	$7.88\text{x}10^{-23}$	$5.80\text{x}10^{-12}$	0.50	0.50
10	0.91	$9.20\text{x}10^{-4}$	$1.2\text{x}10^{-10}$	$1.91\text{x}10^{-21}$	$3.18\text{x}10^{-11}$	0.50	0.50
20	1.92	$1.84\text{x}10^{-3}$	$3.4\text{x}10^{-10}$	$4.78\text{x}10^{-21}$	$2.45\text{x}10^{-10}$	0.50	0.50
30	2.94	$2.76\text{x}10^{-3}$	$1.5\text{x}10^{-9}$	$5.72\text{x}10^{-21}$	$1.42\text{x}10^{-9}$	0.50	0.50
40	3.95	$3.68\text{x}10^{-3}$	$8.4\text{x}10^{-9}$	$1.54\text{x}10^{-20}$	$8.26\text{x}10^{-9}$	0.50	0.50
50	4.96	$4.60\text{x}10^{-3}$	$5.1\text{x}10^{-8}$	$5.44\text{x}10^{-19}$	$5.03\text{x}10^{-8}$	0.50	0.50
60	5.97	$5.52\text{x}10^{-3}$	$3.2\text{x}10^{-7}$	$2.69\text{x}10^{-17}$	$3.18\text{x}10^{-7}$	0.50	0.50
70	6.98	$6.44\text{x}10^{-3}$	$2.1\text{x}10^{-6}$	$1.33\text{x}10^{-15}$	$2.07\text{x}10^{-6}$	0.50	0.50
80	8.00	$7.35\text{x}10^{-3}$	$1.4\text{x}10^{-5}$	$6.84\text{x}10^{-14}$	$1.37\text{x}10^{-5}$	0.50	0.50
90	9.01	$8.28\text{x}10^{-3}$	$9.3\text{x}10^{-5}$	$3.91\text{x}10^{-12}$	$9.24\text{x}10^{-5}$	0.50	0.50
100	10.02	$9.20\text{x}10^{-3}$	$6.3\text{x}10^{-4}$	$2.68\text{x}10^{-10}$	$6.30\text{x}10^{-4}$	0.50	0.50

The value for the minimum total energy of this model system is $9.20\text{x}10^{-3}$.

APPENDIX D: Bibliography

BIBLIOGRAPHY

Adkins, C. J., *Equilibrium Thermodynamics*, Second Edition, McGraw-Hill Book Company (UK) Limited, Maidenhead, England, 1968.

Akasofu, S. I., *Polar and Magnetospheric Substorms*, Springer-Verlag, New York, 1968.

Akasofu, S. I. and L. J. Lanzerotti, "The Earth's Magnetosphere," *Physics Today*, 28-35, 1975.

Akasofu, S. I., "Concluding Remarks," in *Magnetospheric Physics*, edited by Lui, A. T. Y., John Hopkins University Press, Baltimore, 1987.

Axford, W. I., "Tail of the Magnetosphere," *J. Geophys. Res.*, 70, 1231, 1965.

Birn, J., "The Boundary Value Problem of Magnetotail Equilibrium," *J. Geophys. Res.*, 97(A11), 19,441-19,450, 1991.

Burkhart, G. R., J. F. Drake, P. B. Dusenbery, and T. W. Speiser, "A Particle Model for Magnetotail Neutral Sheet Equilibria," *J. Geophys. Res.*, 97(A9), 13,799-13,815, 1992.

Carovillano, R. L., J. F. McClay, and H. R. Radoski, "Physics of the Magnetosphere," Springer-Verlag New York Inc., New York, 1967.

Cattell, C. A., C. W. Carlson, W. Baumjohann, and H. Luhr, "The MHD Structure of the Plasmasheet Boundary: (1) Tangential Momentum Balance and Consistency With Slow Mode Shocks," *J. Geophys. Res. Ltrs.*, 19(20), 2083-2086, 1992.

Clauer, C. R. and R. L. McPherron, "Mapping the Local Time-Universal Time Development of Magnetospheric Substorms Using Mid-latitude Magnetic Observations," *J. Geophys. Res.*, 79(19), 2811-2820, 1974.

Cheng, C. Z., "Magnetospheric Equilibrium With Anisotropic Pressure," *J. Geophys. Res.*, 97(A2), 1497-1510, 1992.

Cowley, S. W. H. and D. J. Southwood, "Some Properties of a Steady-State Geomagnetic Tail," *J. Geophys. Res. Ltrs.*, 7(10), 833-836, 1980.

Eastman, T. E., L. A. Frank, and C. Y. Huang, "The Boundary Layer as the Primary Transport Regions of the Earth's Magnetotail," *J. Geophys. Res.*, 90, 9541, 1985.

Erickson, G. M., "A Quasi-Static Magnetospheric Convection Model in Two Dimensions," *J. Geophys. Res.*, 97(A5), 6505-6522, 1992.

Erickson, G. M. and R. A. Wolf, "Is Steady Convection Possible in the Earth's Magnetotail?" *J. Geophys. Res. Ltrs.*, 7(11), 897-900, 1980.

Fairfield, D. H.,"Magnetotail Energy Storage and the Variability of the Magnetotail Current Sheet," in *Magnetic Reconnection in Space and Laboratory Plasmas*, Geophysical Monograph 30, edited by Hones, E. W. Jr., 168-176, American Geophysical Union, Washington D.C., 1984.

Fairfield, D. H., "Structure of the Geomagnetic Tail," in *Magnetospheric Physics*, edited by Lui, A. T. Y., Chapter 2, 23-33, John Hopkins University Press, Baltimore, 1987.

Goldstein, H., *Classical Mechanics*, Second Edition, Addison-Wesley Publishing Co., Reading, Massachusetts, 1980.

Gosling, J. T., D. N. Baker, and E. W. Hones, Jr., "Journeys of a Spacecraft," *Los Alamos Science*, 33-53, 1984.

Hau, L. N. and G. H. Voigt, "Loss of MHD Equilibrium Caused by the Enhancement of the Magnetic B_y Component in Earth's Magnetotail," *J. Geophys. Res.*, 97(A6), 8707-8711, 1992.

Heikkila, W. J., "Impusive Plasma Transport through the Magnetotpause," *Geophys. Res. Lett.*, 9, 877, 1982

Hill, T. W. and A. J. Dessler, "Plasma Motions in Planetary Magnetospheres," *Science*, 252, 410-415, 1991.

Hones, E. W. Jr., "The Earth's Magnetotail," *Scientific American*, 40-47, 1986.

Kerr, R. A., "Probing the Long Tail of the Magnetosphere," *Science*, 226, 1298-1299, 1984.

King, J. W. and Newman, W. S., *Solar-Terrestrial Physics*, Academic Press, Inc., London, 1967.

Knecht, D. J. and B. M. Shuman, "The Geomagnetic Field," in *Handbook of Geophysics and the Space Environment*, edited by A. S. Jursa, Chapter 4, Air Force Geophysics Laboratory, United States Air Force, 1985.

Lanzerotti, L. J., "Earth's Magnetic Environment," *Sky & Telescope*, 360-362, 1988.

Lanzerotti, L. J. and Krimigis, S. M., "Comparative Magnetospheres," *Physics Today*, 24-34, 1985.

Lee, D. Y. and R. A. Wolf, "Is the Earth's Magnetotail Balloon Unstable?" *J. Geophys. Res.*, 97(A12), 19,251-19,257, 1992.

Lui, A. T. Y., "Observations on the Fluid Aspects of Magnetotail Dynamics," in *Magnetospheric Physics*, edited by Lui, A. T. Y., Chapter 3, 101-118, John Hopkins University Press, Baltimore, 1987.

Lui, A. T. Y., "Road Map to Magnetotail Domains," in *Magnetospheric Physics*, edited by Lui, A. T. Y., Chapter 1, 3-9, John Hopkins University Press, Baltimore, 1987.

Lundin, R., I. Sandahl, and J. Woch, "The Contribution of the Boundary Layer EMF to Magnetospheric Substorms," in *Magnetospheric Substorms*, Geophysical Monograph 64, edited by Kan, J. R., Potemra, T. A., Kokubun S., and Iijima T., American Geophysical Union, Washington D.C., 1991.

McPherron, R. L., "Physical Process Producing Magnetospheric Substorms and Magnetic Storms," in *Geomagnetism*, Vol 4, edited by J. A. Jacobs, Chapter 7, Academic Press, London', 1991.

National Research Council, *Solar-Terrestrial Research for the 1980's*, National Academy Press, 1981.

Ness, N. F., "Magnetotail Research: The Early Years," in *Magnetospheric Physics*, edited by Lui, A. T. Y., Chapter 1, 11-20, John Hopkins University Press, Baltimore, 1987.

Nishida, A., *Geomagnetic Diagnosis of the Magnetosphere*, Springer-Verlag, New York, 1978.

Nishida, A., "Reconnection in Earth's Magnetotail: An Overview," in *Magnetic Reconnection in Space and Laboratory Plasmas*, Geophysical Monograph 30, edited by Hones, E. W. Jr., 159-167, American Geophysical Union, Washington D.C., 1984.

Peterson, I., "Startling Tales From the Magnetotail," *Science News*, 139, 356, 1991.

Pilipp W. and G. Morfill, "The Plasma Mantle as the Origin of the Plasma Sheet," in *Magnetospheric Particles and Fields*, edited by B. M. McCormac, 55, D. Reidel Publ. Co., Dordrecht, Holland, 1974.

Pippard, A. B., *The Elements of Classical Thermodynamics*, Cambridge, London, 1957.

Schindler, K. and J. Birn., "Magnetotail Theory," *Space Science Reviews*, 44, 307-355, 1986.

Scholer, M., "General Discussion on Magnetotail Kinetics," in *Magnetospheric Physics*, edited by Lui, A. T. Y., Chapter 4, 257-259, John Hopkins University Press, Baltimore, 1987.

Sibeck, D. G., "Evidence for Flux Ropes in the Earth's Magnetotail," in *Physics of Magnetic Flux Ropes*, Geophysical Monograph 58, edited by Russell, C. T., Priest, E. R., Lee, L. C., Chapter _, American Geophysical Union, Washington D.C., 1990.

Speiser, T. W., "Kinetic Aspect of Tail Dynamics: Theory and Simulation," in *Magnetospheric Physics*, edited by Lui, A. T. Y., Chapter 4, 277-285, John Hopkins University Press, Baltimore, 1987.

Tascione, Thomas F., "Magnetosphere," in *Introduction to the Space Environment*, Chapter 5, Orbit Book Company, Malabar, Florida, 1988.

Tsurutani, B. T. and von Rosenvinge, T. T., "ISEE-3 Distant Geotail Results," *J. Geophys. Res. Ltrs.*, 11(10), 1027-1029, 1984.

Voigt, G. H. and R. V. Hilmer, "The Influence of the IMF B_y Component on the Earth's Magneto-Hydrostatic Magnetotail," in *Magnetospheric Physics*, edited by Lui, A. T. Y., Chapter 2, 91-97, John Hopkins University Press, Baltimore, 1987.

Walker, R. J., T. Ogino, and M. Ashour-Abdalla, "Simulating the Magnetosphere: The Structure of the Magnetotail," in *Solar System Plasma Physics*, Geophysical Monograph 54, edited by Waite, J. H. Jr., J. L. Burch, and R. L. Moore, 61-68, American Geophysical Union, Washington D.C., 1989.

Williams, D. J., "Ring Current and Radiation Belts," *Rev. of Geophys.* 25(3), 570-578, 1987.

Young, R. and E. Hameiri, "Approximate Magnetotail Equilibria With Parallel Flow," *J. Geophys. Res.*, 97(A11), 16,789-16,802, 1992.

Zwickl, R. D., L. F. Bargatze, D. N. Baker, C. R. Clauer, and R. L. McPherron, "An Evaluation of the Total Magnetospheric Energy Output Parameter, U_T, in *Magnetospheric Physics*, edited by Lui, A. T. Y., Chapter 3, 155-161, John Hopkins University Press, Baltimore, 1987.